

BLEJSKE DELAVNICE IZ FIZIKE

BLED WORKSHOPS IN PHYSICS

LETNIK 14, ŠT. 1

VOL. 14, NO. 1

ISSN 1580-4992

Proceedings of the Mini-Workshop
Looking into Hadrons

Bled, Slovenia, July 7 – 14, 2013

Edited by

Bojan Golli

Mitja Rosina

Simon Širca

University of Ljubljana and Jožef Stefan Institute

DMFA – ZALOŽNIŠTVO
LJUBLJANA, NOVEMBER 2013

The Mini-Workshop *Looking into Hadrons*

was organized by

*Society of Mathematicians, Physicists and Astronomers of Slovenia
Department of Physics, Faculty of Mathematics and Physics, University of Ljubljana*

and sponsored by

*Department of Physics, Faculty of Mathematics and Physics, University of Ljubljana
Jožef Stefan Institute, Ljubljana
Society of Mathematicians, Physicists and Astronomers of Slovenia*

Organizing Committee

Mitja Rosina, Bojan Golli, Simon Širca

List of participants

*Roelof Bijker, UNAM, Mexico, bijker@nucleares.unam.mx
Joseph Day, Graz, jday21@gmail.com
Giuseppe Galata, UNAM, Mexico, giuseppe.galata@nucleares.unam.mx
Bojan Golli, Ljubljana, bojan.golli@ijs.si
Dubravko Klabučar, Zagreb, klabucar@oberon.phy.hr
Christian B. Lang, Graz, christian.lang@uni-graz.at
Marko Petrič, Ljubljana, marko.petric@ijs.si
Willi Plessas, Graz, willibald.plessas@uni-graz.at
Saša Prelovšek, Ljubljana, Sasa.Prelovsek@ijs.si
Mitja Rosina, Ljubljana, mitja.rosina@ijs.si
Wolfgang Schweiger, Graz, wolfgang.schweiger@uni-graz.at
Oliver Senekowitsch, Graz, oliver.senekowitsch@edu.uni-graz.at
Ica Stancu, Liege, fstancu@ulg.ac.be
Simon Širca, Ljubljana, simon.sirca@fmf.uni-lj.si*

Electronic edition

<http://www-f1.ijs.si/BledPub/>

Contents

| | |
|--|-----|
| Preface | V |
| Predgovor | VII |
| The role of valence and sea quarks in light baryons <i>R. Bijker and E. Santopinto</i> | 1 |
| Baryon spectra and nucleon form factors from relativistic quark models and AdS/QCD <i>J. P. Day and W. Plessas</i> | 6 |
| Hybrid mesons spectroscopy <i>Giuseppe Galatà</i> | 8 |
| Hot and dense QCD medium and restoration of $U_A(1)$ symmetry <i>Dubravko Klabučar et al.</i> | 11 |
| Resonance phase shifts from lattice QCD: The pion-nucleon channel <i>C. B. Lang and V. Verduci</i> | 25 |
| Flavor Decomposition of Baryon Electromagnetic Form Factors <i>M. Rohrmoser, Ki-Seok Choi, and W. Plessas</i> | 27 |
| Quark-Pair Contributions to Weak Transition Form Factors of Heavy-Light Mesons <i>Oliver Senekowitsch and Wolfgang Schweiger</i> | 30 |
| Large N_c baryons and Regge trajectories <i>N. Matagne and Fl. Stancu</i> | 37 |
| Electroexcitation of the D-wave resonances <i>Bojan Golli and Simon Širca</i> | 43 |

New results on quarkonium spectroscopy and exotic quarkonium-like resonances at B-factories

Marko Petrič 45

Charmonium-like states and K^* resonances from lattice QCD

Saša Prelovšek 50

Pion coupling to constituent quarks versus coupling to nucleon

Mitja Rosina and Bogdan Povh 52

Real and virtual Compton scattering experiments at MAMI and Jefferson Lab

S. Širca 57

Povzetki v slovenščini 63

Preface

At our traditional Bled Workshop we were indeed “looking into hadrons”. We were studying different perspectives of the fact that nowadays a baryon is no longer a three-body but rather a many-body problem. Electron scattering reveals polarizations and electroexcitation amplitudes whose explanation requires a “sea” of additional quark-antiquark pairs, which may or may not be rendered by a pion cloud and which is characterized by flavour asymmetry. The electroexcitation of the D-wave resonances demonstrates the interplay of the quark and meson degrees of freedom. The description of such observables is model-dependent, and this is the very junction at which the interaction between physicists can clarify the interaction between partons.

The calculation of quark-pair current contributions to weak transition form-factors of heavy-light mesons is still in progress. The $1/N_c$ -expansion method is still popular for classification of high-lying baryon states and for operators describing observables systematically.

The relativistic constituent quark model with Goldstone-boson-exchange interaction has seen an extension of its domain from light to heavy and double-heavy baryons. The latter have not been measured yet and it is here that Lattice QCD is promising to “replace” the experiment. The agreement with other models is reasonable, while experimentalists are encouraged to measure soon the cc -baryons and cc -tetraquarks.

The progress in Lattice QCD is truly impressive: it is now aiming at K^* resonances, charmonium-like states, DD^* -scattering with some evidence for $X(3872)$ in the 1^{++} , $I = 0$ channel. The phase diagram of QCD is exciting the imagination since it is relevant to heavy-ion collisions and the interior of heavy compact stars. The restoration of different symmetries is an important mechanism for this.

We have also had the traditional experimental talks intended to put the stubborn theoreticians on firm ground. Real and virtual Compton scattering experiments at MAMI and Jefferson Lab give support to constituent quark models; further insight is obtained from generalized (dynamical) proton polarizabilities. New results on quarkonium spectroscopy and exotic quarkonium-like resonances from B-factories provide the quantum numbers of the $Z(4430)^+$ and updated results on $Y(4008)$ and $Y(4260)$ — to tease the theoreticians. There remain puzzles of $\Upsilon(5S)$ decays. Properties of new Z_b states and evidence for $\eta_b(2S)$ have been highlighted.

We would like to encourage the readers to think about coming to Bled (again) and continue the discussions on these exciting topics.

Predgovor

V naši tradicionalni blejski delavnici smo zares "gledali v hadrone". Iz raznih perspektiv smo preučevali dejstvo, da dandanes barion ni več problem treh teles, temveč je problem več teles. S sipanjem elektronov spoznavamo polarizacijo in vzbujanje, ki se da razložiti z "morjem" dodatnih parov kvark-antikvark. Le-te imajo značilno asimetrijo glede "okusa" kvarkov in jih smemo marsikdaj oponašati s pionskim oblakom. Vzbujanje resonanc v valu D z elektroni tudi kaže na prepletanje kvarkovskih in mezonskih prostostnih stopenj. Opis vseh teh fizikalnih količin je precej odvisen od izbire modela. Tu je torej prizorišče, kjer lahko sodelovanje med fiziki razčisti, kakšno je sodelovanje med delci.

V delu so še računi, koliko prispevajo dvokvarkovski tokovi k oblikovnim faktorjem pri šibkih prehodih težko-lahkih mezonov. Metoda razvoja po recipročnem številu barv je še priljubljena, zlasti za klasifikacijo visokih barionskih stanj in za sistematično konstrukcijo operatorjev, ki opisujejo fizikalne kolčine.

Relativistični model, v katerem oblečeni kvarki sodelujejo z izmenjavo Goldstonovih bozonov, je doživel razmah od lahkih do težkih in dvojno težkih barionov. Ker slednji še niso bili izmerjeni, je bila tu priložnost za kromodinamiko na mreži, da je "nadomestila" eksperiment. Tudi ujemanje z drugimi modeli je dobro, kar naj bi dodatno vzpodbudilo eksperimentalce, da bi kmalu merili cc-barione in cc-tetrakvarke.

Napredek pri kromodinamiki na mreži je res vzpodbuden: cilja na opis resonanc K^* , na študij stanj podobnih čarmoniju, ter na tolmačenje sipanja DD^* z resonanco $X(3872)$ v kanalu 1^{++} , $I = 0$. Kromodinamski fazni diagram vzbuja domišljijo, saj ga rabimo za tolmačenje trkov težkih ionov, kakor tudi sredice težkih kompaktnih zvezd. Važen mehanizem je pri tem ponovna vzpostavitev raznih simetrij.

Po tradiciji smo povabili tudi eksperimentalce, da postavijo trmaste teoretike na trdna tla. Eksperimenti z realnim in virtualnim comptonским sipanjem v laboratoriju MAMI in v Jeffersonovem laboratoriju podpirajo uspehe kvarkovih modelov; dodaten upogled nudijo posplošene (dinamične) polarizabilnosti protona. Novi rezultati pri spektroskopiji kvarkonijev in eksotičnih kvarkonijem podobnih resonanc v "tovarnah B mezonov" so določili kvantna števila pri resonanci $Z(4430)^+$ in izostrili podatke o $Y(4008)$ in $Y(4260)$ — zato da dražijo teoretike. Uganke pri razpadih $\Upsilon(5S)$ pa ostajajo. Novost pa so stanja Z_b in $\eta_b(2S)$.

Radi bi vzpodbudili bralce, naj razmislijo, kaj če bi (spet) prišli na Bled in nadaljevali razprave o teh zanimivih problemih.

Workshops organized at Bled

- ▷ *What Comes beyond the Standard Model*
(June 29–July 9, 1998), Vol. **0** (1999) No. 1
(July 22–31, 1999)
(July 17–31, 2000)
(July 17–27, 2001), Vol. **2** (2001) No. 2
(July 15–25, 2002), Vol. **3** (2002) No. 4
(July 17–27, 2003), Vol. **4** (2003) Nos. 2-3
(July 19–29, 2004), Vol. **5** (2004) No. 2
(July 18–28, 2005), Vol. **6** (2005) No. 2
(September 16–29, 2006), Vol. **7** (2006) No. 2
(July 18–28, 2007), Vol. **8** (2007) No. 2
(July 15–25, 2008), Vol. **9** (2008) No. 2
(July 14–24, 2009), Vol. **10** (2009) No. 2
(July 12–22, 2010), Vol. **11** (2010) No. 2
(July 11–21, 2011), Vol. **12** (2011) No. 2
(July 9–19, 2012), Vol. **13** (2012) No. 2
(July 15–25, 2013), Vol. **14** (2013) No. 2
- ▷ *Hadrons as Solitons* (July 6–17, 1999)
- ▷ *Few-Quark Problems* (July 8–15, 2000), Vol. **1** (2000) No. 1
- ▷ *Statistical Mechanics of Complex Systems* (August 27–September 2, 2000)
- ▷ *Selected Few-Body Problems in Hadronic and Atomic Physics* (July 7–14, 2001),
Vol. **2** (2001) No. 1
- ▷ *Studies of Elementary Steps of Radical Reactions in Atmospheric Chemistry*
- ▷ *Quarks and Hadrons* (July 6–13, 2002), Vol. **3** (2002) No. 3
- ▷ *Effective Quark-Quark Interaction* (July 7–14, 2003), Vol. **4** (2003) No. 1
- ▷ *Quark Dynamics* (July 12–19, 2004), Vol. **5** (2004) No. 1
- ▷ *Exciting Hadrons* (July 11–18, 2005), Vol. **6** (2005) No. 1
- ▷ *Progress in Quark Models* (July 10–17, 2006), Vol. **7** (2006) No. 1
- ▷ *Hadron Structure and Lattice QCD* (July 9–16, 2007), Vol. **8** (2007) No. 1
- ▷ *Few-Quark States and the Continuum* (September 15–22, 2008),
Vol. **9** (2008) No. 1
- ▷ *Problems in Multi-Quark States* (June 29–July 6, 2009), Vol. **10** (2009) No. 1
- ▷ *Dressing Hadrons* (July 4–11, 2010), Vol. **11** (2010) No. 1
- ▷ *Understanding hadronic spectra* (July 3–10, 2011), Vol. **12** (2011) No. 1
- ▷ *Hadronic Resonances* (July 1–8, 2012), Vol. **13** (2012) No. 1
- ▷ *Looking into Hadrons* (July 7–14, 2013), Vol. **14** (2013) No. 1

Also published in this series

- ▷ *Book of Abstracts, XVIII European Conference on Few-Body Problems in Physics*,
Bled, Slovenia, September 8–14, 2002, Edited by Rajmund Krivec, Bojan Golli,
Mitja Rosina, and Simon Širca, Vol. **3** (2002) No. 1–2





The role of valence and sea quarks in light baryons*

Roelof Bijker^a and Elena Santopinto^b

^a Instituto de Ciencias Nucleares, Universidad Nacional Autónoma de México,
A.P.70-543, 04510 México D.F., México

^b I.N.F.N., Sezione di Genova, via Dodecaneso 33, Genova, I-16146 Italy

Abstract. In this contribution, we discuss the spin and flavor content of the proton in two extensions of the quark model, the unquenched quark model and the chiral quark model, and address the role of valence and sea quarks in light baryons.

1 Introduction

The constituent quark model (CQM) describes the nucleon as a system of three constituent, or valence, quarks. Despite the successes of the CQM (e.g. masses, electromagnetic coupling, magnetic moments), there is compelling evidence for the presence of sea quarks from the measurement of the flavor asymmetry of the proton and the so-called proton spin crisis. The role of the pion cloud in the nucleon has been the subject of many studies [1–3], and was shown to hold the key to understand the flavor asymmetry and the spin-crisis of the proton. Recently, it was pointed out these two properties are closely related: angular momentum conservation of the pionic fluctuations of the nucleon leads to a relation between the flavor asymmetry and the contribution of orbital angular momentum to the spin of the proton $\mathcal{A}(p) = \Delta L$ [4]. This identity can be understood from the fact that the flavor asymmetry is a matrix element in isospin space, and the orbital angular momentum in spin space with the same values of the quantum numbers.

The aim of this contribution is to study two different extensions of the quark model, the unquenched quark model and the chiral quark model, at the level of toy models which may provide important insight into the properties of the nucleon.¹

2 Flavor and spin content

The first model is the unquenched quark model (UQM) in which the effect of the quark-antiquark pairs is taken into account via a 3P_0 creation mechanism. The

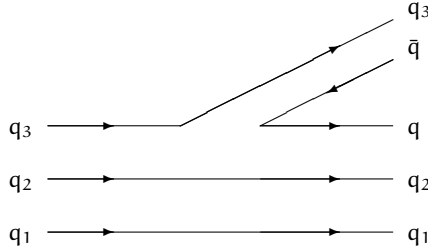
* Talk delivered by R. Bijker

¹ Aage Bohr once remarked that describing the properties of a many-body system like the atomic nucleus in terms of symmetry arguments provides important insight into the properties of the system. On the other hand, when one is able to describe the same system in terms of the detailed motion of the particles (nucleons), and of the couplings to the fields which act upon them (vibration, rotations) one obtains, as a rule, a true understanding of the system under consideration [5].

resulting wave function is given by [6]

$$|\psi_A\rangle = \mathcal{N} \left\{ |A\rangle + \gamma \sum_{BCI} \int d\mathbf{K} k^2 dk |BC, l, J; \mathbf{K}, k\rangle \frac{\langle BC, l, J; \mathbf{K}, k | T^\dagger | A\rangle}{M_A - E_B(k) - E_C(k)} \right\}, \quad (1)$$

where γ is the coupling strength of the 3P_0 whose value is determined from the flavor asymmetry of the proton. In the calculations presented in this section only the contribution from the pions is taken into account.



The second model is the chiral quark model (χ QM) [7, 8] in which the pion is emitted from the individual constituent (up and down) quarks

$$|\psi_{u_\pm}\rangle = \frac{1}{\sqrt{1+g^2}} \left[|u_\pm\rangle \pm \frac{1}{3} g \left(|u_\pm\pi^0\rangle - \sqrt{2}|d_\pm\pi^+\rangle \right)_{l,m=1,0} \mp \frac{\sqrt{2}}{3} g \left(|u_\mp\pi^0\rangle - \sqrt{2}|d_\mp\pi^+\rangle \right)_{l,m=1,\pm 1} \right], \quad (2)$$

and a similar expression for d quarks. Here l, m denote the relative orbital angular momentum between the quark and the pion. In the present version, both the helicity changing and conserving contributions are taken into account. The final quark wave function has the full spin and isospin structure [9].

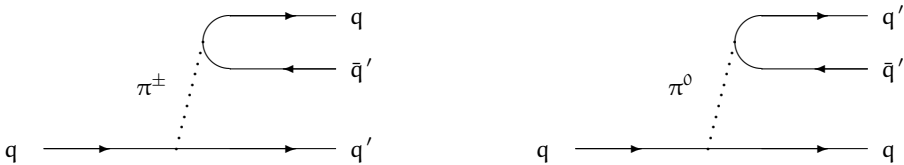


Table 1 shows the results for the flavor and spin content of the proton. The last column for UQM also holds for the meson-cloud model in which the coefficients a and b multiply the $N\pi$ and $\Delta\pi$ components of the nucleon wave function.

The ab term in Table 1 denotes the contribution from the cross terms between the $N\pi$ and $\Delta\pi$ components. In the UQM, the three coefficients a^2 , b^2 and ab all depend on the 3P_0 coupling strength γ , and are expressed in terms of an integral over the relative momentum k . In this case the value of the cross term ab is not the product of a and b , although the numerical value is close. It is interesting to note that in the absence of the contribution of the $\Delta\pi$ component in the UQM, *i.e.* $b^2 = ab = 0$, the two models give the same results for these observables. The same observation was made by Rosina in a comparison of pion couplings to the nucleon and to the quarks [10].

Table 1. Spin and flavor content of the proton in the constituent quark model (CQM), the chiral quark model (χ QM) and the unquenched quark model (UQM).

| | CQM | χ QM | UQM |
|---|----------------|---|--|
| $\mathcal{A}(p) = \Delta L$ | 0 | $\frac{2g^2}{3(1+g^2)}$ | $\frac{2a^2-b^2}{3(1+a^2+b^2)}$ |
| Δu | $\frac{4}{3}$ | $\frac{4}{3} - \frac{38g^2}{27(1+g^2)}$ | $\frac{4}{3} - \frac{38a^2+b^2-16ab\sqrt{2}}{27(1+a^2+b^2)}$ |
| Δd | $-\frac{1}{3}$ | $-\frac{1}{3} + \frac{2g^2}{27(1+g^2)}$ | $-\frac{1}{3} + \frac{2a^2+19b^2-16ab\sqrt{2}}{27(1+a^2+b^2)}$ |
| Δs | 0 | 0 | 0 |
| $\Delta\Sigma = \Delta u + \Delta d + \Delta s$ | 1 | $1 - \frac{4g^2}{3(1+g^2)}$ | $1 - \frac{4a^2-2b^2}{3(1+a^2+b^2)}$ |
| $g_A = \Delta u - \Delta d$ | $\frac{5}{3}$ | $\frac{5}{3} - \frac{40g^2}{27(1+g^2)}$ | $\frac{5}{3} - \frac{40a^2+20b^2-32ab\sqrt{2}}{27(1+a^2+b^2)}$ |

Since both models, UQM and χ QM, contain the full spin and isospin structure, both satisfy the relation between the flavor asymmetry and the contribution of the orbital angular momentum to the spin of the proton $\mathcal{A}(p) = \Delta L$ [4], and therefore $\Delta\Sigma = 1 - 2\Delta L$. This relation does not hold for the chiral quark model of [7, 8] in which the orbital angular momentum is enhanced with respect to the flavor asymmetry $\Delta L = 3\mathcal{A}(p)/2$ as a consequence of the requirement of a helicity flip of the quark.

Table 2 shows the results for the spin and flavor content of the proton normalized to the proton flavor asymmetry. The second and third column are normalized to the E866/NuSea value [11], and the last two to the somewhat higher NMC value [12].

The probability that a proton fluctuates in $n\pi^+$

$$|\langle n\pi^+ | p \rangle|^2 = \frac{2a^2}{3(1+a^2+b^2)} = 0.180, \quad (3)$$

(UQM1 value) is in close agreement with the experimental value 0.17 ± 0.01 determined in an analysis of forward neutron production in electron-proton collisions

at 300 GeV by the H1 and ZEUS Collaborations at DESY [13, 14]. The total probability for a pion fluctuation of the proton is given by

$$|\langle N\pi|p\rangle|^2 + |\langle \Delta\pi|p\rangle|^2 = \frac{a^2 + b^2}{1 + a^2 + b^2} = 0.455, \quad (4)$$

(UQM1 value), in good agreement with the value of 0.470 as determined in an analysis of the quark distribution functions measured in Drell-Yan experiments and semi-inclusive DIS experiments [15].

Finally, Table 3 shows the flavor asymmetry for octet baryons. In the χ QM the flavor asymmetries are given by $\mathcal{A}(\Sigma^+) = 2\mathcal{A}(p) = 2\mathcal{A}(\Xi^0)$ no matter whether one includes only pions or also kaons and eta mesons. In the UQCM, one has $\mathcal{A}(\Sigma^+) > \mathcal{A}(p) > \mathcal{A}(\Xi^0)$. In order to distinguish between the predictions of the different models (see also [6]) and to obtain a better understanding of the non-perturbative structure of QCD, new experiments are needed to measure the flavor asymmetry of hyperons. In particular, the flavor asymmetry of charged Σ hyperons can be obtained from Drell-Yan experiments using charged hyperon beams on the proton [16] or by means of backward K^\pm electroproduction [17].

3 Summary and conclusions

In this contribution, we studied the predictions of two extensions of the quark model, the unquenched quark model and the chiral quark model. In both cases,

Table 2. Spin and flavor content of the proton normalized to the flavor asymmetry, χ QM1 and UQM1 using the E866/NuSea value [11] and χ QM2 and UQM2 using the NMC value [12].

| | CQM | χ QM1 | UQM1 | χ QM2 | UQM2 |
|-----------------------------|------|------------|--------|------------|--------|
| $\mathcal{A}(p) = \Delta L$ | 0 | *0.118 | *0.118 | *0.158 | *0.158 |
| Δu | 4/3 | 1.084 | 1.132 | 1.000 | 1.064 |
| Δd | -1/3 | -0.320 | -0.368 | -0.316 | -0.380 |
| $\Delta\Sigma$ | 1 | 0.764 | 0.764 | 0.684 | 0.684 |
| g_A | 5/3 | 1.404 | 1.500 | 1.316 | 1.444 |

Table 3. Flavor asymmetry of octet baryons relative to that of the proton, $\mathcal{A}/\mathcal{A}(p)$.

| Baryon | χ QM | UQM1 | UQM2 |
|------------|-----------|------|------|
| Σ^+ | 2 | 1.45 | 1.62 |
| Ξ^0 | 1 | 0.64 | 0.81 |

only pion fluctuations were taken into account. The results were normalized to the observed value of the proton flavor asymmetry. It was shown that the pion fluctuations in both schemes lead to a reduction of quark model value of Δu and g_A , and give rise to a sizeable contribution (25 - 30 %) of orbital angular momentum to the spin of the proton. In addition, it was found that the probabilities for pion fluctuations in the UQM are in good agreement with the values determined in analyses of the available experimental data.

In another contribution to these proceedings, Rosina addresses many of the same questions, and suggests to use two-pion probabilities to distinguish between pion couplings to the nucleon versus couplings to quarks [10]. The two contributions give complementary information.

Acknowledgements

It is a pleasure to thank Mitja Rosina for stimulating discussions on the properties of the pion cloud and his kind invitation to participate in the 2013 Bled Workshop. This work was supported in part by research grants from CONACyT and PAPIIT-UNAM.

References

1. S. Kumano, Phys. Rep. **303**, 183 (1998).
2. J. Speth and A.W. Thomas, Adv. Nucl. Phys. **24**, 83 (1998).
3. G.T. Garvey and J.-C. Peng, Prog. Part. Nucl. Phys. **47**, 203 (2001).
4. G.T. Garvey, Phys. Rev. C **81**, 055212 (2010).
5. See Preface of *Fifty years of nuclear BCS* (Eds. Ricardo A. Broglia and Vladimir Zelevinsky), World Scientific, Singapore, 2013
6. R. Bijker and E. Santopinto, Phys. Rev. C **80**, 065210 (2009) [arXiv:0912.4494];
E. Santopinto and R. Bijker, Phys. Rev. C **82**, 062202(R) (2010);
R. Bijker, J. Ferretti and E. Santopinto, Phys. Rev. C **85**, 035204 (2012).
7. E.J. Eichten, I. Hinchcliffe and C. Quigg, Phys. Rev. D **45**, 2269 (1992).
8. T.P. Cheng and Ling-Fong Li, Phys. Rev. Lett. **74**, 2872 (1995).
9. Lang Yu, Xiao-Lin Chen, Wei-Zhen Deng and Shi-Lin Zhu, Phys. Rev. D **73**, 114001 (2006).
10. M. Rosina, these proceedings.
11. R.S. Towell *et al.*, Phys. Rev. D **64**, 052002 (2001).
12. M. Arneodo *et al.*, Nucl. Phys. B **487**, 3 (1997).
13. A. Bunyatyan and B. Povh, Eur. Phys. J. A **27**, 359 (2006).
14. B. Povh and M. Rosina, Bled Workshops in Physics **12**, 82 (2011).
15. Wen-Chen Chang and Jen-Chieh Peng, Phys. Rev. Lett. **106**, 252002 (2011).
16. M.A. Alberg, E.M. Henley, X.-D. Ji and A.W. Thomas, Phys. Lett. B **389**, 367 (1996);
M.A. Alberg, T. Falter and E.M. Henley, Nucl. Phys. A **644**, 93 (1998).
17. R. Osipenko, private communication.



Baryon spectra and nucleon form factors from relativistic quark models and AdS/QCD*

J. P. Day and W. Plessas

Theoretical Physics, Institute of Physics, University of Graz, A-8010 Graz, Austria

Abstract. We give an account of our studies of low-energy hadrons along non-perturbative approaches or effective models. In the first instance, we present a relativistic constituent-quark model that is able to provide a universal framework for the description of all baryons with flavors u , d , s , c , and b that are phenomenologically known hitherto. Its performance is shown with regard to baryon spectroscopy as well as the nucleon electromagnetic, axial, and gravitational form factors. Secondly, we discuss the possibilities offered by anti-de Sitter quantum chromodynamics formulated on the light front to describe the spectra of mesons and baryons as well as the structures of hadrons as seen with electromagnetic, weak, and gravitational probes.

Lacking a rigorous field-theoretical solution of quantum chromodynamics (QCD), there is interest in and need for alternative approaches, such as effective models or field-theoretical substitutes. The aim is to provide an ever widening and consistent framework for the description of the wealth of hadron phenomena and to reach a deeper understanding of essential properties of QCD, like confinement or the spontaneous breaking of chiral symmetry. Several competing approaches are available, which may be considered more or less profound and/or promising. In our recent studies we have investigated a relativistic constituent-quark model (RCQM) that should universally cover all baryons and we have attempted to adapt anti-de Sitter (AdS) QCD with soft-wall dynamics to the spectroscopy as well as form factors of mesons and baryons [1].

The construction of a universal RCQM for baryons has already been presented in ref. [2] together with its parametrization. There also first results regarding baryon spectroscopy have been given. Further properties have been discussed in refs. [3, 4]. Our universal RCQM for baryons of all flavors consists in a generalization of the Goldstone-boson-exchange (GBE) RCQM [5, 6], which has been quite successful in describing the sector of $SU(3)_F$ before (see, e.g., the compact review in ref. [7]). In this domain the new model performs with practically the same quality as the previous one with regard to nucleon, Δ , and hyperon spectroscopy as well as the nucleon electroweak form factors. At the same time it reproduces

* Talk delivered by J. P. Day

the spectroscopy known so far for baryons containing c - and b -flavored quarks. It means that not only the light-light quark dynamics but also the light-heavy as well as the heavy-heavy quark interactions at low energies can be successfully described by Goldstone-boson exchange. Among the observables considered so far we have not found any place disqualifying the assumed GBE dynamics. Furthermore, in cases, where lattice-QCD results are available, the predictions of the universal GBE RCQM are in reasonable agreement with them.

Recent investigations of AdS/QCD [8] and light-front quantization of QCD [9] have opened another way to a non-perturbative treatment of hadron phenomena. So far we have studied the spectroscopy of pseudoscalar and vector mesons as well as the excitation spectra of the nucleons and the Δ 's. The results are found to be in good agreement with Regge trajectories. The extracted light-front wave functions were also applied to calculate pion and nucleon form factors. For the nucleons we have considered electromagnetic, axial, and gravitational form factors. The results turn out to agree favorably with phenomenology. Whenever experimental data are missing, they compare well with results from other approaches such as lattice QCD or the RCQM. All these details will be given in a forthcoming article [10].

Acknowledgment

This work was supported by the Austrian Science Fund, FWF, through the Doctoral Program on *Hadrons in Vacuum, Nuclei, and Stars* (FWF DK W1203-N16).

References

1. Joseph P. Day, PhD Thesis, Univ. of Graz (2013)
2. J. P. Day, W. Plessas, and K.-S. Choi, arXiv:1205.6918 [hep-ph]
3. J. P. Day, K.-S. Choi, and W. Plessas, PoS QNP **2012**, 078 (2012)
4. J. P. Day, K.-S. Choi, and W. Plessas, Few-Body Syst. **54**, 329 (2013)
5. L. Y. Glozman, W. Plessas, K. Varga, and R. F. Wagenbrunn, Phys. Rev. D **58**, 094030 (1998)
6. L. Y. Glozman, Z. Papp, W. Plessas, K. Varga, and R. F. Wagenbrunn, Phys. Rev. C **57**, 3406 (1998).
7. W. Plessas, PoS(LC2010) 017 (2010)
8. S. J. Brodsky, G. F. de Téramond, and H. G. Dosch, arXiv:1302.5399 [hep-ph]
9. S. J. Brodsky, H.-C. Pauli, and S. S. Pinsky, Phys. Rept. **301**, 299 (1998)
10. J. P. Day and W. Plessas, to be published



Hybrid mesons spectroscopy

Giuseppe Galatà

Instituto de Ciencias Nucleares, Universidad Nacional Autonoma de Mexico, Apdo.
Postal 70-543 04510 Mexico, DF, Mexico

Abstract. The hybrids are mesons with constituent gluonic components. The most commonly studied hybrids are composed of a quark, an antiquark and a gluon. These mesons are studied in a variational approach to QCD in the Coulomb gauge. Within the variational approach, a confining linear potential has been shown to emerge from the Dyson-Schwinger equations, at least at the hadronic scale. This potential has been used to first calculate the spectrum of the gluelump, which is an idealized system defined as gluonic excitations bounded to a static, localized color octet source (for example a very heavy quark and antiquark). The next step has been to introduce the quark-antiquark dynamics to calculate the spectrum of heavy hybrid mesons. Our results are in good agreement with the lattice data.

The hybrids are mesons with constituent gluonic components. The most commonly studied hybrids are composed of a quark, an antiquark and a gluon. These mesons are studied in a variational approach to QCD in the Coulomb gauge. This particular gauge has been chosen for its advantages, in particular in the Coulomb gauge the degrees of freedom are physical. This makes the QCD Hamiltonian close in spirit to quantum mechanical models of QCD, for example the constituent quark model, and particularly adapt to calculate the spectrum of particles. In our variational approach we used a variational gaussian vacuum on which the quasiparticle states were built. This variational approach to Coulomb gauge QCD has been developed as a method to introduce effective degrees of freedom (constituent gluons and quarks) in such a way that the connection to QCD is not destroyed. The vacuum expectation value (VEV) of the Coulomb gauge Hamiltonian was calculated and the variational principle applied, resulting in a set of four coupled Dyson-Schwinger equations.

$$\frac{1}{d(\mathbf{k})} = \frac{1}{g} - I_d(\mathbf{k}), \quad f(\mathbf{k}) = 1 + I_f(\mathbf{k}),$$
$$\chi(\mathbf{k}) = I_\chi(\mathbf{k}), \quad \omega_{\mathbf{k}}^2 = \mathbf{k}^2 + \chi(\mathbf{k})^2 + I_\omega(\mathbf{k}) + I_\omega^0,$$

where $d(\mathbf{k})$ is called the ghost form factor, $f(\mathbf{k})$ is called Coulomb form factor, $\chi(\mathbf{k})$ curvature, $\omega_{\mathbf{k}}$ is the gap function and the integral functions I are

$$\begin{aligned} I_d(\mathbf{k}) &= \frac{N_C}{2} \int \frac{d^3 \mathbf{q}}{(2\pi)^3} (1 - (\hat{\mathbf{k}}\hat{\mathbf{q}})^2) \frac{d(\mathbf{k} - \mathbf{q})}{(\mathbf{k} - \mathbf{q})^2 \omega(\mathbf{q})}, \\ I_f(\mathbf{k}) &= \frac{N_C}{2} \int \frac{d^3 \mathbf{q}}{(2\pi)^3} (1 - (\hat{\mathbf{k}}\hat{\mathbf{q}})^2) \frac{d(\mathbf{k} - \mathbf{q}) f(\mathbf{k} - \mathbf{q})}{(\mathbf{k} - \mathbf{q})^2 \omega(\mathbf{q})}, \\ I_\chi(\mathbf{k}) &= \frac{N_C}{4} \int \frac{d^3 \mathbf{q}}{(2\pi)^3} (1 - (\hat{\mathbf{k}}\hat{\mathbf{q}})^2) \frac{d(\mathbf{k} - \mathbf{q}) f(\mathbf{q})}{(\mathbf{k} - \mathbf{q})^2}, \\ I_\omega^0 &= \frac{N_C}{4} g^2 \int \frac{d^3 \mathbf{q}}{(2\pi)^3} \frac{3 - (\hat{\mathbf{k}}\hat{\mathbf{q}})^2}{\omega(\mathbf{q})}, \\ I_\omega(\mathbf{k}) &= \frac{N_C}{4} \int \frac{d^3 \mathbf{q}}{(2\pi)^3} [1 + (\hat{\mathbf{k}}\hat{\mathbf{q}})^2] \frac{d(\mathbf{k} - \mathbf{q})^2 f(\mathbf{k} - \mathbf{q})}{(\mathbf{k} - \mathbf{q})^2} \frac{\omega_{\mathbf{k}}^2 - [\omega(\mathbf{q}) - \chi(\mathbf{q}) + \chi(\mathbf{k})]^2}{\omega_{\mathbf{k}}}. \end{aligned}$$

Unfortunately the VEVs cannot be calculated exactly, mainly due to the difficulty to deal with the Faddeev-Popov operator ($\nabla_i D_i$), and theoretical approximations, such as the rainbow ladder approximation, had to be adopted. This makes the model an effective one but with still strong connection to QCD. Within the variational approach and with the approximations used, a confining linear potential has been shown to emerge from the Dyson-Schwinger equations, at least at the hadronic scale.

$$V_{CL}(\mathbf{k}) = V_C(\mathbf{k}) + V_L(\mathbf{k}),$$

where

$$V_C(\mathbf{k}) = -\frac{4\pi\alpha(\mathbf{k})}{k^2}, \quad \alpha(\mathbf{k}) = \frac{4\pi Z}{\beta^{\frac{3}{2}} \log^{\frac{3}{2}} \left(\frac{k^2}{\Lambda_{\text{QCD}}^2} + c \right)}, \quad V_L(\mathbf{k}) = -\frac{8\pi k}{k^4}.$$

This potential has been used to first calculate the spectrum of the gluelump [1], which is an idealized system defined as gluonic excitations bounded to a static, localized color octet source (for example a very heavy quark and antiquark). The gluelump states could be classified according to the J^{PC} quantum numbers and we found that the ordering of the various spin-parity states matches those found in lattice computations. The absolute energy scale of these levels is set by the variational parameter. We were able to reproduce the lattice data and in particular the inversion of the gluelump unnatural parity state 1^{+-} below the natural parity state 1^{--} [1], which is typical of the lattice results. The next step has been to introduce the quark-antiquark dynamics to calculate the spectrum of heavy hybrid mesons [2]. The relation between heavy hybrids and gluelumps is very close: low hybrids are expected to be approximately classified by the product of gluelump and $\bar{Q}Q$ quantum numbers. The final and more important result is the good agreement found between our results and the lattice ones. Again we reproduced in particular the inversion of the 1^{--} , 0^{++} , 1^{+-} , 2^{++} hybrids (which correspond to the 1^{+-} gluelump) below the 1^{+-} , 0^{++} , 1^{++} , 2^{++} hybrids (which correspond to the 1^{--} gluelump) and we were able to explain the physical reasons of this inversion [2].

References

1. Peng Guo, Adam Szczepaniak, Giuseppe Galatà, Andrea Vassallo and Elena Santopinto, *Phys.Rev. D* **77** (2008) 056005.
2. Peng Guo, Adam Szczepaniak, Giuseppe Galatà, Andrea Vassallo and Elena Santopinto, *Phys.Rev. D* **78** (2008) 056003.



Hot and dense QCD medium and restoration of $U_A(1)$ symmetry*

Dubravko Klabučar^a, Sanjin Benić^a, Davor Horvatić^a and Dalibor Kekez^b

^a Physics Department, Faculty of Science, Zagreb University, Bijenička c. 32, Zagreb 10000, Croatia

^b Rudjer Bošković Institute, Bijenička c. 54, 10000 Zagreb, Croatia

Abstract. Recent RHIC results on η' multiplicity in heavy-ion collisions are of great importance because they clearly signal a partial restoration of $U_A(1)$ symmetry at high temperatures, and thus provide an unambiguous signature of the formation of a new state of matter. To explain these experimental results of STAR and PHENIX collaborations, a minimal generalization of the Witten-Veneziano relation to finite temperatures was proposed. The present paper provides a detailed, pedagogical discussion and explanation thereof. After explaining why these results show that the zero-temperature Witten-Veneziano relation cannot be straightforwardly extended to temperatures T too close to the chiral restoration temperature T_{Ch} and beyond, we find the quantity which should replace, at $T > 0$, the Yang-Mills topological susceptibility appearing in the $T = 0$ Witten-Veneziano relation, in order to avoid the conflict with experiment at $T > 0$. This is illustrated through concrete T -dependences of pseudoscalar meson masses in a chirally well-behaved, Dyson-Schwinger approach, but our results and conclusions are of a more general nature and, essentially, model-independent.

1 Introduction and survey

QCD excitations of our “ordinary”, low-energy world are hadrons, namely baryons and mesons, wherein the fundamental QCD degrees of freedom – quarks and gluons – are confined. At low energies, meaning of the order of the typical hadronic scale ~ 1 GeV and below, QCD is strongly nonperturbative [1]. The confinement of quarks and gluons is not the only important nonperturbative phenomenon of QCD. Another one is the spontaneous, dynamical symmetry breaking of the axial subgroup $SU_A(N_f)$ of the chiral symmetry, where $N_f = 3$ is the number of the light quark flavors $f = u, d, s$. The most conspicuous manifestation of this breaking is the small mass of the octet of the light pseudoscalar mesons: pions (π^0, π^\pm), kaons (K^0, \bar{K}^0, K^\pm) and the η -meson. The smallness of their masses in comparison of the typical hadronic mass scales (such as the vector meson masses, and the nucleon mass $m_N \sim 1$ GeV) illustrates that the chiral symmetry is a reasonable, although rough, approximate symmetry of the physics of light hadrons. In the chiral limit, i.e., in the limit of strictly vanishing Lagrangian quark masses

* Talk delivered by D. Klabučar

(which in reality slightly violate explicitly the chiral symmetry for light quark flavors $q = u, d, s$), these light pseudoscalar mesons would be strictly massless Goldstone bosons of the dynamical chiral symmetry breaking (DChSB).

Nevertheless, the above leaves unexplained why the η' -meson is not the ninth light pseudoscalar meson, i.e., the ninth almost-Goldstone boson of DChSB of the axial $U_A(1)$ symmetry of the QCD Lagrangian. Instead, the η' -meson is somewhat more massive than nucleons due to the breaking of the classical $U_A(1)$ symmetry of QCD by the quantum effects known as the (gluon, or non-Abelian) axial anomaly of QCD. This completes our understanding of the pseudoscalar meson nonet composed of light quarks, which is one of characteristic emergent manifestations [1] of low-energy QCD.

However, this low-energy QCD phase changes if hadrons get sufficiently hot or dense. Because of the asymptotic freedom of QCD at high energies, it is expected that sufficiently high temperatures (T), as well as densities, bring about not only deconfinement of quarks and gluons but also the [flavor $SU_A(3)$] chiral symmetry and the $U_A(1)$ symmetry. Such circumstances were in the early universe, and maybe also in the compact stars. Also, heavy ion collisions in terrestrial laboratories, at RHIC and LHC, seem to find “melting” of hadrons under such extreme conditions into a new phase of matter – the quark-gluon plasma (QGP). It is however still nonperturbative and strongly interacting, and thus designated sQGP. The ongoing experiments at RHIC and LHC, and the future experiments at FAIR and NICA, will explore in detail the properties of the QGP phase in wide intervals of temperatures and densities, especially where the critical point of the QCD phase diagram is expected.

One should stress that the studies of the QGP phase are intricate and difficult, and that clear, compelling signals for the creation of this new form of matter are very much needed. Such an unambiguous, “smoking gun” signal would be the change of a symmetry obeyed by the strong interaction, such as the restoration of the [$SU_A(3)$ flavor] chiral symmetry, or the $U_A(1)$ symmetry.

The nonperturbativity of the low-energy QCD limits theoretical calculations to those on lattice and in effective models. Among the latter, those within the Schwinger-Dyson (SD) approach to the physics of quarks and gluons are especially prominent, since they have a strong basis in QCD. An example of a strong connection with the fundamental theory is that SD approach has the correct chiral behavior of QCD and also reproduces the pseudoscalar meson quark-antiquark ($q\bar{q}$) bound states as the (almost-)Goldstone bosons of DChSB, as in QCD. The SD approach is able to achieve this even with the usage of simplified model interactions, such as the one in the Nambu-Jona Lasinio (NJL) model and its nonlocal generalizations, suitable for model studies of the QCD medium at high temperatures and densities. Using DS approach, we achieved successful description of pseudoscalar mesons at $T = 0$ using various models for nonperturbative QCD interactions (*e.g.*, see [2, 3] and refs. therein), notably including also the isoscalar complex of η - η' mesons [4–8]. The extension of the description of the whole meson nonet (*i.e.*, including η and η') to $T > 0$ was also successfully achieved [9, 10] using the class of models employing the separable approximation to gluon-exchange interactions. However, we noticed that the behavior of

the complex of η - η' mesons at high T depends crucially on the interrelation between the dynamically broken chiral symmetry and the $U_A(1)$ symmetry and their restoration.

The plan of this paper is as follows: the pertinent experimental situation is reviewed in the next section, Sec. 2. Then, Sec. 3 introduces two peculiar relations between quantities of two different theories, namely the full QCD and the pure-gauge, Yang-Mills (YM) theory. Thanks to these relations, Sec. 4 presents how recent RHIC results on increased η' multiplicity can be theoretically explained [11, 12] if the restoration of $U_A(1)$ symmetry is directly linked with the chiral symmetry restoration. The concrete mechanism proposed to accomplish this, amounts to expressing the Yang-Mills topological susceptibility through quark condensate. We conclude in Sec. 5.

2 Experimental status of $U_A(1)$ symmetry

The ultrarelativistic heavy-ion collider facilities like RHIC at BNL and LHC at CERN strive to produce a new form of hot QCD matter. The experiments show [13, 14] that it has very intricate properties and presents a big challenge especially for theoretical understanding. While above the (pseudo)critical temperature $T_c \sim 170$ MeV this matter is often called the quark-gluon plasma (QGP), it cannot be a perturbatively interacting quark-gluon gas (as widely expected before RHIC results [13,14]) until significantly higher temperatures $T \gg T_c$. Instead, the interactions and correlations in the hot QCD matter are still strong (e.g., see Refs. [15, 16]) so that its more recent and more precise name is *strongly coupled QGP* (sQGP) [16]. One of its peculiarities seems to be that strong correlations in the form of $q\bar{q}$ bound states and resonances still exist [15, 17] in the sQGP well above T_c . In the old QGP paradigm, even deeply bound charmonium ($c\bar{c}$) states such as J/Ψ and η_c were expected to unbind at $T \approx T_c$, but lattice QCD simulations of mesonic correlators now indicate they persist till around $2T_c$ [18, 19] or even above [20]. Similar indications for light-quark mesonic bound states are also accumulating from lattice QCD [21] and from other methods [15, 22, 23]. This agrees well with the findings on the lattice (e.g., see Ref. [24] for a review) that for realistic explicit chiral symmetry breaking (ChSB), i.e., for the physical values of the current quark masses, the transition between the hadron phase and the phase dominated by quarks and gluons, is not an abrupt, singular phase transition but a smooth, analytic crossover around the *pseudocritical* temperature T_c . It is thus not too surprising that a clear experimental signal of, e.g., deconfinement, is still hard to find and identify unambiguously.

The most compelling signal for production of a new form of QCD matter, i.e., sQGP, would be a restoration - in hot and/or dense matter - of the symmetries of the QCD Lagrangian which are broken in the vacuum. One of them is the $[SU_A(N_f)$ flavor] chiral symmetry, whose dynamical breaking results in light, (almost-)Goldstone pseudoscalar (P) mesons - namely the octet $P = \pi^0, \pi^\pm, K^0, \bar{K}^0, K^\pm, \eta$, as we consider all three light-quark flavors, $N_f = 3$. The second one is the $U_A(1)$ symmetry. Its breaking by the non-Abelian axial Adler-Bell-Jackiw anomaly ('gluon anomaly' for short) makes the remaining pseudoscalar meson

of the light-quark sector, the η' , much heavier, preventing its appearance as the ninth (almost-)Goldstone boson of dynamical chiral symmetry breaking (DChSB) in QCD.

The first experimental signature of a partial restoration of the $U_A(1)$ symmetry seems to have been found in the $\sqrt{s_{NN}} = 200$ GeV central Au+Au reactions at RHIC. Namely, Csörgő *et al.* [25,26] analyzed combined data of PHENIX [27] and STAR [28] collaborations very robustly, through six popular models for hadron multiplicities, and found that at 99.9% confidence level, the η' mass, which in the vacuum is $M_{\eta'} = 957.8$ MeV, is reduced by at least 200 MeV inside the fireball. It is the sign of the disappearing contribution of the gluon axial anomaly to the η' mass, which would drop to a value readily understood together with the (flavor-symmetry-broken) octet of $q\bar{q}'$ ($q, q' = u, d, s$) pseudoscalar mesons. This is the issue of the “return of the prodigal Goldstone boson” predicted [29] as a signal of the $U_A(1)$ symmetry restoration.

Another related but less obvious issue to which we want to draw attention, concerns the status, at $T > 0$, of the famous Witten-Veneziano relation (WVR) [30,31]

$$M_{\eta'}^2 + M_{\eta}^2 - 2M_K^2 = \frac{2N_f \chi_{YM}}{f_{\pi}^2} \quad (1)$$

between the η' , η and K-meson masses $M_{\eta',\eta,K}$, pion decay constant f_{π} , Yang-Mills (YM) topological susceptibility χ_{YM} , and the number of the light quark flavors $N_f = 3$. WVR was obtained in the limit of large number of colors N_c [30,31]. It is well satisfied at $T = 0$ for χ_{YM} obtained by lattice calculations (e.g., [32–35]). Nevertheless, the T -dependence of χ_{YM} is such [9] that the straightforward extension of Eq. (1) to $T > 0$ [9], i.e., replacement of all quantities¹ therein by their respective T -dependent versions $M_{\eta'}(T)$, $M_{\eta}(T)$, $M_K(T)$, $f_{\pi}(T)$ and $\chi_{YM}(T)$, leads to a conflict with experiment [25,26]. Since this extension of Eq. (1) to $T > 0$ was studied in Ref. [9] before the pertinent experimental analysis [25,26], one of the purposes of this paper is to revisit the implications of the results of Ref. [9] for WVR at $T > 0$, and demonstrate explicitly that they are practically model-independent. The other, more important purpose is to propose a mechanism which can enable WVR to agree with experiment at $T > 0$.

3 Relations connecting two theories, QCD and YM

Both issues pointed out before Eq. (1) and around it, are best understood in a model-independent way if one starts from the chiral limit of vanishing current quark masses ($m_q = 0$) for all three light flavors, $q = u, d, s$. Then not only pions and kaons are massless, but is also η , which is then (since the situation is also SU(3)-flavor-symmetric) a purely SU(3)-octet state, $\eta = \eta_8$. In contrast, η' is then purely singlet, $\eta' = \eta_0$; since the divergence of the singlet axial quark current $\bar{q}\gamma^{\mu}\gamma_5\frac{1}{2}\lambda^0q$ is nonvanishing even for $m_q = 0$ due to the gluon anomaly,

¹ Throughout this paper, all quantities are for definiteness assumed at $T = 0$ unless their T -dependence is specifically indicated in formulas or in the text.

the η' mass squared receives the anomalous contribution $\Delta M_{\eta'}^2$, ($= \lambda^4/f_{\eta'}^2$, in the notation of Ref. [29]) which is nonvanishing even in the chiral limit:

$$\frac{\lambda^4}{f_{\eta'}^2} = \Delta M_{\eta_0}^2 = \Delta M_{\eta'}^2 = \frac{6\chi_{\text{YM}}}{f_{\pi}^2} + \mathcal{O}\left(\frac{1}{N_c}\right). \quad (2)$$

However, λ^4 and $f_{\eta'}$ are known accurately² only in the large N_c limit. There, in the leading order in $1/N_c$, λ^4 is given by the YM (i.e., “pure glue”) topological susceptibility χ_{YM} times $2N_f = 6$ [30, 31], and the “ η' decay constant” $f_{\eta'}$ is the same as f_{π} [37]. Thus, keeping only the leading order in $1/N_c$, the last equality is WVR in the chiral limit.

The consequences of Eq. (2) remain qualitatively the same realistically away from the chiral limit. This will soon become clear on the basis of, e.g., Eq. (3) below. Namely, due to DChSB in QCD, for relatively light current quark masses m_q ($q = u, d, s$), the $q\bar{q}'$ bound-state pseudoscalar meson masses (including the *nonanomalous* parts of the η' and η masses) behave as

$$M_{q\bar{q}'}^2 = \text{const} (m_q + m_{q'}), \quad (q, q' = u, d, s). \quad (3)$$

The pseudoscalar mesons (including η') thus obtain relatively light nonanomalous contributions $M_{q\bar{q}'}$ to their masses M_p , allowing them to reach the empirical values. That is, instead of the eight strictly massless Goldstone bosons, $\pi^0, \pi^{\pm}, K^0, \bar{K}^0, K^{\pm}$ and η are relatively light almost-Goldstones. Among them, in the limit of isospin symmetry ($m_u = m_d$), only η now receives also the gluon-anomaly contribution since the explicit SU(3) flavor breaking between the nonstrange (NS) u, d -quarks and s -quarks causes the mixing between the isoscalars η and η' . For $m_q \neq 0$, Eq. (2) is replaced by the usual WVR (1) containing also the nonanomalous contributions to meson masses. Nevertheless, these contributions largely cancel due to the approximate SU(3) flavor symmetry and to DChSB [i.e., Eq. (3)].

This can be seen assuming the usual SU(3) $q\bar{q}$ content of the pseudoscalar meson nonet with well-defined isospin³ quantum numbers, in particular the isoscalar ($I = 0$) octet and singlet etas,

$$\eta_8 = \frac{1}{\sqrt{6}} (u\bar{u} + d\bar{d} - 2s\bar{s}), \quad \eta_0 = \frac{1}{\sqrt{3}} (u\bar{u} + d\bar{d} + s\bar{s}), \quad (4)$$

whose mixing yields the physical particles η and η' . Since the *nonanomalous* parts of the η_0 and η_8 masses squared, $M_{\eta_0}^2$ and $M_{\eta_8}^2$, are respectively $M_{00}^2 \approx \frac{2}{3}M_K^2 + \frac{1}{3}M_{\pi}^2$ and $M_{88}^2 \approx \frac{4}{3}M_K^2 - \frac{1}{3}M_{\pi}^2$ (see, e.g., Ref. [7]), and since $M_{\eta_8}^2 + M_{\eta_0}^2 = M_{\eta}^2 + M_{\eta'}^2$, the nonanomalous parts of the η and η' masses are canceled by $2M_K^2$ in WVR (1). Another way of seeing this is expressing the nonanomalous parts of $M_{\eta}^2 + M_{\eta'}^2 = M_{\eta_8}^2 + M_{\eta_0}^2$ by Eq. (3). Thus again $M_{\eta}^2 + M_{\eta'}^2 - 2M_K^2 \approx \Delta M_{\eta_0}^2$,

² Also note that a unique “ η' decay constant” $f_{\eta'}$ is, strictly speaking, not a well-defined quantity, as *two* η' decay constants are actually needed: the singlet one, $f_{\eta'}^0$, and the octet one, $f_{\eta'}^8$; e.g., see an extensive review [36] or the short Appendix of Ref. [5].

³ The effects of the small difference between m_u and m_d are not important for the present considerations. We thus stick to the isospin limit throughout the present paper.

showing again that already WVR's chiral-limit-nonvanishing part (2) reveals the essence of the influence of the gluon anomaly on the masses in the η' - η complex. This is important also for the presently pertinent finite-T context because thanks to this, below it will be shown model-independently that WVR (1) containing the YM topological susceptibility χ_{YM} implies T-dependence of η' mass in conflict with the recent experimental results [25,26].

Namely, the anomaly contribution (2) is established at $T = 0$ but it is not expected to persist at high temperatures. Ultimately, η' should also become a massless Goldstone boson at sufficiently high T, where $\chi_{\text{YM}}(T) \rightarrow 0$. However, according to WVR, $\Delta M_{\eta'}(T)$ falls only for T where $f_{\pi}(T)^2$ does not fall faster than $6\chi_{\text{YM}}(T)$, as stressed in Ref. [9].

The WVR's chiral-limit version (2) manifestly points out the ratio

$$\chi_{\text{YM}}(T)/f_{\pi}(T)^2$$

as crucial for the anomalous η' mass, but the above discussion shows that this remains essentially the same away from the chiral limit.

In the present context, it is important for practical calculations to go realistically away from the chiral limit, in which the chiral restoration is a sharp phase transition at its critical temperature T_{Ch} where the chiral-limit pion decay constant vanishes very steeply, i.e., as steeply as the chiral quark condensate. In contrast, for realistic explicit ChSB, i.e., m_u and m_d of several MeV, this transition is a *smooth crossover* (e.g., see Ref. [24]). For the pion decay constant, this implies that $f_{\pi}(T)$ still falls relatively steeply around *pseudocritical* temperature T_{Ch} , but less so than in the chiral case, and even remains finite, enabling the usage of WVR (1) for the temperatures across the chiral and $U_A(1)$ symmetry restorations.

WVR is very remarkable because it connects two different theories: QCD with quarks and its pure-gauge, YM counterpart. The latter, however, has much higher characteristic temperatures than QCD with quarks: the "melting temperature" T_{YM} where $\chi_{\text{YM}}(T)$ starts to decrease appreciably was found on lattice to be, for example, $T_{\text{YM}} \approx 260$ MeV [38,39] or even higher, $T_{\text{YM}} \approx 300$ MeV [40]. In contrast, the pseudocritical temperatures for the chiral and deconfinement transitions in the full QCD are lower than T_{YM} by some 100 MeV or more (e.g., see Ref. [24]) due to the presence of the quark degrees of freedom.

This difference in characteristic temperatures, in conjunction with $\chi_{\text{YM}}(T)$ in WVRs (1) and (2) would imply that the (partial) restoration of the $U_A(1)$ symmetry (understood as the disappearance of the anomalous η_0/η' mass) should happen well after the restoration of the chiral symmetry. But, this contradicts the RHIC experimental observations of the reduced η' mass [25,26] *if* WVRs (1), (2) hold unchanged also close to the QCD chiral restoration temperature T_{Ch} , around which $f_{\pi}(T)$ decreases still relatively steeply⁴ [9] for realistic explicit ChSB, thus leading to the increase of $6\chi_{\text{YM}}(T)/f_{\pi}(T)^2$ and consequently also of $M_{\eta'}$.

There is still more to the relatively high resistance of $\chi_{\text{YM}}(T)$ to temperature: not only does it start falling at rather high T_{YM} , but $\chi_{\text{YM}}(T)$ found on the lattice

⁴ Relative to decay constants of mesons containing a strange quark; e.g., compare $f_{ss}(T)$ of the unphysical $s\bar{s}$ pseudoscalar with $f_{\pi}(T)$ in Fig. 1.

is falling with T *relatively* slowly. In some of the applications in the past (e.g., see Refs. [41,42]), it was customary to simply rescale a temperature characterizing the pure-gauge, YM sector to a value characterizing QCD with quarks. (For example, Refs. [41, 42] rescaled $T_{YM} = 260$ MeV found by Ref. [38] to 150 MeV). However, even if we rescale the critical temperature for melting of the topological susceptibility $\chi_{YM}(T)$ from T_{YM} down to T_{Ch} , the value of $6\chi_{YM}(T)/f_\pi(T)^2$ still increases a lot [9] for the pertinent temperature interval starting already below T_{Ch} . This happens because $\chi_{YM}(T)$ falls with T more slowly than $f_\pi(T)^2$. (It was found [9] that the rescaling of T_{YM} would have to be totally unrealistic, to less than 70% of T_{Ch} , in order to achieve sufficiently fast drop of the anomalous contribution that would allow the observed enhancement in the η' multiplicity.)

These WVR-induced enhancements of the η' mass for $T \sim T_{Ch}$ were first noticed in Ref. [9]. This reference used a concrete dynamical model (with an effective, rank-2 separable interaction, convenient for computations at $T \geq 0$) [43] of low energy, nonperturbative QCD to obtain mesons as $q\bar{q}'$ bound states in SD approach [44–46], which is a bound-state approach with the correct chiral behavior (3) of QCD. Nevertheless, this concrete dynamical SD model was used in Ref. [9] to get concrete values for only the nonanomalous parts of the meson masses, but was essentially *not* used to get model predictions for the mass contributions from the gluon anomaly, in particular $\chi_{YM}(T)$. On the contrary, the anomalous mass contribution was included, in the spirit of $1/N_c$ expansion, through WVR (1). Thus, the T -evolution of the η' - η complex in Ref. [9] was not dominated by dynamical model details, but by WVR, i.e., the ratio $6\chi_{YM}(T)/f_\pi(T)^2$. Admittedly, $f_\pi(T)$ was also calculated within this model, causing some *quantitative* model dependence of the anomalous mass in WVR, but this cannot change the qualitative observations of Ref. [9] on the η' mass enhancement. Namely, our model $f_\pi(T)$, depicted as the dash-dotted curve in Fig. 1, obviously has the right crossover features [24]. It also agrees qualitatively with $f_\pi(T)$'s calculated in other realistic dynamical models [22, 45]. Various modifications were tried in Ref. [9] but could not reduce much the η' mass enhancement caused by this ratio, let alone bring about the significant η' mass reduction found in the RHIC experiments [25, 26].

One must therefore conclude that either WVR breaks down as soon as T approaches T_{Ch} , or that the T -dependence of its anomalous contribution is different from the pure-gauge $\chi_{YM}(T)$. We will show that the latter alternative is possible, since WVR can be reconciled with experiment thanks to the existence of another relation which, similarly to WVR, connects the YM theory with full QCD. Namely, using large- N_c arguments, Leutwyler and Smilga derived [37], at $T = 0$,

$$\chi_{YM} = \frac{\chi}{1 + \chi \frac{N_f}{m \langle \bar{q}q \rangle_0}} \quad (\equiv \tilde{\chi}) , \quad (5)$$

the relation (in our notation) between the YM topological susceptibility χ_{YM} , and the full-QCD topological susceptibility χ , the *chiral-limit* quark condensate $\langle \bar{q}q \rangle_0$, and m , the harmonic average of N_f current quark masses m_q . That is, m is N_f times the reduced mass. In the present case of $N_f = 3$, $q = u, d, s$, so that

$$\frac{N_f}{m} = \sum_{q=u,d,s} \frac{1}{m_q} . \quad (6)$$

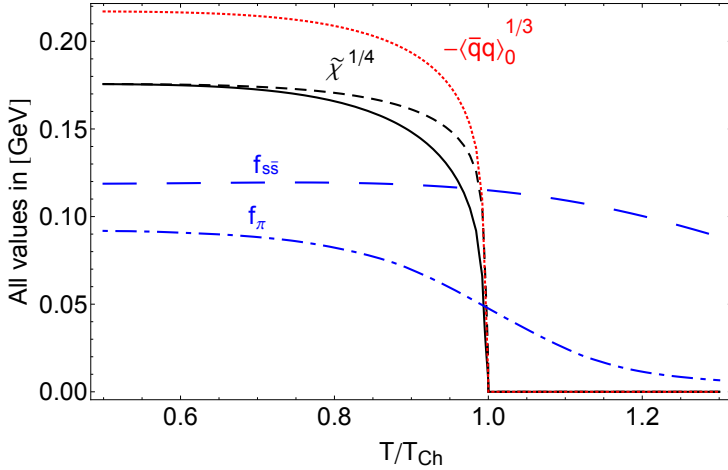


Fig. 1. The relative-temperature dependences, on T/T_{Ch} , of $\tilde{\chi}^{1/4}$, $\langle \bar{q}q \rangle_0^{1/3}$, f_π and $f_{s\bar{s}}$, i.e., the T/T_{Ch} -dependences of the quantities entering in the anomalous contributions to various masses in the $\eta' - \eta$ complex – see Eq. (10) and formulas below it. The solid curve depicts $\tilde{\chi}^{1/4}$ for $\delta = 0$ in Eq. (10), and the short-dashed curve is $\tilde{\chi}^{1/4}$ for $\delta = 1$. At $T = 0$, the both $\tilde{\chi}$'s are equal to $\chi_{\text{YM}} = (0.1757 \text{ GeV})^4$, the weighted average [9] of various lattice results for χ_{YM} . The dotted (red) curve depicts $-\langle \bar{q}q \rangle_0^{1/3}$, the dash-dotted (blue) curve is f_π , and the long-dashed (blue) curve is $f_{s\bar{s}}$. (Colors in the electronic version.)

Leutwyler-Smilga relation, Eq. (5), is a remarkable relation between the two pertinent theories. For example, in the limit of all very heavy quarks ($m_q \rightarrow \infty$, $q = u, d, s$), it correctly leads to the result that χ_{YM} is equal to the value of the topological susceptibility in *quenched* QCD, $\chi_{\text{YM}} = \chi(m_q = \infty)$. This holds because χ is by definition the vacuum expectation value of a gluonic operator, so that the absence of quark loops would leave only the pure-gauge, YM contribution. However, the Leutwyler-Smilga relation (5) also holds in the opposite (and presently pertinent) limit of light quarks. This limit still presents a problem for getting the full-QCD topological susceptibility χ on the lattice [47], but we can use the light-quark-sector result [37, 48]

$$\chi = -\frac{m \langle \bar{q}q \rangle_0}{N_f} + C_m, \quad (7)$$

where C_m stands for corrections of higher orders in small m_q , and thus of small magnitude. The leading term is positive (as $\langle \bar{q}q \rangle_0 < 0$), but C_m is negative, since Eq. (5) shows that $\chi \leq \min(-m \langle \bar{q}q \rangle_0 / N_f, \chi_{\text{YM}})$.

Although small, C_m should not be neglected, since $C_m = 0$ would imply, through Eq. (5), that $\chi_{\text{YM}} = \infty$. Instead, its value (at $T = 0$) is fixed by Eq. (5):

$$C_m = C_m(0) = \frac{m \langle \bar{q}q \rangle_0}{N_f} \left(1 - \chi_{\text{YM}} \frac{N_f}{m \langle \bar{q}q \rangle_0} \right)^{-1}. \quad (8)$$

4 η - η' complex at high temperatures

All this starting from Eq. (5) has so far been at $T = 0$. If the left- and right-hand side of Eq. (5) are extended to $T > 0$, it is obvious that the equality cannot hold at arbitrary temperature $T > 0$. The relation (5) must break down somewhere close to the (pseudo)critical temperatures of full QCD ($\sim T_{\text{Ch}}$) since the pure-gauge quantity χ_{YM} is much more temperature-resistant than the right-hand side, abbreviated as $\tilde{\chi}$. The quantity $\tilde{\chi}$, which may be called the effective susceptibility, consists of the full-QCD quantities χ and $\langle \bar{q}q \rangle_0$, the quantities of full QCD with quarks, characterized by T_{Ch} , just as $f_\pi(T)$. As $T \rightarrow T_{\text{Ch}}$, the chiral quark condensate $\langle \bar{q}q \rangle_0(T)$ drops faster than the other DChSB parameter in the present problem, namely $f_\pi(T)$ for realistically small explicit ChSB. (See Fig. 1 for the results of the dynamical model adopted here from Ref. [9], and, e.g., Refs. [22, 45] for analogous results of different SD models). Thus, the troublesome mismatch in T -dependences of $f_\pi(T)$ and the pure-gauge quantity $\chi_{\text{YM}}(T)$, which causes the conflict of the temperature-extended WVR with experiment at $T \gtrsim T_{\text{Ch}}$, is expected to disappear if $\chi_{\text{YM}}(T)$ is replaced by $\tilde{\chi}(T)$, the temperature-extended effective susceptibility. The successful zero-temperature WVR (1) is, however, retained, since $\chi_{\text{YM}} = \tilde{\chi}$ at $T = 0$.

Extending Eq. (7) to $T > 0$ is something of a guesswork as there is no guidance from the lattice for $\chi(T)$ [unlike $\chi_{\text{YM}}(T)$]. Admittedly, the leading term is straightforward as it is plausible that its T -dependence will simply be that of $\langle \bar{q}q \rangle_0(T)$. Nevertheless, for the correction term \mathcal{C}_m such a plausible assumption about the form of T -dependence cannot be made and Eq. (8), which relates YM and QCD quantities, only gives its value at $T = 0$. We will therefore explore the T -dependence of the anomalous masses using the following Ansatz for the $T \geq 0$ generalization of Eq. (7):

$$\chi(T) = -\frac{m \langle \bar{q}q \rangle_0(T)}{N_f} + \mathcal{C}_m(0) \left[\frac{\langle \bar{q}q \rangle_0(T)}{\langle \bar{q}q \rangle_0(T=0)} \right]^\delta, \quad (9)$$

where the correction-term T -dependence is parametrized through the power δ of the presently fastest-vanishing (as $T \rightarrow T_{\text{Ch}}$) chiral order parameter $\langle \bar{q}q \rangle_0(T)$.

The $T \geq 0$ extension (9) of the light-quark χ , Eq. (7), leads to the $T \geq 0$ extension of $\tilde{\chi}$:

$$\tilde{\chi}(T) = \frac{m \langle \bar{q}q \rangle_0(T)}{N_f} \left(1 - \frac{m \langle \bar{q}q \rangle_0(T)}{N_f \mathcal{C}_m(0)} \left[\frac{\langle \bar{q}q \rangle_0(T=0)}{\langle \bar{q}q \rangle_0(T)} \right]^\delta \right).$$

We now use $\tilde{\chi}(T)$ in WVR instead of $\chi_{\text{YM}}(T)$ used by Ref. [9]. This gives us the temperature dependences of the masses in the η - η' complex, such as those in Fig. 2 and in Fig. 3, illustrating the respective cases $\delta = 0$ and $\delta = 1$.

It is clear that $\tilde{\chi}(T)$ (10) blows up as $T \rightarrow T_{\text{Ch}}$ if the correction term there vanishes faster than $\langle \bar{q}q \rangle_0(T)$ squared. Thus, varying δ between 0 and 2 covers the cases from the T -independent correction term, to (already experimentally excluded) enhanced anomalous masses for δ noticeably above 1, to even sharper mass blow-ups for $\delta \rightarrow 2$ when $T \rightarrow T_{\text{Ch}}$. On the other hand, it does not seem

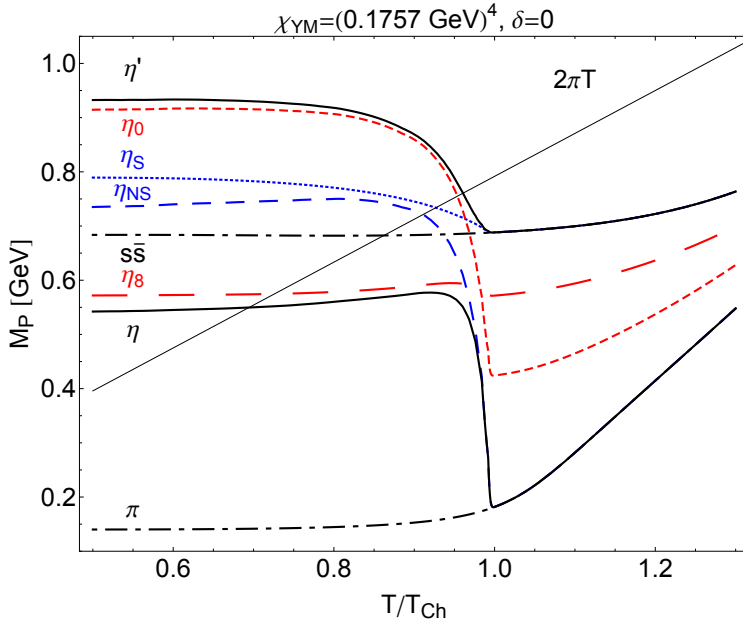


Fig. 2. The relative-temperature dependence, on T/T_{Ch} , of the pseudoscalar meson masses for $\tilde{\chi}(T)$, namely Eq. (10), with $\delta = 0$. The meaning of the symbols is as follows: the masses of η' and η are, respectively, the upper and lower solid curve, those of the pion and nonanomalous $s\bar{s}$ pseudoscalar are, respectively, the lower and upper dash-dotted curve, M_{η_0} and M_{η_8} are, respectively, the short-dashed (red) and long-dashed (red) curve, $M_{\eta_{NS}}$ is the medium-dashed (blue), and M_{η_S} is the dotted (blue) curve. (Colors in the electronic version.) The straight line $2\pi T$ is twice the lowest Matsubara frequency.

natural that the correction term vanishes faster than the fastest-vanishing order parameter $\langle \bar{q}q \rangle_0(T)$. Indeed, already for the same rate of vanishing of the both terms ($\delta = 1$), one can notice in Fig. 3 the start of the precursors of the blow-up of various masses in the η' - η complex as $T \rightarrow T_{\text{Ch}}$ although these small mass bumps are still experimentally acceptable. Thus, in Fig. 3 we depict the $\delta = 1$ case, and the case with $\delta = 0$ (T -independent correction term) is depicted in Fig. 2 as the other acceptable extreme. Since they turn out to be not only qualitatively, but also quantitatively so similar that the present era experiments cannot discriminate between them, there is no need to present any 'in-between results', for $0 < \delta < 1$.

To clarify completely how the results in Figs. 2 and 3 were obtained, we now give some additional explanations.

Using $\tilde{\chi}(T)$ in WVR instead of $\chi_{\text{YM}}(T)$ used by Ref. [9], does not change anything at $T = 0$, where $\tilde{\chi}(T) = \chi_{\text{YM}}(0)$, which remains an excellent approximation even well beyond $T = 0$. Nevertheless, this changes drastically as T approaches T_{Ch} . For $T \sim T_{\text{Ch}}$, the behavior of $\tilde{\chi}(T)$ is dominated by the T -dependence of the chiral condensate, tying the restoration of the $U_A(1)$ symmetry to the chiral symmetry restoration.

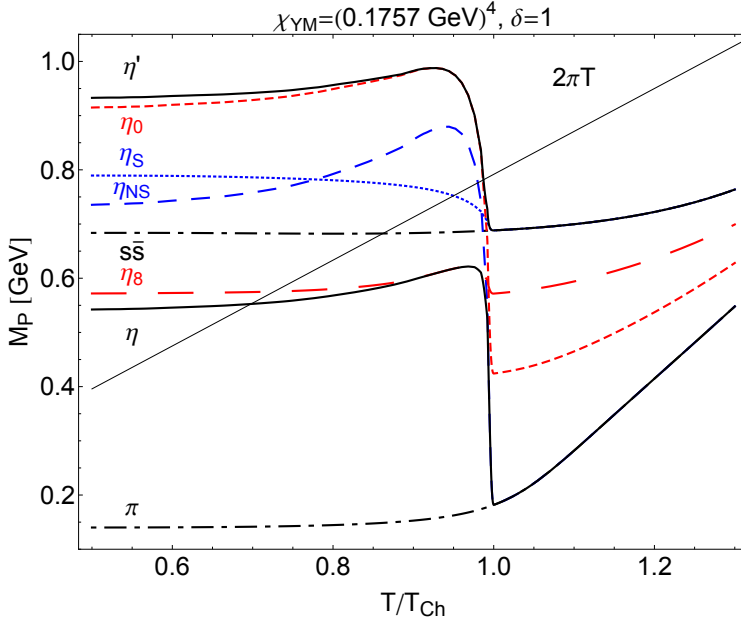


Fig. 3. The relative-temperature dependence, on T/T_{Ch} , of the pseudoscalar meson masses for $\tilde{\chi}(T)$, Eq. (10), with $\delta = 1$. The meaning of all symbols is the same as in the preceding Fig. 2.

As for the nonanomalous contributions to the meson masses, we use the same SD model (and parameter values) as in Ref. [9], since it includes both DChSB and correct QCD chiral behavior as well as realistic explicit ChSB. That is, all nonanomalous results (M_π, f_π, M_K, f_K , as well as $M_{s\bar{s}}$ and $f_{s\bar{s}}$, the mass and decay constant of the unphysical $s\bar{s}$ pseudoscalar meson) in the present paper are, for all T , taken over from Ref. [9]. We used this same model also for computing the chiral quark condensate $\langle \bar{q}q \rangle_0$, including its T -dependence displayed in Fig. 1.

This defines completely how the results displayed in Figs. 2 and 3 were generated. For details, see Ref. [9] (and Ref. [7] for M_{η_0} and M_{η_8}). Here we list only the formulas which, in conjunction with Fig. 1, enable the reader to understand easily the T -dependences of the masses in Figs. 2 and 3: the theoretical η' and η mass eigenvalues are

$$M_{\eta'}^2(T) = \frac{1}{2} [M_{\eta_{NS}}^2(T) + M_{\eta_S}^2(T) + \Delta_{\eta\eta'}(T)], \quad (10)$$

$$M_{\eta}^2(T) = \frac{1}{2} [M_{\eta_{NS}}^2(T) + M_{\eta_S}^2(T) - \Delta_{\eta\eta'}(T)], \quad (11)$$

where $\Delta_{\eta\eta'} \equiv \sqrt{[M_{\eta_{NS}}^2 - M_{\eta_S}^2]^2 + 8\beta^2 X^2}$, $\beta = \frac{1}{2 + X^2} \frac{6\tilde{\chi}}{f_\pi^2}$, $X \equiv \frac{f_\pi}{f_{s\bar{s}}}$,

$$M_{\eta_{NS}}^2 = M_\pi^2 + 2\beta, \quad M_{\eta_S}^2 = M_{s\bar{s}}^2 + \beta X^2,$$

$$M_{\eta_0}^2 = M_{00}^2 + \frac{1}{3}(2 + X)^2 \beta, \quad M_{\eta_8}^2 = M_{88}^2 + \frac{2}{3}(1 - X)^2 \beta,$$

$$M_{88}^2 = \frac{2}{3} M_{s\bar{s}}^2 + \frac{1}{3} M_{\pi}^2, \quad M_{00}^2 = \frac{1}{3} M_{s\bar{s}}^2 + \frac{2}{3} M_{\pi}^2.$$

In all expressions after Eq. (11), the T-dependence is understood.

In both cases considered for the topological susceptibility (9) [$\delta = 0$, i.e., the constant correction term, and $\delta = 1$, i.e., the strong T-dependence $\propto \langle \bar{q}q \rangle_0(T)$ of both the leading and correction terms in $\chi(T)$], the results are consistent with the experimental findings on the decrease of the η' mass of Csörgő *et al.* [25,26].

5 Summary, discussion and conclusions

The recent experimental results on the η' multiplicity in heavy-ion collisions [25,26] are of great importance because they clearly signal a partial restoration of $U_A(1)$ symmetry at high temperatures, and thus provide an unambiguous signature of the formation of a new state of matter.

In the light of this important experimental find, we revisited the earlier theoretical work [9] concerning the thermal behavior of the η' - η complex following from WVR straightforwardly extended to $T > 0$. We have confirmed the results of Ref. [9] on WVR where the ratio $\chi_{YM}(T)/f_{\pi}(T)^2$ dominates the T-dependence, and clarified that these results are practically model-independent. It is important to note the difference between our approach and those that attempt to give model predictions for topological susceptibility, such as Refs. [49,50]. By contrast, in Refs. [9] and here, as well as earlier works [4–7] at $T = 0$, a SD dynamical model is used (as far as masses are concerned) to obtain only the nonanomalous part of the light pseudoscalar meson masses (where the model dependence is however dominated by their almost-Goldstone character), while the anomalous part of the masses in the η' - η complex is, through WVR, dictated by $6\chi_{YM}/f_{\pi}^2$. In this ratio, $f_{\pi}(T)$ is admittedly model-dependent in quantitative sense, but other realistic models yield qualitatively similar crossover behaviors [51] of $f_{\pi}(T)$ for $m_q \neq 0$, as exemplified by our Fig. 1, and Fig. 2 in Ref. [9], and by Fig. 6 in Ref. [22]. Such $f_{\pi}(T)$ behaviors are also in agreement with the T-dependence expected of the DChSB order parameter on general grounds: a pronounced fall-off around T_{Ch} – but exhibiting, in agreement with lattice [24], a smooth crossover pattern for nonvanishing explicit ChSB, a crossover which gets slower with growing m_q [e.g., compare $f_{\pi}(T)$ with $f_{s\bar{s}}(T)$ in Fig. 1]. In contrast to the QCD topological susceptibility χ , the YM topological susceptibility and even its T-dependence $\chi_{YM}(T)$, including its “melting” temperature T_{YM} , can be extracted [9] reasonably reliably from the lattice [34,38]. Thus, it was not modeled in Ref. [9]. Hence our assertion that the results of Ref. [9] unavoidably imply that the straightforward extension of WVR to $T > 0$ is falsified by experiment [25,26], especially if one recalls that even the sizeable T-rescaling [41,42] $T_{YM} \rightarrow T_{Ch}$ was among the attempts to control the η' mass enhancement [9].

Nevertheless, we have also shown that there is a plausible way to avoid these problems of the straightforward, naive extension of WVR to $T > 0$, and this is

the main result of the present paper. Thanks to the existence of another relation, Eq. (5), connecting the YM quantity χ_{YM} with QCD quantities χ and $\langle \bar{q}q \rangle_0$, it is possible to define a quantity, $\tilde{\chi}$, which can meaningfully replace $\chi_{YM}(T)$ in finite-T WVR. It remains practically equal to χ_{YM} up to some 70% of T_{Ch} , but beyond this, it changes following the T-dependence of $\langle \bar{q}q \rangle_0(T)$. In this way, the successful zero-temperature WVR is retained, but the (partial) restoration of $U_A(1)$ symmetry [understood as the disappearing contribution of the gluon anomaly to the η' (η_0) mass] is naturally tied to the restoration of the $SU_A(3)$ flavor chiral symmetry and to its characteristic temperature T_{Ch} , instead of T_{YM} .

It is very pleasing that this fits in nicely with the recent *ab initio* theoretical analysis using functional methods [52], which finds that the anomalous breaking of $U_A(1)$ symmetry is related to DChSB (and confinement) in a self-consistent manner, so that one cannot have one of these phenomena without the other.

Of course, the most important thing is that this version of the finite-T WVR, obtained by $\chi_{YM}(T) \rightarrow \tilde{\chi}(T)$, is consistent with experiment [25,26] for all reasonable strengths of T-dependence [$0 \leq \delta \lesssim 1$ in Eq. (9)]. Namely, the both Figs. 2 and 3 show, first, that η' mass close to T_{Ch} suffers the drop of more than 200 MeV with respect to its vacuum value. This satisfies the minimal experimental requirement abundantly. Second, Figs. 2 and 3 show an even larger drop of the η_0 mass, to some 400 MeV, close to the “best” value of the in-medium η' mass (340 MeV, albeit with large errors) obtained by Csörgő *et al.* [25,26]. This should be noted because the η_0 mass inside the fireball is possibly even more relevant. Namely, although it is, strictly speaking, not a physical meson, η_0 is the state with the $q\bar{q}$ content closest to the $q\bar{q}$ content of the physical η' *in the vacuum*. Thus, among the isoscalar $q\bar{q}$ states inside the fireball, η_0 has the largest projection on, and thus the largest amplitude to evolve, by fireball dissipation, into an η' in the vacuum.

We should also note that our proposed mechanism, tying $\tilde{\chi}$ to the chiral quark condensate $\langle \bar{q}q \rangle_0$, suggests that the partial $U_A(1)$ -symmetry restoration would also happen if, instead of temperature, matter density is increased sufficiently, so that the chiral symmetry restoration takes place and $\langle \bar{q}q \rangle_0$ vanishes.

References

1. C. D. Roberts, arXiv:1203.5341 [nucl-th].
2. D. Kekez, B. Bistrovic and D. Klabucar, Int. J. Mod. Phys. A **14**, 161 (1999).
3. D. Kekez and D. Klabucar, Phys. Rev. D **71**, 014004 (2005) [hep-ph/0307110].
4. D. Klabucar and D. Kekez, Phys. Rev. D **58**, 096003 (1998) [hep-ph/9710206].
5. D. Kekez, D. Klabucar and M. D. Scadron, J. Phys. G **26**, 1335 (2000) [hep-ph/0003234].
6. D. Kekez and D. Klabucar, Phys. Rev. D **65**, 057901 (2002) [hep-ph/0110019].
7. D. Kekez and D. Klabucar, Phys. Rev. D **73**, 036002 (2006) [hep-ph/0512064].
8. D. Horvatic, D. Blaschke, Y. Kalinovsky, D. Kekez and D. Klabucar, Eur. Phys. J. A **38**, 257 (2008) [arXiv:0710.5650 [hep-ph]].
9. D. Horvatic, D. Klabucar and A. E. Radzhabov, Phys. Rev. D **76**, 096009 (2007) [arXiv:0708.1260 [hep-ph]].
10. D. Horvatic, D. Blaschke, D. Klabucar and A. E. Radzhabov, Phys. Part. Nucl. **39**, 1033 (2008) [hep-ph/0703115 [HEP-PH]].

11. S. Benic, D. Horvatic, D. Kekez and D. Klabucar, Phys. Rev. D **84**, 016006 (2011) [arXiv:1105.0356 [hep-ph]].
12. S. Benic, D. Horvatic, D. Kekez and D. Klabucar, Acta Phys. Polon. Supp. **5**, 941 (2012) [arXiv:1207.3068 [hep-ph]].
13. STAR, J. Adams *et al.*, Nucl. Phys. **A757**, 102 (2005), [nucl-ex/0501009].
14. B. Muller and J. L. Nagle, Ann. Rev. Nucl. Part. Sci. **56**, 93 (2006).
15. E. V. Shuryak and I. Zahed, Phys. Rev. **D70**, 054507 (2004), [hep-ph/0403127].
16. M. A. Stephanov, PoS **LAT2006**, 024 (2006) [arXiv:hep-lat/0701002].
17. D. B. Blaschke and K. A. Bugaev, Fizika **B13**, 491 (2004), [nucl-th/0311021].
18. S. Datta, F. Karsch, P. Petreczky and I. Wetzorke, Nucl. Phys. Proc. Suppl. **119**, 487 (2003), [hep-lat/0208012].
19. M. Asakawa and T. Hatsuda, Phys. Rev. Lett. **92**, 012001 (2004), [hep-lat/0308034].
20. E. Shuryak, Nucl. Phys. **A774**, 387 (2006), [hep-ph/0510123].
21. F. Karsch *et al.*, Nucl. Phys. **A715**, 701 (2003), [hep-ph/0209028].
22. P. Maris, C. D. Roberts, S. M. Schmidt and P. C. Tandy, Phys. Rev. C **63**, 025202 (2001) [arXiv:nucl-th/0001064].
23. M. Mannarelli and R. Rapp, Phys. Rev. **C72**, 064905 (2005), [hep-ph/0505080].
24. Z. Fodor and S. D. Katz, arXiv:0908.3341 [hep-ph].
25. T. Csorgo, R. Vertesi and J. Sziklai, Phys. Rev. Lett. **105**, 182301 (2010).
26. R. Vertesi, T. Csorgo and J. Sziklai, Phys. Rev. C **83**, 054903 (2011).
27. S. S. Adler *et al.* [PHENIX Collaboration], Phys. Rev. Lett. **93**, 152302 (2004).
28. J. Adams *et al.* [STAR Collaboration], Phys. Rev. C **71**, 044906 (2005).
29. J. I. Kapusta, D. Kharzeev and L. D. McLerran, Phys. Rev. D **53**, 5028 (1996).
30. E. Witten, Nucl. Phys. **B156**, 269 (1979).
31. G. Veneziano, Nucl. Phys. **B159**, 213 (1979).
32. B. Lucini, M. Teper and U. Wenger, Nucl. Phys. **B715**, 461 (2005), [hep-lat/0401028].
33. L. Del Debbio, L. Giusti and C. Pica, Phys. Rev. Lett. **94**, 032003 (2005).
34. B. Alles, M. D'Elia and A. Di Giacomo, Phys. Rev. **D71**, 034503 (2005).
35. S. Dürr, Z. Fodor, C. Hoelbling and T. Kurth, JHEP **0704**, 055 (2007).
36. T. Feldmann, Int. J. Mod. Phys. **A15**, 159 (2000), [hep-ph/9907491].
37. H. Leutwyler and A. V. Smilga, Phys. Rev. D **46**, 5607 (1992).
38. B. Alles, M. D'Elia and A. Di Giacomo, Nucl. Phys. **B494**, 281 (1997).
39. G. Boyd *et al.*, Nucl. Phys. **B469**, 419 (1996), [hep-lat/9602007].
40. C. Gattringer, R. Hoffmann and S. Schaefer, Phys. Lett. **B535**, 358 (2002).
41. K. Fukushima, K. Ohnishi and K. Ohta, Phys. Rev. **C63**, 045203 (2001).
42. J. Schaffner-Bielich, Phys. Rev. Lett. **84**, 3261 (2000), [hep-ph/9906361].
43. D. Blaschke, G. Burau, Yu. L. Kalinovsky, P. Maris and P. C. Tandy, Int. J. Mod. Phys. **A 16**, 2267 (2001) [arXiv:nucl-th/0002024].
44. For reviews, see, e.g., Refs. [45,46].
45. C. D. Roberts and S. M. Schmidt, Prog. Part. Nucl. Phys. **45**, S1 (2000).
46. R. Alkofer and L. von Smekal, Phys. Rept. **353**, 281 (2001) [arXiv:hep-ph/0007355].
47. T. DeGrand and S. Schaefer, arXiv:0712.2914 [hep-lat].
48. P. Di Vecchia and G. Veneziano, Nucl. Phys. **B171**, 253 (1980).
49. G.A. Contrera, D. Gomez Dumm and N.N. Scoccola, Phys. Rev. D **81**, 054005 (2010).
50. P. Costa, M. C. Ruivo, C. A. de Sousa, H. Hansen and W. M. Alberico, Phys. Rev. D **79**, 116003 (2009) [arXiv:0807.2134 [hep-ph]].
51. E.g., within SD approach, compare our $f_{\pi}(T)$ and the one in Ref. [22] and in reviews such as Ref. [45].
52. R. Alkofer, PoS **FACESQCD**, 030 (2011), [arXiv:1102.3166 [hep-th]].



Resonance phase shifts from lattice QCD: The pion-nucleon channel^{*}

C. B. Lang¹ and V. Verduci²

¹Institut für Physik, Universität Graz, A-8010 Graz, Austria

²School of Physics and Astronomy, University of Edinburgh, Edinburgh EH9 3JZ, Scotland

We discuss recently published results for the negative parity nucleon channel [1,2] and the problem of baryonic resonances in lattice calculations.

The Euclidean space-time lattice regularisation is the only controllable non-perturbative regularisation of QCD. It defines the quantum field theory as a limit from a finite to an infinite number of points and from non-zero to vanishing lattice spacing. The last decades have shown an enormous progress towards computing hadronic properties that way, mainly by large scale Monte Carlo simulations.

The ground states can be computed from the asymptotic decay of the correlation function of hadronic operators $\langle \mathcal{O}(t)\mathcal{O}(0) \rangle$ in the corresponding quantum channel. In nature, however, most hadrons are unstable. In the lattice world, due to the finiteness of the spatial volume, correlation functions have a discrete energy spectrum – as opposed to the continuous spectral function in the continuum – and one has to retrieve all information on resonances from the measured energy levels. Also the quark mass may be set to unphysically large values and thus some decay thresholds lie higher than in the physical situation and the respective lowest state appears to be (artificially) stable. Towards the physical limit the decay poses a serious problem in the analysis. Two- (and more-) hadron intermediate states should have an impact on the energy spectrum.

In recent years there have been several studies determining baryonic excitations. One common feature was the absence of hadron-hadron decay state signals (except for possibly the s -wave states). This was especially blatant in the $\rho \rightarrow \rho$ studies, which on the lattice should exhibit p -wave $\pi\pi$ intermediate states. These should show up as discrete energy levels of the spectral decomposition of the hadron correlation function, but were not observed. In the meson sector the cure was to include meson-meson interpolators in the set of operators of the correlation matrix. In the baryon studies, the baryon interpolators were exclusively three-quark operators and the statements above applied. In order to clarify the situation we studied the negative parity nucleon channel including s -wave $N\pi$ ($4+1$ quark) operators [1]. Indeed we find significant differences in the energy spectrum.

^{*} Talk delivered by C. B. Lang

Our study is for gauge configurations with two mass degenerate dynamical quarks. The used parameters correspond to a lattice spacing of 0.1239 fm on a $16^3 \times 32$ lattice with a pion mass of 266 MeV. For the nucleon interpolator we use the standard 3-quark operators, For the $N\pi$ system in the rest frame the leading s -wave contribution comes from the interpolator with both particles at rest, $N\pi(\mathbf{p} = 0) = \gamma_5 N_+(\mathbf{p} = 0)\pi(\mathbf{p} = 0)$, where N_+ denotes the positive parity nucleon and the factor γ_5 ensures negative parity for the interpolator.

We determine the energy levels of the coupled N and $N\pi$ system with help of the so-called variational method [3]. For this approach one determines and diagonalizes the cross-correlation matrix between several operators with the given quantum numbers. In order to compute this correlation matrix we had to first compute the Wick decomposition of the correlators in terms of the quark propagators. For $N \leftrightarrow N$ these are of only two types, while the complete $(N_-, N_+\pi) \leftrightarrow (N_-, N_+\pi)$ system requires the evaluation of 29 graphs. Among all these contraction terms there are some involving backtracking propagators. Hence special tools are necessary in order to obtain statistically reliable signals. We used the so-called distillation method [4].

We find that the energy spectrum changes when allowing for the $N\pi$ coupled channel. We find now a clear signal for the lowest $N(0)\pi(0)$ state, lying closely below threshold, as expected. Indeed, also the quality of the energy levels improves. Lüscher [5] derived a relation between the energy levels at finite volume and the phase shifts of the infinite volume, valid in the elastic region. We apply this relation up to the region of the second resonance. More detailed studies would have to include more operators and deal with the coupled channel problem. In a Breit-Wigner fit to the corresponding phase shift values the resonance masses lie approximately 150 MeV above the physical values, similar to the nucleon mass, due to the unphysical pion mass of 266 MeV. Further details can be found in Refs. [1] and [2].

CBL thanks Mitja Rosina for organizing such a relaxed and enjoyable meeting. VV has been supported by the Austrian Science Fund (FWF) under Grant No. DK W1203-N16.

References

1. C. B. Lang and V. Verduci, *Phys. Rev. D* **87**, 054502 (2013).
2. C. B. Lang and V. Verduci, *Nucleon excited states on the lattice*, (2013), arXiv:1304.4114.
3. C. Michael, *Nucl. Phys. B* **259**, 58 (1985). M. Lüscher and U. Wolff, *Nucl. Phys. B* **339**, 222 (1990). B. Blossier, M. DellaMorte, G. von Hippel, T. Mendes, and R. Sommer, *JHEP* **0904**, 094 (2009).
4. Hadron Spectrum Collaboration, M. Peardon *et al.*, *Phys. Rev. D* **80**, 054506 (2009).
5. M. Lüscher, *Commun. Math. Phys.* **104**, 177 (1986), *ibid.* **105**, 153 (1986); *Nucl. Phys. B* **354**, 531 (1991); *Nucl. Phys. B* **364**, 237 (1991).



Flavor Decomposition of Baryon Electromagnetic Form Factors[★]

M. Rohrmoser[†], Ki-Seok Choi^{*}, and W. Plessas[†]

[†] Theoretical Physics, Institute of Physics, University of Graz, A-8010 Graz, Austria

^{*} Department of Physics, Soongsil University, Seoul 156-743, Republic of Korea

Abstract. We report of testing the relativistic constituent-quark model based on Goldstone-boson-exchange dynamics with regard to phenomenological data that have recently become available on the flavor content in nucleon electromagnetic form factors. Corresponding studies have furthermore been extended to all other baryon ground states with flavors u , d , and s . Beyond the nucleons comparisons of our results are possible with some data available from calculations within lattice quantum chromodynamics. It is found that in all respects the relativistic constituent-quark model relying on $\{QQQ\}$ degrees of freedom only performs reasonably well in describing the electromagnetic structures up to momentum transfers of $Q^2 \sim 4\text{-}5 \text{ GeV}^2$.

Exploring the structure of hadrons with different probes provides valuable insight into their composition of constituents and the prevailing interactions. The longest tradition belongs to the nucleons, specifically the proton, whose electromagnetic structure has now already been measured since more than half a century ago. The nucleons are furthermore tested under weak interactions with regard to their axial form factors. Theoretically one further explores their form factors under (strong) scalar and gravitational interactions. These latter quantities are not (yet) directly accessible to experiments.

Due to the advent of recent phenomenological data [1–3], it has become quite exciting to dissect the nucleon electromagnetic form factors with regard to their flavor contents. The observables measured in elastic electron scattering on the nucleons shed valuable light on various aspects of Sachs as well as Dirac and Pauli form factors. Especially, some of their ratios and the pertinent flavor contributions represent sensitive quantities in discussing the role of different quark flavors.

We have performed a comprehensive study of the flavor decomposition of the nucleon form factors within relativistic constituent-quark models (first results having appeared in refs. [4, 5]). Various aspects of our theoretical investigations were further discussed at the Workshop. In particular, we highlighted issues regarding additional degrees of freedom beyond three-quark configurations, quark-diquark clustering, spin-flavor symmetries of the wave functions,

^{*} Talk delivered by W. Plessas

relativistic effects etc. For instance, the fall off of the ratios of the d to u flavor contributions in the Dirac and Pauli form factors, claimed to be a signal for di-quark clustering [6], is also obtained by the relativistic constituent-quark model relying on explicit three-Q degrees of freedom (see fig. 1). Very importantly we also hinted to intriguing discrepancies among the data sets, especially for the ratio F_2^d/F_2^u of u and d flavor contributions to the Pauli form factor F_2 from the three different phenomenological analyses of refs. [1–3] (also visible from fig. 1). While all analyses differ among each other, our theoretical predictions seem to agree best with the data obtained by Qattan and Arrington.

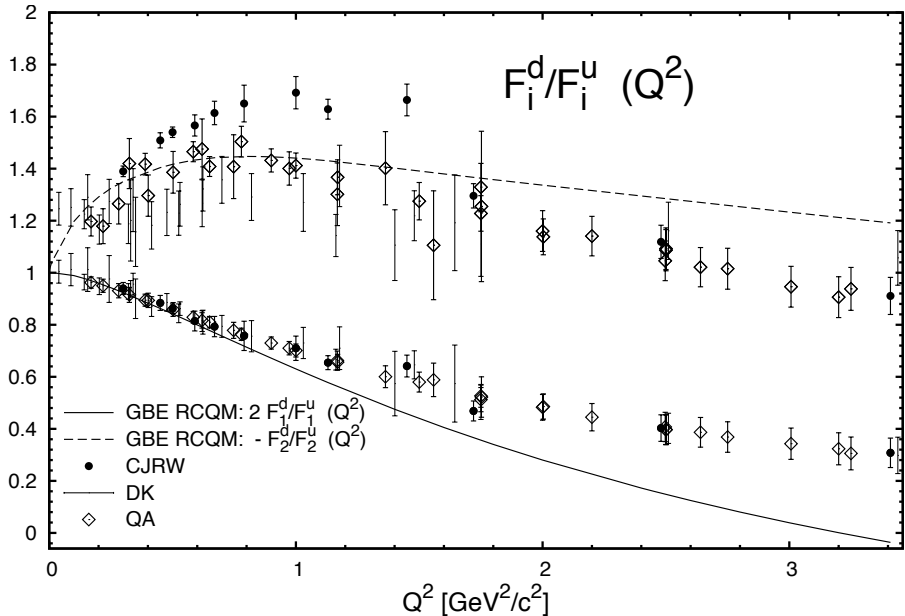


Fig. 1. Predictions of the Goldstone-boson-exchange relativistic constituent-quark model [7] for the ratio of d to u flavor contributions to the Dirac and Pauli form factors of the nucleons in comparison to phenomenological data produced in the analyses of refs. [1–3].

Our theoretical flavor decompositions have furthermore been extended to all other octet and decuplet baryon ground states [8]. Interesting aspects have thereby been revealed about the contributions of u, d, and s flavors to the electric and magnetic form factors as well as electric radii and magnetic moments. For instance, it has been found that the magnetic form factor of the octet Λ^0 is almost exclusively carried by the s quark, see fig. 2. Furthermore, baryons with the same flavor contents but belonging to different flavor multiplets as, e.g., the Σ and Σ^* or the Ξ and Ξ^* , receive for their electromagnetic form factors quite different contributions from their constituent flavors. Beyond the comparisons with available experimental data we also contrasted our results in detail with predictions from

other approaches, such as lattice quantum chromodynamics, and found reasonable agreement.

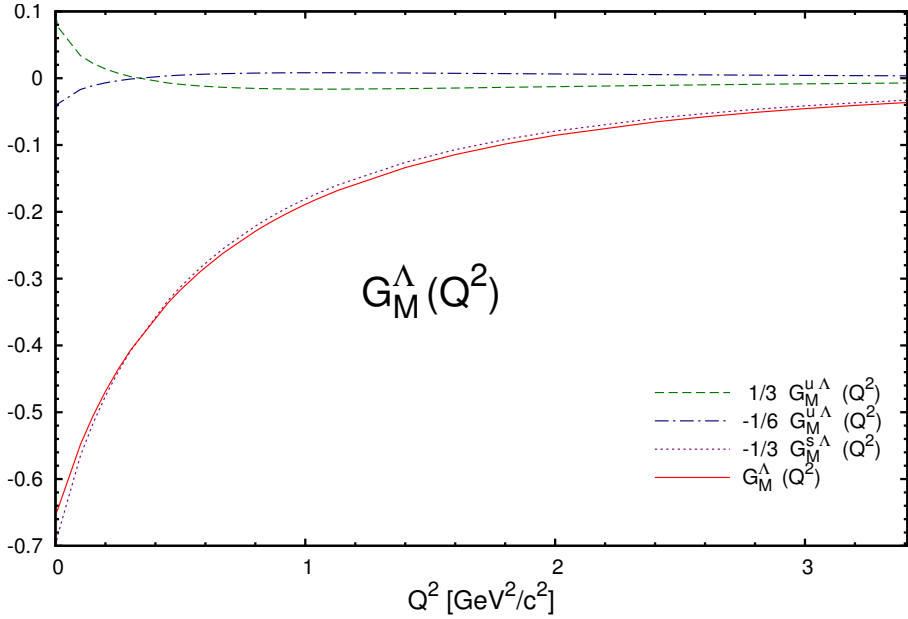


Fig. 2. Predictions of the Goldstone-boson-exchange relativistic constituent-quark model [7] for the magnetic form factor of Λ^0 and the individual u , d , and s flavor contributions therein.

Acknowledgment

This work was supported by the Austrian Science Fund, FWF, through the Doctoral Program on *Hadrons in Vacuum, Nuclei, and Stars* (FWF DK W1203-N16).

References

1. G. D. Cates, C. W. de Jager, S. Riordan, and B. Wojtsekhowski, *Phys. Rev. Lett.* **106**, 252003 (2011)
2. I. A. Qattan and J. Arrington, *Phys. Rev. C* **86**, 065210 (2012)
3. M. Diehl and P. Kroll, *Eur. Phys. J. C* **73**, 2397 (2013)
4. M. Rohrmoser, K. -S. Choi, and W. Plessas, arXiv:1110.3665v2 [hep-ph]
5. M. Rohrmoser, K. -S. Choi, and W. Plessas, *Acta Phys. Pol. Suppl.* **6**, 371 (2013)
6. I. C. Cloet, G. Eichmann, B. El-Bennich, T. Klahn, and C. D. Roberts, *Few-Body Syst.* **46**, 1 (2009)
7. L. Y. Glozman, W. Plessas, K. Varga, and R. F. Wagenbrunn, *Phys. Rev. D* **58**, 094030 (1998)
8. M. Rohrmoser, Diploma Thesis, Univ. of Graz, 2013



Quark-Pair Contributions to Weak Transition Form Factors of Heavy-Light Mesons*

Oliver Senekowitsch and Wolfgang Schweiger

Institut für Physik, Universität Graz, A-8010 Graz, Austria

Abstract. Weak transition form factors of heavy-light mesons are discussed within a relativistic constituent-quark model employing the point-form of relativistic quantum mechanics. We study such form factors in the space- and the time-like momentum-transfer regions for heavy-light to heavy-light and heavy-light to light-light transitions. We investigate the influence of non-valence degrees-of-freedom which lead to, so called, “quark-pair contributions” in the weak transition current. To this aim the weak transition form factors are first calculated for space-like momentum transfers in a frame where quark-pair contributions are supposed to be suppressed. Analytical continuation to time-like momentum transfers and subsequent comparison with the time-like transition form factors obtained from a direct decay calculation gives us an estimate of the role quark-pair contributions may play for decay kinematics. A simple dynamical mechanism for quark-pair contributions based on the 3P_0 quark-pair creation model is suggested.

Our goal is to describe the electroweak structure of mesons within a constituent-quark model in a relativistically invariant way. To this aim we make use of the Bakamjian-Thomas construction [1, 2] and choose the point-form of relativistic dynamics [3]. The point form is characterized by the property that interaction terms enter all four components of the 4-momentum operator, whereas the generators of Lorentz transformations stay free of interactions. This makes it comparably simple to boost and rotate wave functions and add angular momenta. The essence of the Bakamjian-Thomas construction in point form is that the 4-momentum operator factorizes into an interaction-dependent mass operator and a free 4-velocity operator

$$\hat{p}^\mu = \hat{\mathcal{M}} \hat{V}_{\text{free}}^\mu = (\hat{\mathcal{M}}_{\text{free}} + \hat{\mathcal{M}}_{\text{int}}) \hat{V}_{\text{free}}^\mu. \quad (1)$$

The dynamics of the system is thus completely encoded in the mass operator.

Since we are dealing with processes during which the particle number is not necessarily conserved, we have to allow for particle creation and annihilation. This is accomplished by using a coupled-channel framework with a matrix mass operator $\hat{\mathcal{M}}$ that acts on the direct sum of the pertinent multiparticle Hilbert spaces. The diagonal entries $\hat{\mathcal{M}}_i$ of this matrix mass operator are the sum of the

* Talk delivered by Oliver Senekowitsch

relativistic kinetic energies of the particles in channel i . In addition, the \hat{M}_i may contain instantaneous interactions between the particles, like the confinement potential between quark and antiquark. Off-diagonal entries of the matrix mass operator are vertex operators $\hat{K}_{i \rightarrow j}$ and $\hat{K}_{j \rightarrow i} = \hat{K}_{i \rightarrow j}^\dagger$ which describe the absorption and emission of particles and hence the transition from one channel to the other. The vertex interactions we use are derived from common field-theoretical interaction Lagrangean densities [4,5].

A most convenient basis to represent all these operators is formed by a complete set of velocity states [6]. A velocity state is a multiparticle momentum state in the rest frame

$$|\mathbf{k}_i, \mu_i\rangle \equiv |\mathbf{k}_1, \mu_1; \mathbf{k}_2, \mu_2; \dots; \mathbf{k}_n, \mu_n\rangle, \text{ with } \sum_{i=1}^N \mathbf{k}_i = 0, \quad (2)$$

which is boosted to an overall 4-velocity V ($V_\mu V^\mu = 1$)

$$|V; \mathbf{k}_1, \mu_1; \mathbf{k}_2, \mu_2; \dots; \mathbf{k}_n, \mu_n\rangle = \hat{U}_{B_c(V)} |\mathbf{k}_1, \mu_1; \mathbf{k}_2, \mu_2; \dots; \mathbf{k}_n, \mu_n\rangle \quad (3)$$

by means of a rotationless boost $B_c(V)$. Using velocity states, matrix elements of vertex operators can be simply related to appropriate interaction Lagrangean densities [4,5]

$$\langle V'; \mathbf{k}'_j, \mu'_j | \hat{K} | V; \mathbf{k}_i, \mu_i \rangle \propto V^0 \delta^3(\mathbf{V} - \mathbf{V}') \langle \mathbf{k}'_j, \mu'_j | \hat{\mathcal{L}}_{\text{int}}(0) | \mathbf{k}_i, \mu_i \rangle. \quad (4)$$

At this point it is worthwhile to remark that conservation of the overall 3-velocity at interaction vertices is a specific feature of the Bakamjian-Thomas construction and does not hold, in general, for point-form quantum-field theories. It is this overall velocity-conserving delta function that leads to wrong cluster properties, an unwanted feature of the Bakamjian-Thomas construction which is observed in any form of relativistic dynamics and is not just specific to the point form [2]. The physical consequences of wrong cluster properties in our case are that the gauge-boson-hadron vertices, which we analyze to obtain the transition form factors, may not only depend on the momenta attached to the vertex, but also on the lepton momenta. Formally such wrong cluster properties could be cured by means of, so called, "packing operators", but practically these are hard to construct. We will therefore adopt another strategy to end up with sensible results for the weak transition form factors.

Neutrino-Meson Scattering

Our first goal is to derive weak $B \rightarrow D$ transition form factors for space-like momentum transfers as they can, in principle, be measured in $\nu_e B^- \rightarrow e^- D^0$ scattering. In order to account for dynamical exchange of W -bosons we set up a 4-channel problem that includes all states which occur during such a scattering process if considered within a valence-quark picture (i.e. $|\nu_e, b, \bar{u}\rangle, |e, W^+, b, \bar{u}\rangle, |e, c, \bar{u}\rangle, |\nu_e, W^-, c, \bar{u}\rangle$). An instantaneous confinement potential between quark and antiquark is included in the diagonal entries of the matrix mass operator.

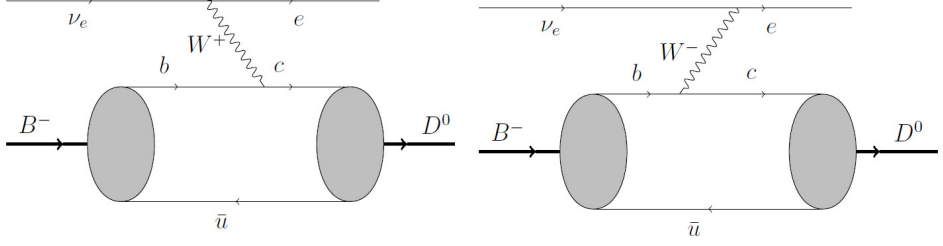


Fig. 1. Time-ordered contributions to the invariant 1W-exchange amplitude for $\nu_e B^- \rightarrow e^- D^0$ scattering.

Using perturbation theory for the weak coupling we calculate the invariant 1W-exchange amplitude for $\nu_e B^- \rightarrow e^- D^0$ scattering. It is the sum of two time-ordered contributions which are given by the (velocity-state) matrix elements

$$\begin{aligned}\Gamma_1 &= \langle V'; \mathbf{k}'_D; \mathbf{k}'_e, \mu'_e | \hat{K}_W (m - \hat{M}_{\bar{u}bW_e})^{-1} \hat{K}_W^\dagger | V; \mathbf{k}_B; \mathbf{k}_{\nu_e}, \mu_{\nu_e} \rangle, \\ \Gamma_2 &= \langle V'; \mathbf{k}'_D; \mathbf{k}'_e, \mu'_e | \hat{K}_W (m - \hat{M}_{\bar{u}cW_{\nu_e}})^{-1} \hat{K}_W^\dagger | V; \mathbf{k}_B; \mathbf{k}_{\nu_e}, \mu_{\nu_e} \rangle\end{aligned}$$

that correspond to the graphs shown in Fig. 1. As expected, the sum of both contributions is proportional to the contraction of a lepton with a meson current times the covariant W-boson propagator. This allows us to identify the weak meson current in a unique way:

$$\begin{aligned}\tilde{J}_{B \rightarrow D}^{\nu}(\mathbf{k}'_D, \mathbf{k}_B) &= \int d^3 \tilde{\mathbf{k}}'_{\bar{u}} f_{\text{kinem}} \sum_{\mu'_c \mu_b} \mathcal{W}_{\mu_b \mu'_c} \left[\tilde{u}_{\mu'_c}(\mathbf{k}'_c) \gamma^\nu \frac{1 - \gamma^5}{2} u_{\mu_b}(\mathbf{k}_b) \right] \\ &\quad \times \Psi_D^*(|\tilde{\mathbf{k}}'_{\bar{u}}|) \Psi_B(|\tilde{\mathbf{k}}_{\bar{u}}|).\end{aligned}\quad (5)$$

Momenta with a tilde refer to the $Q\bar{u}$ rest frame ($Q = b, c$), whereas momenta without tilde rather refer to the $\nu_e b\bar{u}$ or $e c\bar{u}$ rest frame, respectively. Momenta with and without tilde are connected by means of Lorentz boosts which also give rise to the Wigner-rotation factor $\mathcal{W}_{\mu_b \mu'_c}$. f_{kinem} is an uniquely determined kinematical factor (see, e.g., Ref. [7]) and Ψ_D, Ψ_B are the D- and B-meson bound-state wave functions – in our case for simplicity pure s-wave. The expression within the square brackets represents the weak quark current.

Since we have worked with a velocity-state representation the bound-state current in Eq. (5) still does not transform like a 4-vector under Lorentz transformations, it rather transforms by a Wigner rotation. Only after going back to the physical particle momenta $\mathbf{p}_B = B_c(V)\mathbf{k}_B$ and $\mathbf{p}'_D = B_c(V)\mathbf{k}'_D$ we end up with a meson current that transforms like a 4-vector:

$$J^\mu(\mathbf{p}'_D, \mathbf{p}_B) := B_c(V)^\mu{}_\nu \tilde{J}_{B \rightarrow D}^\nu(\mathbf{k}'_D, \mathbf{k}_B).\quad (6)$$

Table 1. Model parameters

| | | |
|----------------------------|-------------------------------|------------------------------|
| $M_B = 5.2795 \text{ GeV}$ | $M_D = 1.869 \text{ GeV}$ | $M_\pi = 0.1396 \text{ GeV}$ |
| $m_b = 4.8 \text{ GeV}$ | $m_d, m_u = 0.25 \text{ GeV}$ | $m_c = 1.6 \text{ GeV}$ |
| $\alpha_B = 0.55$ | $\alpha_D = 0.46$ | $\alpha_\pi = 0.33$ |

For pseudoscalar to pseudoscalar transitions the covariant decomposition of this current reads [8]:

$$J^\mu(\mathbf{p}'_D, \mathbf{p}_B) = \left[(\mathbf{p}_B + \mathbf{p}_D) - \frac{m_B^2 - m_D^2}{q^2} \mathbf{q} \right]^\mu F_1(Q^2, s) + \frac{m_B^2 - m_D^2}{q^2} q^\mu F_0(Q^2, s). \quad (7)$$

The physical consequences of wrong cluster properties, inherent in the Bakamjian-Thomas construction, become obvious in this decomposition. The form factors cannot be chosen such that they are functions of the squared 4-momentum transfer at the W -meson vertex, they also depend on Mandelstam s , i.e. the invariant mass squared of the whole neutrino-B-meson (or equivalently electron-D-meson) system. This does not spoil Poincaré invariance of the scattering amplitude, it just means that the WBD-vertex is also influenced by the presence of the scattering lepton. The Mandelstam- s dependence may also be interpreted as a frame dependence of the $W^*B \rightarrow D$ subprocess. We consider two extreme cases, namely the minimum value of s necessary to reach a particular $q^2 < 0$ and $s \rightarrow \infty$. The first choice corresponds to the Breit frame (BF), the second to the infinite-momentum frame (IF).

Using simple harmonic-oscillator wave functions with the oscillator parameters and masses given in Tab. 1 we obtain the results that are plotted in Figs. 2 and 3 for the $B \rightarrow D$ and, in addition, also for the $B \rightarrow \pi$ transition, respectively.¹ Whereas the differences between IF and BF are small for F_1 , they can be sizeable for F_0 .

Semileptonic Meson Decay

In the time-like momentum transfer region these form factors can be measured in semileptonic weak decay processes. Theoretically it is straightforward to adapt our relativistic multichannel approach such that one can deal with decay processes like $B \rightarrow D e \bar{\nu}_e$. Working in the velocity-state representation the decaying B-meson has to be at rest. For this kinematical situation it is, however, known from front-form calculations [11] that non-valence contributions leading to, so called, “Z-graphs” may become important. A similar observation can be made for space-like momentum transfers, if the form factors are calculated in the Breit frame. For kinematical reasons Z-graphs are, however, suppressed for space-like momentum transfers, if the form factors are calculated in the infinite-momentum

¹ The physical meson masses are the PDG values [9]. The constituent quark masses and wave-function parameters are taken from a corresponding front-form calculation [10].

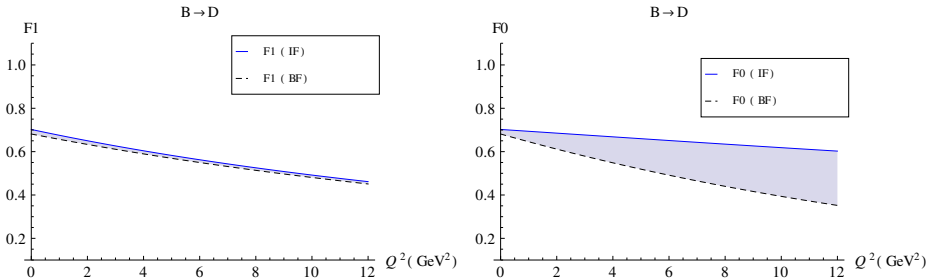


Fig. 2. The weak form factors F_1 and F_0 for the $B \rightarrow D$ transition in the space-like region as functions of $Q^2 = -(\mathbf{p}_B - \mathbf{p}'_D)^2$. The solid and dashed lines refer to calculations in the infinite momentum frame and the Breit frame, respectively. The shaded area indicates the frame dependence caused by the violation of cluster separability.

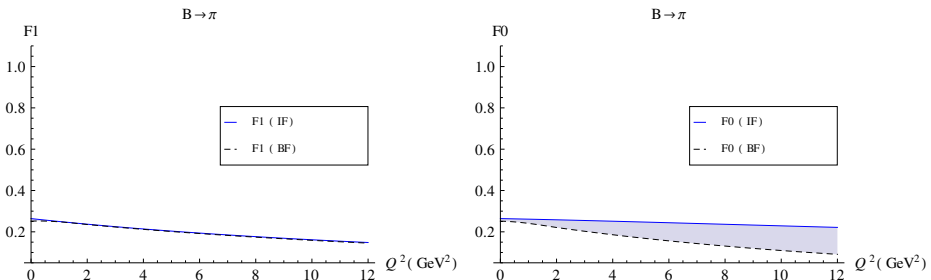


Fig. 3. Same as in Fig. 2, but for the $B \rightarrow \pi$ transition.

frame. In order to avoid problems with Z-graphs it is thus suggestive to take the form factor expressions obtained in the IF for space-like momentum transfers and continue them analytically to time-like momentum transfers by the replacement $Q \rightarrow iQ$. This is done in Figs. 4 and 5 for the $B \rightarrow D$ and $B \rightarrow \pi$ transitions, respectively (solid lines). In these figures the results of a direct decay calculation [7] (Z-graphs absent) are also shown (dashed lines). The differences may be considered as an estimate of the size of Z-graph (or “quark-pair”) contributions. From the considerations just made it is clear that the solid line should be closer to experiment than the dashed one. This is indeed the case. What one knows experimentally is the slope of F_1 at zero recoil as measured in $B \rightarrow D e \bar{\nu}_e$ decays. It agrees approximately with the value which we get from our analytic continuation, whereas the decay calculation provides a much smaller value.

Outlook

Our next task is now the explicit inclusion of Z-graphs in the decay calculation. A typical Z-graph contribution to the $B \rightarrow D e \bar{\nu}_e$ decay is shown in Fig. 6. The non-valence contribution is easily accommodated within our coupled-channel approach, but in addition one has to say, how the $c\bar{c}$ -pair is created. We plan to use a simple 3P_0 pair-creation model [12]. In this way we hope to achieve a

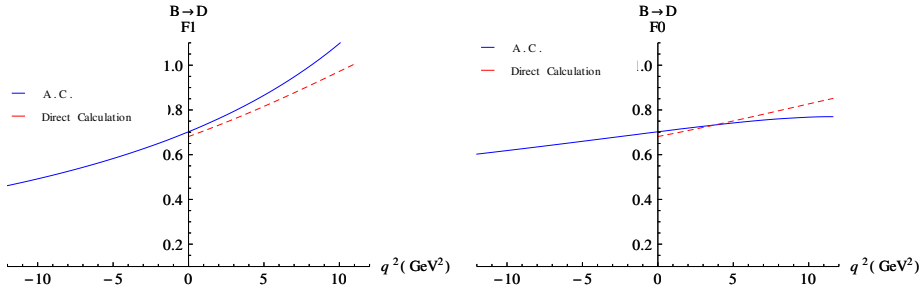


Fig. 4. The weak form factors F_1 and F_0 for the $B \rightarrow D$ transition for space- and time-like momentum transfers. The solid line refers to the analytic continuation from space- to time-like momentum transfers by making the replacement $Q \rightarrow iQ$ in the IF result. The dashed line is the outcome of a decay calculation in the B rest frame [7].

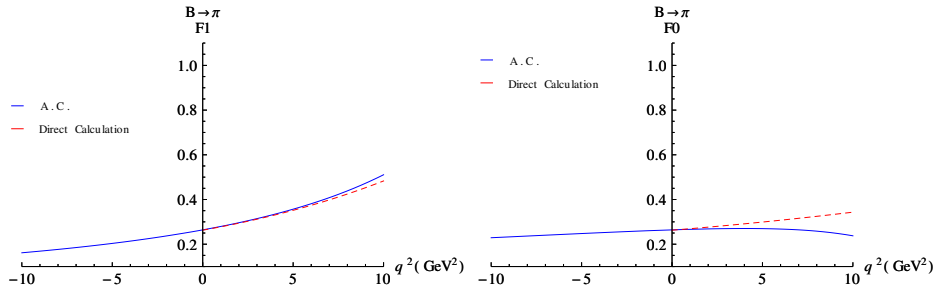


Fig. 5. Same as in Fig. 4, but for the $B \rightarrow \pi$ transition.

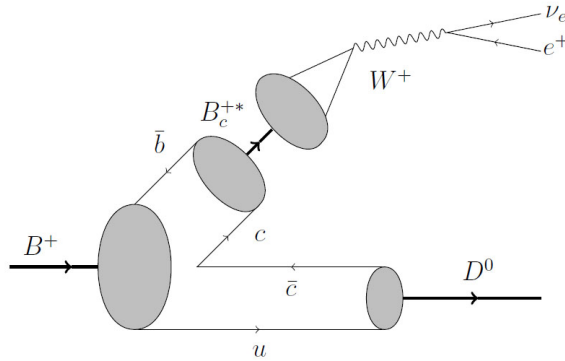


Fig. 6. Z -graph contribution to the $1W$ -exchange amplitude of the semileptonic $B \rightarrow D e \bar{\nu}_e$ decay

more quantitative estimate of Z -graph contributions in weak meson decay form factors.

References

1. B. Bakamjian and L. H. Thomas, Phys. Rev. 92, 1300 (1953).

2. B. D. Keister and W. N. Polyzou, *Adv. Nucl. Phys.* 20, 225 (1991).
3. P. A. M. Dirac, *Rev. Mod. Phys.* 21, 392 (1949).
4. W. H. Klink, *Nucl. Phys.* A716, 123 (2003).
5. E. P. Biernat, "Electromagnetic properties of few-body systems within a point-form approach", PhD thesis, University Graz (2011), arXiv:nucl-th/1110.3180.
6. W. H. Klink, *Phys. Rev.* C58, 3617 (1998).
7. M. Gomez-Rocha and W. Schweiger, *Phys. Rev.* D86, 053010 (2012).
8. M. Wirbel, B. Stech and M. Bauer, *Z. Phys.* C29, 637 (1985).
9. J. Beringer et al. [Particle Data Group], *Phys. Rev.* D86, 010001 (2012).
10. H.-Y. Cheng, C.-Y. Cheung and C.-W. Hwang, *Phys. Rev.* D55, 1559 (1997).
11. H.-M. Choi and C.-R. Ji, *Nucl. Phys.* A679, 735 (2001).
12. J. Segovia, D.R. Entem and F. Fernández, *Phys. Lett.* B715, 322 (2012).



Large N_c baryons and Regge trajectories*

N. Matagne^a and Fl. Stancu^b

^a Service de Physique Nucléaire et Subnucléaire, University of Mons, Place du Parc, B-7000 Mons, Belgium,

^b Institute of Physics, B5, University of Liège, Sart Tilman, B-4000 Liège 1, Belgium

Abstract. The mixed symmetric positive and negative parity baryons are described in a similar way in the $1/N_c$ expansion method of QCD by using a procedure where the permutation symmetry is incorporated exactly. This allows to express the mass formula in terms of a small number of linearly independent operators. We show that the leading term follows a different Regge trajectory from that found for symmetric states, when plotted as a function of the band number N .

1 Introduction

The large N_c or alternatively the $1/N_c$ expansion method of QCD [1] became a valuable and systematic tool to study baryon properties in terms of the parameter $1/N_c$ where N_c is the number of colors. According to Witten's intuitive picture [2], a baryon containing N_c quarks is seen as a bound state in an average self-consistent potential of a Hartree type and the corrections to the Hartree approximation are of order $1/N_c$. Also, it has been shown that QCD has an exact contracted $SU(2N_f)_c$ symmetry when $N_c \rightarrow \infty$, N_f being the number of flavors [3,4]. For ground state baryons the $SU(2N_f)$ symmetry is broken by corrections proportional to $1/N_c$ [5,6].

For excited states the symmetry has to be extended to $SU(2N_f) \times O(3)$. In the spirit of the Hartree approximation a procedure for constructing large N_c baryon wave functions with mixed symmetric spin-flavor parts has been proposed [7] and an operator analysis was performed for $\ell = 1$ baryons [8]. It was proven that, for such states, the $SU(2N_f)$ breaking occurs at order N_c^0 , instead of $1/N_c$, as for the ground and symmetric excited states [9,10]. The procedure has been extended to positive parity nonstrange baryons belonging to the $[70, \ell^+]$ with $\ell = 0$ and 2 [11].

More recently the $[70, 1^-]$ multiplet was reanalyzed by using an exact wave function, instead of the Hartree-type wave function, with the Pauli principle satisfied at any stage of the calculations [12]. The novelty was that the isospin-isospin term, neglected previously [8] becomes as dominant in Δ resonances as the spin-spin term in N^* resonances.

* Talk delivered by Fl. Stancu

In the present work we follow the approach of Ref. [12] both for positive and negative parity mixed symmetric states and compare the leading mass term with that of symmetric states. We show that in each case it follows a distinct Regge trajectory as a function of the band number.

Evidence for Regge trajectories in large N_c QCD is of current interest for mesons and glueballs as well, as shown, for example, in Ref. [13].

2 The mass operator

The most general form of the mass operator is [14]

$$M = \sum_i c_i O_i + \sum_i d_i B_i. \quad (1)$$

The formula contains two types of terms. In the first category are the operators O_i , which are invariant under $SU(N_f)$ and are defined as

$$O_i = \frac{1}{N_c^{n-1}} O_\ell^{(k)} \cdot O_{SF}^{(k)}, \quad (2)$$

where $O_\ell^{(k)}$ is a k -rank tensor in $SO(3)$ and $O_{SF}^{(k)}$ a k -rank tensor in $SU(2)$ -spin. For the ground state one has $k = 0$. The excited states also require $k = 1$ and $k = 2$ terms. The rank $k = 2$ tensor operator of $SO(3)$ is

$$L^{(2)ij} = \frac{1}{2} \{L^i, L^j\} - \frac{1}{3} \delta_{i,-j} \mathbf{L} \cdot \mathbf{L}, \quad (3)$$

which acts on the orbital wave function $|\ell m_\ell\rangle$ of the whole system of N_c quarks. The second category are the operators B_i which are $SU(3)$ breaking and are defined to have zero expectation values for non-strange baryons.

3 Symmetric states

If an excited baryon belongs to a symmetric [56]-plet the three-quark system can be treated similarly to the ground state in the flavour-spin degrees of freedom, but one has to take into account the presence of an orbital excitation in the space part of the wave function [9, 10]. As an example, in Table 1 we reproduce the results of Ref. [10] for [56, 4⁺] where $\chi_{\text{dof}}^2 = 0.26$. One can see that the number of dominant operators turns out to be very small. The first operator is a spin-flavor singlet of order $\mathcal{O}(N_c)$. This is the leading operator in the mass formula, needed for obtaining the Regge trajectories below. As compared to the ground state, there is one more operator needed for excited symmetric states. This is the spin-orbit operator O_2 . Note that in the case of symmetric states this is order $\mathcal{O}(1/N_c)$. For a symmetric spin-flavor state the matrix elements of the spin operator O_3 are identical to those of the flavor operator defined as $\frac{1}{N_c} T^\alpha T^\alpha$. As we shall see below, this is not the case for mixed symmetric states. The operator B_1 is defined as the negative of the strangeness S .

Table 1. List of dominant operators and their coefficients in the mass formula (1) for the multiplet $[56, 4^+]$ (from Ref. [10]).

| Operator | Fitted coef. (MeV) |
|-------------------------------|--------------------|
| $O_1 = N_c \mathbf{1}$ | $c_1 = 736 \pm 30$ |
| $O_2 = \frac{1}{N_c} L^i S^i$ | $c_2 = 4 \pm 40$ |
| $O_3 = \frac{1}{N_c} S^i S^i$ | $c_3 = 135 \pm 90$ |
| $B_1 = -S$ | $d_1 = 110 \pm 67$ |

4 Mixed symmetric states

There are two ways of studying mixed symmetric [70]-plets. The standard one is inspired by the Hartree approximation [7] where an excited baryon is described by a symmetric core plus an excited quark, see *e.g.* [8, 11, 15, 16].

As an alternative, in Ref. [12] we have proposed a method where all identical quarks are treated on the same footing and we deal with an exact wave function in the orbital-flavor-spin space. The procedure has been successfully applied to the $N = 1, 2$ and 3 bands [17–20]. In Table 2 we illustrate it by the results obtained in Ref. [19] for the mixed symmetric states $[70, \ell^+]$ with $\ell = 0, 2$ of the $N = 2$ band. The leading operator O_1 is the same as above. On the other hand we identify the spin-orbit operator O_2 with the the single-particle operator

$$\ell \cdot s = \sum_{i=1}^{N_c} \ell(i) \cdot s(i), \quad (4)$$

the matrix elements of which are of order N_c^0 . The analytic expression of the matrix elements of O_2 can be found in the Appendix A of Ref. [8]. Similarly, we ignore the two-body part of the spin-orbit operator as being of a lower order. The spin operator O_3 and the flavor operator O_4 are two-body and linearly independent. The expectation value of O_3 is $\frac{1}{N_c} S(S+1)$ where S is the spin of the entire system of N_c quarks. The expression of the operator O_4 given in Table 2 is consistent with the usual $1/N_c(T^a T^a)$ definition in $SU(4)$. In extending it to $SU(6)$ we had to subtract the quantity $(N_c + 6)/12$ as explained in Ref. [17].

By construction, the operators O_5 and O_6 have non-vanishing contributions for orbitally excited states only. They are also two-body, which means that they carry a factor $1/N_c$ in the definition. The operator O_6 contains the irreducible spherical tensor (3) and the $SU(6)$ generator G^{j^a} both acting on the whole system. The latter is a coherent operator which introduces an extra power N_c so that the order of the matrix elements of O_6 is $\mathcal{O}(1)$.

Table 2 gives three distinct numerical fits which suggest that O_5 is not so important but O_6 is crucial in obtaining a satisfactory χ_{dof}^2 . The Fit 2 is used in Fig. 1.

Table 2. List of dominant operators and the corresponding coefficients, c_i or d_i , in the mass formula (1) obtained in three distinct numerical fits for $[70, \ell^+]$ with $\ell = 0, 2$ [19].

| Operator | Fit 1 | Fit 2 | Fit 3 |
|--|---------------|--------------|---------------|
| $O_1 = N_c \mathbf{1}$ | 616 ± 11 | 616 ± 11 | 616 ± 11 |
| $O_2 = \ell^i s^i$ | 150 ± 239 | 52 ± 44 | 243 ± 237 |
| $O_3 = \frac{1}{N_c} S^i S^i$ | 149 ± 30 | 152 ± 29 | 136 ± 29 |
| $O_4 = \frac{1}{N_c} [T^a T^a - \frac{1}{12} N_c (N_c + 6)]$ | 66 ± 55 | 57 ± 51 | 86 ± 55 |
| $O_5 = \frac{3}{N_c} L^i T^a G^i$ | -22 ± 5 | | -25 ± 52 |
| $O_6 = \frac{15}{N_c} L^{(2)ij} G^{ia} G^{ja}$ | 14 ± 5 | 14 ± 5 | |
| $B_1 = -S$ | 23 ± 38 | 24 ± 38 | -22 ± 35 |
| χ_{dof}^2 | 0.61 | 0.52 | 2.27 |

5 Regge trajectories

The linear Regge trajectories are a manifestation of the nonperturbative aspect of QCD dynamics, which at long distance becomes dominated by the confinement [21]. In our previous studies we have tried to establish a connection between the $1/N_c$ method and a simple semi-relativistic quark model with a Y-junction confinement potential plus a hyperfine interaction generated by one gluon exchange [22,23]. We showed that the band number N emerged naturally from both approaches so that one can plot the coefficients c_i as a function of N . Also we found that c_1 contains the effect of kinetic energy and the confinement.

Presently, we have a consistent description of mixed symmetric positive and negative parity states corresponding to $N = 1, 2$ and 3 bands. It is interesting to revisit the Regge trajectory problem [22,23]. In Fig. 1 we plot c_1^2 as a function of the band number N for $N \leq 4$. One can see that two distinct trajectories emerge from this new picture, one for symmetric [56]-plets, the other for mixed symmetric [70]-plets. This behavior is different from that found in Refs. [22,23] but reminds that of Ref. [24] where the symmetric and mixed symmetric states have distinct trajectories for $(N_c c_1)^2$ as a function of the angular momentum $\ell \leq 6$ (Chew-Frautschi plots). Note that in Ref. [24] the mixed symmetric states were described within the ground state core + excited quark approach. The mass operator was reduced to the $\mathcal{O}(N_c)$ spin-flavor singlet, the $\mathcal{O}(1/N_c)$ hyperfine spin-spin interaction, acting between core quarks only, and $SU(3)$ breaking terms. There are no $\mathcal{O}(N_c^0)$ contributions. For a consistent treatment, in Ref. [24] the hyperfine interaction was restricted to core quarks in symmetric states as well.

In our case, the symmetric and mixed symmetric states are treated on an equal basis: there is no distinction between the core and an excited quark (the core may be excited as well), and the Pauli principle is always fulfilled. The existence of two distinct Regge trajectories, one for symmetric, another for mixed

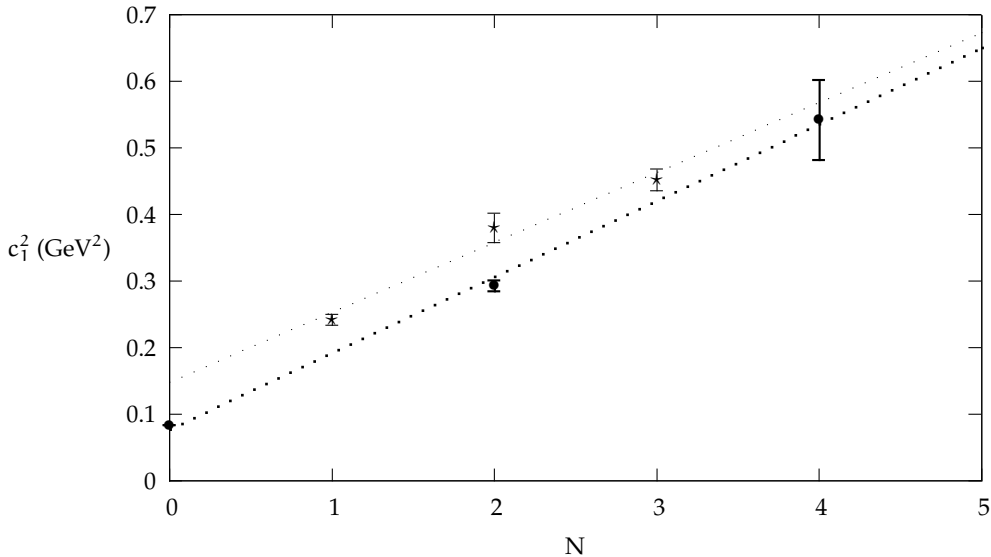


Fig. 1. The coefficient c_1^2 (GeV²) as a function of the band number N . The numerical values of c_1 were taken from Ref. [22] for $N = 0$, from Ref. [18] Fit 3 for $N = 1$, from Ref. [9] for $N = 2$ [56, 2⁺], from Ref. [19] Fit 2 for $N = 2$ [70, ℓ^+] ($\ell = 0, 2$), from Ref. [20] Fit 3 for $N = 3$ [70, ℓ^-] ($\ell = 1, 2, 3$), from Ref. [10] for $N = 4$ [56, 4⁺]. The heavy dots refer to [56]-plets and the stars to [70]-plets. The best fit of these data was obtained with two distinct linear trajectories.

symmetric states, may be due to their distinct structure in the orbital-spin-flavor space.

We are most grateful to Willi Plessas for useful comments.

References

1. G. 't Hooft, Nucl. Phys. **72** (1974) 461.
2. E. Witten, Nucl. Phys. **B160** (1979) 57.
3. J. L. Gervais and B. Sakita, Phys. Rev. Lett. **52** (1984) 87; Phys. Rev. **D30** (1984) 1795.
4. R. Dashen and A. V. Manohar, Phys. Lett. **B315** (1993) 425; *ibid* **B315** (1993) 438.
5. R. F. Dashen, E. Jenkins and A. V. Manohar, Phys. Rev. **D51** (1995) 3697.
6. E. Jenkins, Ann. Rev. Nucl. Part. Sci. **48** (1998) 81; AIP Conference Proceedings, Vol. 623 (2002) 36, arXiv:hep-ph/0111338; PoS E **FT09** (2009) 044 [arXiv:0905.1061 [hep-ph]].
7. J. L. Goity, Phys. Lett. **B414** (1997) 140.
8. C. E. Carlson, C. D. Carone, J. L. Goity and R. F. Lebed, Phys. Rev. **D59** (1999) 114008.
9. J. L. Goity, C. Schat and N. N. Scoccola, Phys. Lett. **B564** (2003) 83.
10. N. Matagne and F. Stancu, Phys. Rev. **D71** (2005) 014010.
11. N. Matagne and F. Stancu, Phys. Lett. **B631** (2005) 7.
12. N. Matagne and F. Stancu, Nucl. Phys. A **811** (2008) 291.
13. M. Bochicchio, arXiv:1308.2925 [hep-th].
14. E. Jenkins and R. F. Lebed, Phys. Rev. **D52** (1995) 282.

15. C. L. Schat, J. L. Goity and N. N. Scoccola, *Phys. Rev. Lett.* **88** (2002) 102002; J. L. Goity, C. L. Schat and N. N. Scoccola, *Phys. Rev.* **D66** (2002) 114014.
16. N. Matagne and F. Stancu, *Phys. Rev.* **D74** (2006) 034014; *Nucl. Phys. Proc. Suppl.* **174** (2007) 155.
17. N. Matagne and F. Stancu, *Nucl. Phys. A* **826** (2009) 161.
18. N. Matagne and F. Stancu, *Phys. Rev. D* **83** (2011) 056007.
19. N. Matagne and F. Stancu, *Phys. Rev. D* **87** (2013) 076012.
20. N. Matagne and F. Stancu, *Phys. Rev. D* **85** (2012) 116003.
21. A. Karch, E. Katz, D. T. Son and M. A. Stephanov, *Phys. Rev. D* **74** (2006) 015005.
22. C. Semay, F. Buisseret, N. Matagne and F. Stancu, *Phys. Rev. D* **75** (2007) 096001.
23. F. Buisseret, C. Semay, F. Stancu and N. Matagne, *Proceedings of the Mini-workshop Bled 2008, "Few Quark States and the Continuum"*, *Bled Workshops in Physics*, vol. 9, no. 1, eds. B. Golli, M. Rosina and S. Sirca. arXiv:0810.2905 [hep-ph].
24. J. L. Goity and N. Matagne, *Phys. Lett. B* **655**, 223 (2007).



Electroexcitation of the D-wave resonances*

Bojan Golli^{a,c} and Simon Širca^{b,c}

^a Faculty of Education, University of Ljubljana, 1000 Ljubljana, Slovenia

^b Faculty of Mathematics and Physics, University of Ljubljana, 1000 Ljubljana, Slovenia

^c Jožef Stefan Institute, 1000 Ljubljana, Slovenia

Abstract. The meson scattering and electroproduction amplitudes in the D13, D33 and D15 partial waves are calculated in a coupled-channel approach incorporating quasi-bound quark-model states. In contrast to our previous results involving the P11, P33 and S11 partial waves the meson and photon couplings obtained in the quark model turned out to be underestimated, but otherwise our results exhibit a consistent behaviour in all channels.

We have developed a coupled-channel formalism which provides a unified treatment of meson scattering and electroproduction. The formalism incorporates in a consistent way quark-model resonance states as excitations of the quark core supplemented by a meson cloud. The approach has been used to systematically study the interplay of quark and meson degrees of freedom in the region of the low lying nucleon resonances as well as in the intermediate region.

In our earlier work we have pointed out the important role of the pion cloud in the electro-excitation of the $\Delta(1232)$ resonance in which case the cloud contributes almost a half to the strength of the M_{1+} amplitude and dominates the E_{1+} amplitude [1–3]. Next we have investigated the meson degrees of freedom in the case of the $N(1440)$ resonance [4] and confirmed the important contribution of the σN and $\pi\Delta$ inelastic channels to scattering in the P11 partial wave [5]. We have further demonstrated that the zero crossing of the helicity amplitude for electroexcitation of the Roper resonance at $Q^2 \approx 0.5 \text{ GeV}^2/c^2$ can be explained as an effect of the pion cloud which dominates the amplitude at small Q^2 and has the opposite sign with respect to the contribution of the quark core [6].

In the case of the negative parity resonances in the S11 partial wave we have shown that the quark model extended to pseudoscalar meson octet correctly predicts the behaviour of the πN and ηN amplitudes in the region of the lower resonance as well as the admixture of the $K\Lambda$ channel at somewhat higher energies [7–9].

In the recent work [10, 11] we have applied the same formalism to the description of scattering and electroproduction of mesons in the resonance region in the D13, D33 and D15 partial waves. In contrast to our results for the P11, P33 and S11 resonances, the results for the D-wave resonances show a more pronounced

* Talk delivered by Bojan Golli

disagreement with experiment, in particular for the prediction of the d-wave meson coupling to the quark core. The model predicts too small helicity amplitudes – though in accordance with other quark model calculations – and consequently also the electro-production amplitudes for the considered resonances. Nonetheless, our calculation exhibits a consistent overall qualitative agreement with the multipole analysis in the D13, D33 and D15 partial waves. Our results, in particular for the D33 wave, show that the meson cloud effects are important in describing the long-range part of the wave-function. We expect that a more elaborate description of the quark core, supplemented by the meson cloud, may eventually bring the results in the ballpark of acceptable values.

References

1. M. Fiolhais, B. Golli, S. Širca, *Phys. Lett. B* **373**, 229 (1996)
2. B. Golli, S. Širca, L. Amoreira, M. Fiolhais *Phys. Lett. B* **553** (2003) 51-60
3. P. Alberto, L. Amoreira, M. Fiolhais, B. Golli, and S. Širca, *Eur. Phys. J. A* **26**, 99 (2005).
4. P. Alberto, M. Fiolhais, B. Golli, and J. Marques, *Phys. Lett. B* **523**, 273 (2001).
5. B. Golli and S. Širca, *Eur. Phys. J. A* **38**, (2008) 271.
6. B. Golli, S. Širca, and M. Fiolhais, *Eur. Phys. J. A* **42**, 185 (2009)
7. B. Golli, S. Širca, *Eur. Phys. J. A* **47** (2011) 61.
8. B. Golli, talk given at the 6th International Workshop on Pion-Nucleon Partial-Wave Analysis and the Interpretation of Baryon Resonances, 23–27 May, 2011, Washington, DC, U.S.A., http://gwdac.phys.gwu.edu/pwa2011/Thursday/b_golli.pdf
9. Simon Širca, Bojan Golli, Manuel Fiolhais and Pedro Alberto, in *Proceedings of the XIV International Conference on Hadron Spectroscopy (hadron2011)*, Munich, 2011, edited by B. Grube, S. Paul, and N. Brambilla, eConf C110613 (2011) [<http://arxiv.org/abs/1109.0163>].
10. B. Golli, S. Širca, *Eur. Phys. J. A* **49** (2013) 111.
11. B. Golli, talk given at the 7th International Workshop on Pion-Nucleon Partial-Wave Analysis and the Interpretation of Baryon Resonances, 23–27 September 2013, Camogli, Italy, http://www.ge.infn.it/pwa7/talks/20_golli.pdf



New results on quarkonium spectroscopy and exotic quarkonium-like resonances at B-factories*

Marko Petrič**

Jožef Stefan Institute, Ljubljana, Slovenia

Abstract. These proceedings covers recent results from spectroscopy measurements with data collected at the Belle experiment, which has been operating at the KEKB asymmetric e^+e^- collider at KEK in Tsukuba, Japan. The data sample can be used for various novel searches in spectroscopy. The paper discusses the discovery of exotic Z_b states, the measurement of radiative $h_b(1, 2P) \rightarrow \eta_b(1, 2S)$ transitions including the first evidence for the $h_b(2S)$ state, and the discovery of the charmed state $Z^+(3900)$.

1 Introduction

The Belle experiment [1] was taking data between 1999 and 2010 at the asymmetric e^+e^- collider KEKB [2] in Tsukuba, Japan. During this time more than 1 ab^{-1} of data was collected, mostly at the $\Upsilon(4S)$ resonance, but also on resonances $\Upsilon(1S)$, $\Upsilon(2S)$ and $\Upsilon(5S)$, as well as in the nearby continuum. The Belle detector was a large-solid-angle magnetic spectrometers that consisted of Drift Chambers, a silicon vertex detectors [3], an electromagnetic calorimeter and a superconducting solenoid that provided a 1.5 T magnetic field. The amount of collected experimental data and superb detector performance enables many interesting analyses, including searches for new hadronic states and studies of their properties. In this paper we will cover interesting spectroscopic measurements performed of charmonium(-like) and bottomonium(-like) states.

2 Discovery of charged and neutral Z_b states

In the past years a myriad of new exotic states has been discovered at different experiments and different energies. A broad selection of interpretations for these states is being proposed, e.g. molecules of mesons, tetraquarks or hadrocharmonia [4]. The observed high rate of $\Upsilon(5S) \rightarrow h_b(mP)\pi^+\pi^-$ ($m = 1, 2$) decays, which is expected to be suppressed compared to $\Upsilon(5S) \rightarrow \Upsilon(nS)\pi^+\pi^-$ ($n = 1, 2, 3$) decays, since it requires a spin flip of one bottom quark [5] is a clear sign of an exotic decay mechanism in $\Upsilon(5S)$ decays. Consequent studies of $\Upsilon(5S)$ decays have shown the existence of two new charged states, $Z_b^+(10610) \equiv Z_{b1}^+$

* Talk delivered by Marko Petrič

** on behalf of the Belle Collaboration

and $Z_b^+(10650) \equiv Z_{b2}^+$. These studies are based on the known initial energy at B-factories to observe unreconstructed particles in the recoil mass distribution of the reconstructed particles:

$$M_{\text{miss}}^{\text{recoil}} = \sqrt{((E_{\text{beam}} - E_{\text{recon}})^2 - p_{\text{recon}}^2)} \quad ,$$

where E_{beam} is half of the centre of mass energy, and all quantities are boosted to the centre of mass system of the colliding beams. This technique is not applicable in measurements at hadron colliders like the LHC. A direct observation of the Z^+

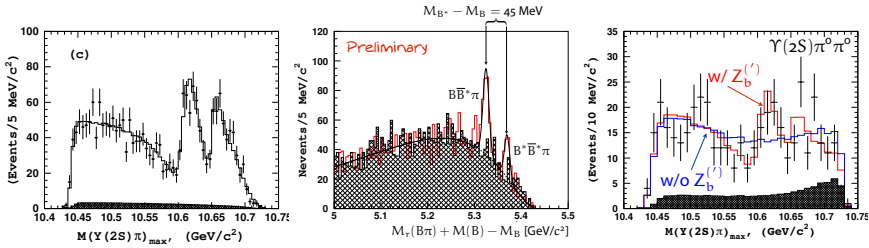


Fig. 1. Discovery of the Z_b states; (LEFT) $M(\Upsilon(2S)\pi)_{\text{max}}$ spectrum in reconstructed $\Upsilon(5S) \rightarrow \Upsilon(2S)\pi^+\pi^-$ decays [6], (MIDDLE) M_{mis} spectrum of reconstructed $\Upsilon(5S) \rightarrow B\pi X$ decays [7], (RIGHT) $M(\Upsilon(2S)\pi)_{\text{max}}$ distribution in reconstructed $\Upsilon(5S) \rightarrow \Upsilon(2S)\pi^0\pi^0$ decays [8].

signals is possible in the $M(\Upsilon(nS)\pi)_{\text{max}}$ distributions of exclusively reconstructed $\Upsilon(5S) \rightarrow \Upsilon(nS)[\mu^+\mu^-]\pi^+\pi^-$ decays (Figure 1). The subscript ‘max’ denotes the choice of the $\Upsilon\pi$ combination with the higher invariant mass. A Dalitz analysis with non-resonant Z_{b1}^+ , Z_{b2}^+ , $f_0(980)$ and $f_2(1270)$ components in the variables $M^2(\Upsilon(\pi S)\pi^+)_{\text{max}} \times M^2(\pi^+\pi^-)$ favours the quantum numbers $I^G(J^P) = 1^+(1^+)$. This hypothesis is supported by a more complex six dimensional Dalitz analysis. During the analysis of the decays $\Upsilon(5S) \rightarrow Z_{b1,2}[h_b(mP)\pi^\mp]\pi^\pm$ the recoil mass technique is applied twice: firstly the $h_b(mP)$ yield is determined from fits to the M_{mis} spectrum, which are performed in bins of M_{mis} , where the Z^+ mass peaks can be observed. The measured masses and the widths of the Z_{b1}^+ and Z_{b2}^+ are in agreement for all channels. The averages are [6]:

$$\begin{aligned} Z_{b1}^+ & : \quad M = (10607.2 \pm 2.0)\text{MeV}/c^2 \quad \Gamma = (18.4 \pm 2.5)\text{MeV} \quad , \\ Z_{b2}^+ & : \quad M = (10652.2 \pm 1.5)\text{MeV}/c^2 \quad \Gamma = (11.5 \pm 2.2)\text{MeV} \quad . \end{aligned}$$

The observed new states have a mass close to the mass of B^*B and B^*B^* pairs suggesting a molecular structure. In the analyses of decays $\Upsilon(5S) \rightarrow B\pi^\pm X$ transitions of $Z_{b1,2}$ to $B^{(*)}\bar{B}^*$ are observed, where the B is a fully reconstructed B^+ or B^0 meson. The second B is measured in the recoil mass $M_{\text{mis}}^{B\pi}$ distribution (Figure 1). The determined branching fractions are $\mathcal{B}(\Upsilon(5S) \rightarrow BB\pi) < 0.60\%$ at 90% C. L., $\mathcal{B}(\Upsilon(5S) \rightarrow BB^*\pi) = (4.25 \pm 0.44 \pm 0.69)\%$ and $\mathcal{B}(\Upsilon(5S) \rightarrow B^*B^*\pi) = (2.12 \pm 0.29 \pm 0.36)\%$. To address the question if these decays proceed via the intermediate $Z_{b1,2}^+$ states an amplitude analysis of the M_{mis} distributions in the B

and B^* signal regions of M_{mis} was made. It is found that the $BB^*\pi$ sample can be described by the sum of a Z_{b1}^+ and a Z_{b2}^+ component or Z_{b1}^+ and a non-resonant component. Whereas the $B^*B^*\pi$ sample is described well by a Z_{b2}^+ alone or a Z_{b2}^+ with a non-resonant admixture. A significant $Z_{b1,2}$ signal is found in all cases. Assuming that the only decay modes are to $\Upsilon(nS)\pi^+$, $h_b(mP)\pi^+$ and $B^*\bar{B}^*$ the Z_{b1}^+ and Z_{b2}^+ states decay predominantly to BB^* and B^*B^* pairs with branching fractions of $(86.0 \pm 3.6)\%$ and $(73.4 \pm 7.0)\%$, respectively [7].

The discovery of Z states prompted the search for their neutral counterparts in fully reconstructed decays $\Upsilon(5S) \rightarrow \Upsilon(nS)[\ell^+\ell^-]\pi^0\pi^0$, where $\Upsilon(2S)$ was additionally reconstructed in the $\Upsilon(1S)[\ell^+\ell^-]\pi^+\pi^-$ channel. From fits to the M_{mis} distributions the $\Upsilon(nS)$ yields are extracted and the resulting branching fractions are $B(\Upsilon(5S) \rightarrow \Upsilon(1S)\pi^0\pi^0) = (2.25 \pm 0.11 \pm 0.20) \times 10^3$, $B(\Upsilon(5S) \rightarrow \Upsilon(2S)\pi^0\pi^0) = (3.79 \pm 0.24 \pm 0.49) \times 10^3$ and $B(\Upsilon(5S) \rightarrow \Upsilon(3S)\pi^0\pi^0) = (2.09 \pm 0.24 \pm 0.34) \times 10^3$. As in the charged channel a Dalitz analysis is performed. No significant $Z_{b1,2}^0$ signal is found in the $\Upsilon(1S)\pi^0\pi^0$ sample, nor can it be excluded. However, a Z_{b1}^0 signal is observed with in the $\Upsilon(2S)\pi^0\pi^0$ sample (4.9σ) and the $\Upsilon(3S)\pi^0\pi^0$ sample (4.3σ); with the mass being $(10609 \pm 8 \pm 6)\text{MeV}/c^2$ which is consistent with the Z_{b1}^+ mass. The Z_{b2}^0 signal was not significant (2.9σ) [8].

3 Observation of $h_b(mP) \rightarrow \eta'_b(mS)$ transitions and first evidence for $\eta_b(2S)$

Belle has recently discovered the $h_b(mP)$ states [5] which are expected to decay significantly via $h_b(mP) \rightarrow \eta_b(m'P)\gamma$. This prompted the collaboration to search for these radiative transitions [9] and the measurement of the $\eta_b(m'P)$ masses and widths in the production chain $\Upsilon(5S) \rightarrow Z_{b1,2}^+\pi^- \rightarrow h_b(mP)\pi^+\pi^-$. In this analysis only two pions and the photon from the $h_b(mP)$ decay are reconstructed. Events with a $Z_{b1,2}^+$ are selected in the $Z_{b1,2}^+$ mass window of the M_{mis} distribution and the $h_b(mP)$ yield is determined from fits to the $M_{\text{mis}}^{\pi\pi}$ distribution (Figure 2). These fits are performed in bins of $M_{\text{mis}}^{\pi\pi(m)} = M_{\text{mis}}^{\pi\pi\gamma} - M_{\text{mis}}^{\pi\pi} - M(h_b(mP))$. With the help of this transformation correlation of $M_{\text{mis}}^{\pi\pi}$ and $M_{\text{mis}}^{\pi\pi\gamma}$ in the signal region are minimised. Figure 2 shows the $\eta(2S)$ signal peak in the $M_{\text{mis}}^{\pi\pi\gamma(2)}$ distribution, which is the first evidence for this state. The measured branching fractions are $\mathcal{B}(h_b(1P) \rightarrow \eta_b(1S)\gamma) = (49.2 \pm 5.7_{-3.3}^{+5.6})\%$, $\mathcal{B}(h_b(2P) \rightarrow \eta_b(1S)\gamma) = (22.3 \pm 3.8_{-3.3}^{+3.1})\%$, $\mathcal{B}(h_b(2P) \rightarrow \eta_b(2S)\gamma) = (47.5 \pm 10.5_{-7.7}^{+6.8})\%$. The extracted masses and widths of the $\eta_b(m'S)$ states are:

$$\begin{aligned} \eta_b(1S) &: M = (9402.4 \pm 1.5 \pm 1.8)\text{MeV}/c^2 \quad \Gamma = (10.8_{-3.7}^{+4.0} \pm 4.5)\text{MeV} \quad , \\ \eta_b(2S) &: M = (9999.0 \pm 3.5_{-1.8}^{+2.8})\text{MeV}/c^2 \quad \Gamma < 24\text{MeV} \quad . \end{aligned}$$

These results are needed for the calculation of the hyperfine splitting $\Delta M_{\text{HF}}(mS) = M_{\Upsilon(mS)} - M_{\eta_b(mS)}$, through which the spin dependence of bound state energy levels can be probed, and at the same time puts a constraint on theoretical descriptions of spin-spin interactions. The results are in agreement with lattice calculations [4, 10].

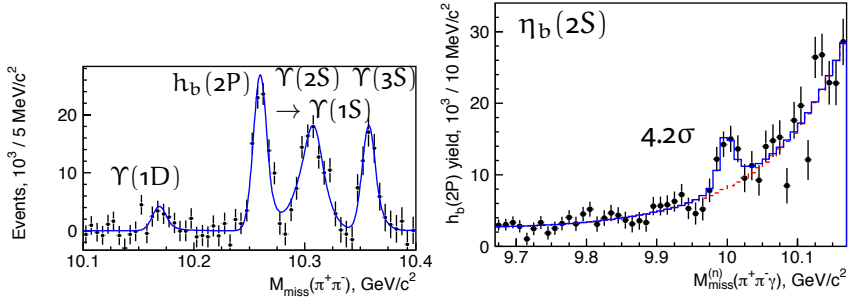


Fig. 2. Study of $\Upsilon(5S) \rightarrow \pi^+\pi^-X$; (LEFT) Distribution of the recoil mass of the two pions, after subtraction of the combinatorial background – the peaks from left to right correspond to $\Upsilon(1D)$, $h_b(2P)$, $\Upsilon(2S) \rightarrow \Upsilon(1S)$ and $\Upsilon(2S)$, (RIGHT) Yield of $h_b(2P)$ mass fits to the M_{miss} distribution in bins of $M_{\text{miss}}^{\pi\pi\gamma}$ – the significance of the $\eta_b(2S)$ peak is 4.2σ [9].

4 Observation of a Charged Charmonium-like State $Z^+(3900)$

The Belle collaboration measured the cross section for $e^+e^- \rightarrow \pi^+\pi^-J/\psi$ between 3.8 GeV and 5.5 GeV on a data sample of 967 fb^{-1} [11]. In this analysis the $Y(4260)$ state is observed, and its resonance parameters are determined. Additionally, an excess of $\pi^+\pi^-J/\psi$ production around 4 GeV is observed, which

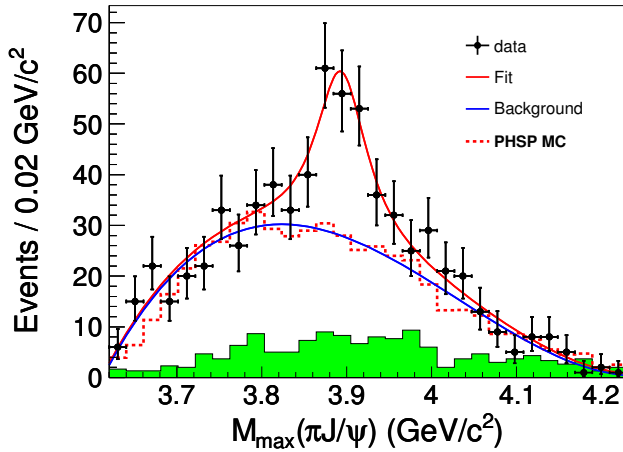


Fig. 3. Unbinned maximum likelihood fit to the distribution of the $M_{\text{max}}(\pi J/\psi)$. Points with error bars are data, the curves are the best fit, the dashed histogram is the phase space distribution and the shaded histogram is the non- $\pi^+\pi^-J/\psi$ background estimated from the normalized J/ψ sidebands [11].

was parametrized with a Breit-Wigner distribution and the results are consistent with the state $Y(4008)$ which was previously reported by Belle. In the subsequent Dalitz analysis of $Y(4260) \rightarrow \pi^+\pi^-J/\psi$ decays, the collaboration observes

a structure is in the $M(\pi^\pm J/\psi)$ mass spectrum with 5.2σ significance, with mass $M = (3894.5 \pm 6.6 \pm 4.5) \text{ MeV}/c^2$ and width $\Gamma = (63 \pm 24 \pm 26) \text{ MeV}/c^2$ [11] (Figure 3). This structure can be interpreted as a new charged charmonium-like state. This state is close to the $D\bar{D}^*$ mass threshold; however, no enhancement is observed near the $D^*\bar{D}^*$ mass threshold. Since this Z state has a strong coupling to charmonium and is charged, it can be concluded that it cannot be a conventional $c\bar{c}$ state.

References

1. A. Abashian et al., Nucl. Instrum. Methods A **479**, 117 (2002).
2. S. Kurokawa and E. Kikutani, Nucl. Instrum. Methods A **499** (2003).
3. Z. Natkaniec et al., Nucl. Instrum. Methods A **560**, 1 (2006).
4. N. Brambilla et al., Eur.Phys. J. C **71**, 1534 (2011).
5. I. Adachi et al. (Belle Collaboration), Phys. Rev. Lett. **108**, 032001 (2012).
6. A. Bondar et al. (Belle Collaboration), Phys. Rev. Lett. **108**, 122001 (2012).
7. I. Adachi et al. (Belle Collaboration), [arxiv:1209.6450](https://arxiv.org/abs/1209.6450)[hep-ph].
8. I. Adachi et al. (Belle Collaboration), [arxiv:1207.4345](https://arxiv.org/abs/1207.4345)[hep-ph].
9. R. Mizuk et al. (Belle Collaboration), Phys. Rev. Lett. **109**, 232002 (2012), [arxiv:1205.6351](https://arxiv.org/abs/1205.6351)[hep-ph].
10. S. Meinel, Phys. Rev. D **82**, 114502 (2010).
11. Z. Liu et al. (Belle Collaboration), Phys. Rev. Lett. **110**, 252002 (2013).



Charmonium-like states and K^* resonances from lattice QCD

Saša Prelovšek^{a,b}

^a Jozef Stefan Institute, Jamova 39, 1000 Ljubljana, Slovenia

^b Department of Physics, University of Ljubljana, Jadranska 19, 1000 Ljubljana, Slovenia

Abstract. I presented the first evidence for $X(3872)$ from lattice QCD, the first search for $Z_c^+(3900)$ and the first extraction of $K^*(892)$ strong decay width.

The charmonium-like state $X(3872)$ with $J^{PC} = 1^{++}$ has never been unambiguously identified from the lattice, since it was not established in addition to the discrete scattering states like DD^* . These should namely appear as energy levels with the same quantum number $J^{PC} = 1^{++}$ and are particularly important as $X(3872)$ lies almost on top of DD^* threshold. In the simulation [1] we established $X(3872)$ with $I = 0$ in addition to all the nearby DD^* and $J/\psi \omega$ scattering states for the first time. We found large and negative DD^* scattering length, which agrees with the presence of a very shallow bound state $X(3872)$ in view of the Levinson's theorem. We did not find $X(3872)$ in the $I = 1$ channel in our simulation with exact isospin.

We performed the first lattice QCD search for manifestly exotic $Z_c(3900)$ [2]. During 2013, the experiments BESIII, Belle and CLEOc reported a discovery of $Z_c^+(3900)$ in the decay to $J/\psi \pi^+$, while J and P are experimentally unknown. We simulated the most popular channel with $J^{PC} = 1^{+-}$ and $I = 1$, and we did not find a candidate for $Z_c^+(3900)$. Instead, we only found discrete scattering states DD^* and $J/\psi \pi$, which inevitably have to be present in a dynamical QCD. The possible reasons for not finding Z_c^+ may be that its quantum numbers are not 1^{+-} or that the employed interpolating fields were not diverse enough. A simulation with additional interpolating fields will be required for a more conclusive result.

The simulation of $K\pi$ scattering in p wave with $I = 1/2$ was aimed at calculating the scattering phase shift [3]. This was determined from each energy level using Luscher's relation, where we simulated scattering system with three choices of total momenta $P = 0, \frac{2\pi}{L}e_z, \frac{2\pi}{L}(e_x + e_y)$. The Breit Wigner type fit of the resulting phase shift lead the mass and the decay width (or rather the $K^* \rightarrow K\pi$) coupling that agrees with the experimental values within the errors. This presents the first lattice determination of the $K^*(892)$ strong decay width.

References

1. Sasa Prelovsek and Luka Leskovec, [arXiv:1307.5172](#).
2. Sasa Prelovsek and Luka Leskovec, [arXiv:1308.2097](#).
3. Sasa Prelovsek, Luka Leskovec, C.B. Lang and Daniel Mohler, *Phys. Rev. D* **88** (2013) 054508, [arXiv:1307.0736](#).



Pion coupling to constituent quarks versus coupling to nucleon ^{*}

Mitja Rosina^{a,b} and Bogdan Povh^c

^aFaculty of Mathematics and Physics, University of Ljubljana, Jadranska 19, P.O. Box 2964, 1001 Ljubljana, Slovenia

^bJ. Stefan Institute, 1000 Ljubljana, Slovenia

^cMax-Planck-Institut für Kernphysik, Postfach 103980, D-69029 Heidelberg, Germany

Abstract. We compare the model in which the pion cloud is coupled to individual constituent quarks with the model with pions coupled to the whole nucleon. We show that many single-particle observables such as flavour asymmetry, spin polarizations and some electroexcitation amplitudes are the same in both models. We predict that the forward proton production will distinguish between both models.

1 Introduction

The importance of the pion cloud in the nucleon has been demonstrated in the study of the magnetic polarizabilities, electroexcitation, spin properties of the nucleon [1]- [9] and, more recently, in deep inelastic scattering [10]. Adding pions either directly to constituent quarks or jointly to the nucleon improves dramatically the agreement between the quark model and experiment, as compared to the "pure" constituent quark model. We have discussed some features already at the Bled Workshop 2011 [1].

In this contribution we study the coupling of one pion either to each constituent quark or to the nucleon. We assume the spatial extent of the pions to be large so that the position of a constituent quark does not matter. Then the pions from different constituent quarks can interfere. The full expansion in terms of multipion states around a nucleon-like cluster and Δ -like cluster would be equivalent in both models. The leading term, however, differs, and we study which model is more promising when using only the leading term. The situation is reminiscent to the dilemma in atomic and nuclear physics whether it is better to use LS-coupling or jj-coupling. In our case, we ask whether it is better to first couple a pion to each quark, and then couple such constituent quarks to a nucleon, or to couple first the quarks to a nucleon cluster and then to add a pion.

^{*} Talk delivered by M. Rosina

2 The two models

The chiral constituent up-quark (u) in the “ $q\pi$ -model” can be written as

$$|u\rangle = \sqrt{\left(1 - \frac{3}{2}a\right)} |u\rangle - \sqrt{a} |d\pi^+\rangle + \sqrt{\frac{a}{2}} |u\pi^0\rangle,$$

and of the down quark (d)

$$|d\rangle = \sqrt{\left(1 - \frac{3}{2}a\right)} |d\rangle + \sqrt{a} |u\pi^-\rangle - \sqrt{\frac{a}{2}} |d\pi^0\rangle.$$

In the alternative model (“ $N\pi$ -model”) we couple the pion to the nucleon

$$|p\rangle = \sqrt{\left(1 - \frac{3}{2}\alpha\right)} |p\rangle - \sqrt{\alpha} |n\pi^+\rangle + \sqrt{\frac{\alpha}{2}} |p\pi^0\rangle.$$

The basis of pure flavour quarks (or nucleons) is denoted by boldface u , d , p and n . The pions are assumed to be in a p -state and Clebsch-Gordan-coupled with the quark (or nucleon) to isospin and spin $1/2$. The isospin coupling is written explicitly and the spin coupling is tacitly assumed.

3 The flavour and spin observables

Structure functions of quarks in the nucleon refer to the number of quarks per the fraction of the nucleon momentum x they carry. The quark symbol indicates the quark flavour. Integrated values (total quark numbers) are denoted by the symbol alone ($u = \int_0^1 u(x)$, etc.). Structure functions are determined from electron and neutrino scattering.

The quantities without superscript p or n refer to proton. Isospin symmetry is assumed: $u^n = d$, $d^n = u$ and $s^n = s$.

$$\hat{u}(x) = u(x) + \bar{u}(x).$$

$$u = u^\uparrow + u^\downarrow, \quad d = d^\uparrow + d^\downarrow, \quad s = s^\uparrow + s^\downarrow;$$

$$\Delta u = u^\uparrow - u^\downarrow, \quad \Delta d = d^\uparrow - d^\downarrow, \quad \Delta s = s^\uparrow - s^\downarrow.$$

Particularly interesting are the polarized structure functions $I_p = g_1^p$ and $I_{\text{deuteron}} = \frac{1}{2}(I_p + I_n)$, the quark spin contribution to the nucleon spin $\Delta\Sigma = \Delta\hat{u} + \Delta\hat{d} + \Delta\hat{s}$, as well as the *Gottfried sum rule* which expresses the flavour asymmetry of the nucleon sea

$$\text{Gottfried} = I_G = 2(F_1^p - F_1^n) = \frac{1}{3}(\hat{u} - \hat{d}) = \frac{1}{3} + \frac{2}{3}(\bar{u} - \bar{d}).$$

Here $F_1^p = \frac{1}{2}(\frac{4}{9}\hat{u} + \frac{1}{9}\hat{d} + \frac{1}{9}\hat{s})$ and $F_1^n = \frac{1}{2}(\frac{4}{9}\hat{d} + \frac{1}{9}\hat{u} + \frac{1}{9}\hat{s})$ refer to the unpolarized structure functions. It should be noted that also the “low-energy observable”, the

| observable | definition | model value | |
|-------------------------------------|--|---------------------------------------|---------|
| $g_A = 1.269 \pm 0.003$ | $\Delta u - \Delta d$ | $\frac{5}{3}(1 - \frac{4}{3}\alpha)$ | = input |
| $I_G = 0.216 \pm 0.033$ | $\frac{1}{3} + \frac{2}{3}(\bar{u} - \bar{d})$ | $\frac{1}{3}(1 - 2\alpha)$ | = 0.214 |
| $I_p = 0.120 \pm 0.017$ | $\frac{1}{2}(\frac{4}{9}\Delta u + \frac{1}{9}\Delta d)$ | $\frac{5}{18}(1 - \frac{5}{3}\alpha)$ | = 0.194 |
| $I_{\text{deut}} = 0.043 \pm 0.006$ | $\frac{5}{36}(\Delta u + \Delta d)$ | $\frac{5}{36}(1 - 2\alpha)$ | = 0.089 |
| $\Delta\Sigma = 0.330 \pm 0.064$ | $\Delta u + \Delta d$ | $(1 - 2\alpha)$ | = 0.642 |

Table 1. The π^+ probability, $\alpha = 0.179$ is used.

neutron decay constant $g_A^{\text{np}} = \Delta\hat{u} - \Delta\hat{d}$ can be expressed in terms of few-GeV structure functions due to the good validity of the *Bjorken sum rule*. In the present study we restrict ourselves to two flavours only ($s = \bar{s} = \Delta s = \Delta\bar{s} = 0$).

In the N- π -model with $\alpha = \alpha$ the results are the same! This means, that these observables cannot distinguish between these two models.

It is remarkable that the flavour asymmetry of the pion cloud (I_G) agrees so well with the spin observable g_A . Other observables, however, agree only qualitatively; they show the correct trend but reduce the observables only half-way. Part of the defect might be due to the omission of strange flavour. It is easy to fit a few strange admixtures but the number of the additional free parameters would be the same as the three improved observables.

It should be noted that previous authors [6–8, 10] did not couple quark and pion to spin 1/2, they only used a “spin-flip” configuration ($|\mathbf{d}\pi^+\rangle \equiv |\mathbf{d}^\downarrow\pi_{m=1}^+\rangle$, etc.) so that their dressed quarks do not have a definite spin. Their results for $\alpha = 0.239$ are partially worse and partially better, for unknown reason:

$$g_A = \frac{5}{3}(1 - \alpha) = 1.269, \quad I_G = \frac{1}{3}(1 - 2\alpha) = 0.174,$$

$$I_p = \frac{5}{18}(1 - 2\alpha) = 0.145, \quad I_{\text{deut}} = \frac{5}{36}(1 - 3\alpha) = 0.039, \quad \Delta\Sigma = (1 - 3\alpha) = 0.283.$$

In our study we corrected this deficiency.

4 More direct evidence of the pion fluctuation

The analysis of the forward neutron production in the $e + p \rightarrow e + n + X$ collisions at 300 GeV measured by the H1 and ZEUS Collaborations at DESY suggests [10]

$$\langle n\pi^+|p \rangle^2 = 0.17 \pm 0.01$$

in reasonable agreement with the theoretical value

$$|\langle n\pi^+ | p \rangle|^2 = |\langle d\pi^+ | u \rangle|^2 = (1 - \frac{3}{2} a) a = 0.13.$$

Again, this experiment does not distinguish between the two models.

5 Leading proton production

Due to the isospin symmetry, the probability of the forward proton production $e + p \rightarrow e + p + \pi^0$ is twice smaller than for forward neutron production.

$$|\langle p\pi^0 | p \rangle|^2 = \frac{1}{2} |\langle n\pi^+ | p \rangle|^2 = \frac{1}{2} (1 - \frac{3}{2} a) a = 0.065.$$

The preliminary analysis of leading proton spectrum from DIS at HERA [11] suggests a much larger probability of leading proton production. Their contribution of π_0 exchange is in fact small, but they include also two-pion exchanges which they relate to “reggeon” and “pomeron” exchanges.

This result suggests the importance of two-pion contributions. The squared amplitude for $e + p \rightarrow e + p + \pi^+ \pi^-$ is even smaller than the probability for the $e + p \rightarrow e + p + \pi^0$ production:

$$|\langle p\pi^+ \pi^- | p \rangle|^2 = (1 - \frac{3}{2} a)^2 a^2 = 0.017.$$

One possibility to increase the probability of leading proton production is to use the **extended model**:

We add a scalar two-pion configuration to constituent quarks

$$|u\rangle = \sqrt{(1 - \frac{3}{2} a - \frac{3}{2} b^2)} |u\rangle - \sqrt{a} |d\pi^+\rangle + \sqrt{\frac{a}{2}} |u\pi^0\rangle + b |u(\pi^+ \pi^- - \pi^0 \pi^0 / \sqrt{2})\rangle,$$

$$|d\rangle = \sqrt{(1 - \frac{3}{2} a - \frac{3}{2} b^2)} |d\rangle + \sqrt{a} |u\pi^-\rangle - \sqrt{\frac{a}{2}} |d\pi^0\rangle + b |d(\pi^+ \pi^- - \pi^0 \pi^0 / \sqrt{2})\rangle.$$

Since the added sea is flavor symmetric (isoscalar) it does not change the Gottfried sum rule. Since it is also isotropic (scalar) it does not contribute to polarization observables. Therefore, no refitting of a is needed. The main point is, that the amplitudes for kicking two pions from different quarks and from the same quark add coherently.

$$A_{i \neq j} = (1 - \frac{3}{2} a - \frac{3}{2} b^2) a = 0.122,$$

$$A_{ii} = 3 \times (1 - \frac{3}{2} a - \frac{3}{2} b^2) b = 0.366,$$

$$A = A_{i \neq j} + A_{ii} = 0.488, \quad A^2 = 0.24.$$

In principle, the amplitude of the two-pion configuration b should be a model parameter to be fitted. However, since we are interested only in the qualitative effect, we assumed that each addition of a charged pion brings the same factor \sqrt{a} in the amplitude so that $b = a$. We did use $b = a = 0.179$ in the amplitudes above.

Such calculation of the two-pion contribution is consistent with [11]. This agreement suggests that their reggeon in fact consists of a scalar two-pion state present in our model. The pomeron exchange is not relevant for our study since it is related to gluon interaction.

CONCLUSION

We encourage a careful analysis of leading proton production in deep inelastic scattering on protons and possibly committed future experiments. This offers a possibility to distinguish between the two models – pion cloud as a part of the constituent quark versus global pion cloud of the nucleon.

References

1. B. Povh and M. Rosina, Bled Workshops in Physics **12** (2011) No.1, 82-87.
2. B. Golli and R. Sraka, Phys. Lett. B **312** (1993) 24-29.
3. M. Fiolhais, B. Golli and S. Širca, Phys. Lett. B **373** (1996) 229-234.
4. B. Golli and S. Širca, Eur. Phys. J. A **38** (2008) 271-286.
5. B. Golli, S. Širca and M. Fiolhais, Pion electro-production in the Roper region in chiral quark models, Eur. Phys. J. A **42** (2009) 185-193.
6. E.J.Eichten, I.Hinchliffe and C.Quigg, Phys. Rev. D **45** (1992) 2269.
7. S. Baumgaertner, H. J. Pirner, K. Koenigsmann, B. Povh, Z. Phys. A **353** (1996) 397.
8. H. J. Pirner, Prog. Part. Nucl. Phys. **36** (1996) 19-28.
9. T. P. Cheng and Ling-Fong Li, Phys. Rev. Lett. **74** (1995) 2872-2875.
10. A. Bunyatyan and B. Povh, Eur. Phys. J. A **27** (2006) 359-364.
11. A. Szczurek, N. N. Nikolaev and J. Speth, Phys. Lett. **B428** (1998) 383-390.
12. K. Nakamura et al. (Particle Data Group), J. Phys. G **37** (2010) 075021.
13. K. Rith, Prog. Part. Nucl. Phys. **49** (2002) 245.
14. A. Airapetian et al., Phys. Rev. D **75** (2007), 012007.



Real and virtual Compton scattering experiments at MAMI and Jefferson Lab

S. Širca^{a,b}

^a Faculty of Mathematics and Physics, University of Ljubljana, Jadranska 19, 1000 Ljubljana, Slovenia

^b Jožef Stefan Institute, Jamova 39, 1000 Ljubljana, Slovenia

Abstract. Real and virtual Compton scattering are among the most elementary electromagnetic processes on the proton. Two active directions of experimental pursuits are described: virtual Compton scattering experiment at Mainz aiming at the determination of proton generalized polarizabilities, and a recent initiative at Jefferson Lab to enrich the existing data set on real Compton scattering by extending it to higher s and t .

1 Virtual Compton scattering at low Q^2

Virtual Compton scattering (VCS) is a generalization of Compton scattering from real to virtual photons, i. e. the photon in the final state of the scattering process is electro-produced by inelastic scattering of electrons on protons:

$$e + p \longrightarrow e' + p + \gamma.$$

(The kinematics is indeed quite similar to pure elastic scattering. The final-state photon is identified by missing-mass technique.) The two nucleon static scalar polarizabilities measured by scattering of real photons, the electric α_E and the magnetic β_M , become *generalized polarizabilities*, $\alpha_E \rightarrow \alpha_E(Q^2)$, $\beta_M \rightarrow \beta_M(Q^2)$. The leading-order Feynman graphs corresponding to VCS are shown in Fig. 1.

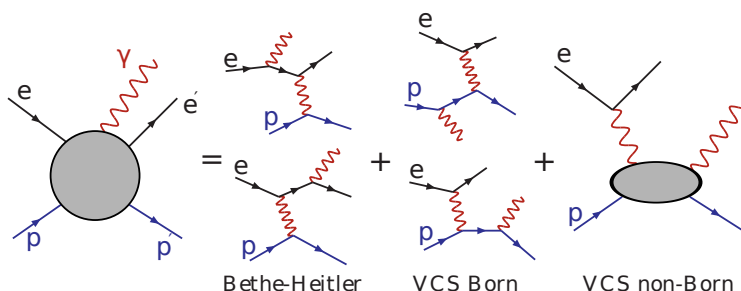


Fig. 1. Leading-order Feynman graphs for virtual Compton scattering.

1.1 Low-energy expansion

There are two main theoretical tools to analyze the VCS process. Both are aimed at the extractions of polarizabilities by comparing the calculated and measured cross-sections in an intricate fit procedure. In the approach that exploits the **low-energy theorem** (LET or “LEX”) [1, 2] one needs to stay below the pion production threshold. In LEX, the differential cross-section is expanded to first power of outgoing photon momentum in the center of mass:

$$d^5\sigma = d^5\sigma_{\text{BH+B}} + (\Phi q'_{\text{cm}}) \left[v_{\text{LL}} \left(P_{\text{LL}} - \frac{P_{\text{TT}}}{\varepsilon} \right) + v_{\text{LT}} P_{\text{LT}} \right] + \mathcal{O}(q'^2),$$

where $d^5\sigma = d^5\sigma/dk'_{\text{lab}}d\Omega'_{\text{lab}}d\Omega_{\gamma\text{cm}}$ (there are also other options for combinations of independent variables). The main point is that $d^5\sigma_{\text{BH+B}}$ contains no polarizability effect and is “exactly” calculable if one assumes that the proton elastic form-factors are well known. Hence, by a simultaneous fit to the measured cross-section divided by the cross-section expanded to lowest order in q' over a large mesh of the photon emission angles one obtains the VCS response (or structure) functions $P_{\text{LL}} - P_{\text{TT}}/\varepsilon$ and P_{LT} that contain specific combinations of generalized and spin polarizabilities:

$$P_{\text{LL}} - \frac{P_{\text{TT}}}{\varepsilon} = \frac{4m_{\text{p}}}{\alpha} G_{\text{E}}^{\text{p}}(Q^2) \alpha_{\text{E}}(Q^2) + [\text{spin-flip GPs}],$$

$$P_{\text{LT}} = -\frac{-2m_{\text{p}}}{\alpha} \sqrt{\frac{q_{\text{cm}}^2}{Q^2}} G_{\text{E}}^{\text{p}}(Q^2) \beta_{\text{M}}(Q^2) + [\text{spin-flip GPs}].$$

Note that additional assumptions on spin-flip polarizabilities are needed in order to extract α_{E} and β_{M} .

1.2 Dispersion-relations analysis

The second approach relies on **dispersion relations** (“DR”) [3, 4] and is — in principle — applicable above the pion threshold if enough information on cross-sections for processes other than VCS are available. This method yields structure functions *as well as* polarizabilities $\alpha_{\text{E}}(Q^2)$ and $\beta_{\text{M}}(Q^2)$. The non-Born amplitudes are computed in terms of dispersive integrals, while the πN part (above the pion production threshold) is given by the $\gamma^*\text{N} \rightarrow \pi\text{N}$ multipoles as obtained from the MAID unitary isobar model. The spin generalized polarizabilities are fixed, while the scalar ones have an unconstrained part which must be parameterized, typically in dipole forms like

$$\alpha_{\text{E}}(Q^2) - \alpha_{\text{E}}^{\pi\text{N}}(Q^2) = \frac{\alpha_{\text{E}}(0) - \alpha_{\text{E}}^{\pi\text{N}}(0)}{\left[1 + \frac{Q^2}{\Lambda_{\alpha}^2}\right]^2}$$

for the electric and similarly for the magnetic polarizability. Ultimately Λ_{α}^2 and Λ_{β}^2 are extracted from experimental data.

Only a few measurements of the VCS structure functions $P_{LL} - P_{TT}/\epsilon$ and P_{LT} exist. Figure 2 shows the world supply of data. Apart from the real-photon values, there are the low- Q^2 measurements by the OOPS Collaboration from MIT-Bates [6], previous measurements at $Q^2 = 0.33$ (GeV/c²) by the A1 Collaboration at MAMI [7, 8], as well as the high- Q^2 data points from Jefferson Lab [9]. The programme to determine $P_{LL} - P_{TT}/\epsilon$ and P_{LT} at various values of Q^2 in a single group of runs, and in turn to extract the generalized polarizabilities $\alpha_E(Q^2)$ and $\beta_M(Q^2)$, is presently underway at MAMI [5]. The aim is to provide additional and more precise data points at $Q^2 = 0.1, 0.3$ and 0.5 (GeV/c²). The measurements will be performed in-plane, out-of-plane, and at low- q' normalization settings in order to better control the systematics.

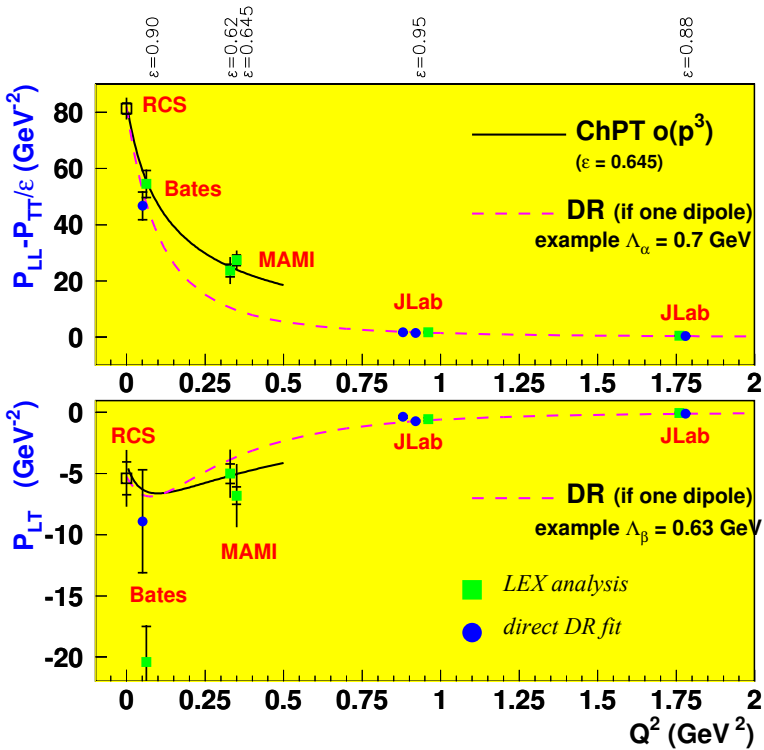


Fig. 2. The world supply of data for the structure functions $P_{LL} - P_{TT}/\epsilon$ and P_{LT} for virtual Compton scattering on the proton. (Figure courtesy of H. Fonvieille.)

2 Real Compton scattering at high s and t

Compton scattering on the proton, in particular in its wide-angle regime where $s, -t, -u \gg M^2$, is a powerful and under-utilized probe of nucleon structure. As the process involves only real photons and only the ground state of the proton in

both initial and final states, it is elegantly simple. The physics involved is closely related to elastic electron-proton elastic scattering or DVCS, yielding the electromagnetic response of the nucleon without complications due to presence of other hadrons. However, wide-angle Compton scattering (WACS) remains one of the least understood fundamental processes in the several-GeV regime.

Several approaches to WACS have been proposed over the years, ranging from relativistic constituent quark models, investigations of the two-gluon exchange mechanism within pQCD, studies of the handbag mechanism in terms of generalized parton distributions (GPDs) [10] and, most recently, soft collinear effective theory [11]. In spite of the progress on all these fronts, WACS continues to pose many questions. Does large $-t$ ensure dominance of short-distance physics? What factorization scheme is valid? Is it true that the WACS reaction proceeds through the interaction of a photon with individual quarks? What information on the structure of proton can be extracted from the measurement of WACS form-factors? Given the fact that pQCD is not expected to be valid at this kinematic scale, why are the scaling predictions (see e.g. [12, 13]) so close to the observed values?

2.1 Factorization schemes in real Compton scattering

Obviously a thorough understanding of the possible underlying factorization schemes in real Compton scattering (RCS) is needed. In these schemes, the “hard scale” implies that all Mandelstam variables, s , $-t$, and $-u$, are large compared to m_p^2 or, equivalently, the transverse momentum transfer, p_{\perp} , is large. Only in this regime the transition amplitude is expected to become factorized as a convolution of a perturbative hard scattering amplitude, which involves the coupling of the external photon to the active quarks, with an overlap of initial and final soft (non-perturbative) wave-functions, which describes the coupling of the active quarks to the proton:

$$T_{if}(s, t) = \Psi_f \otimes K(s, t) \otimes \Psi_i,$$

where $K(s, t)$ is the perturbative hard scattering amplitude and the Ψ 's are the soft wave functions.

Different factorization schemes for RCS are distinguished by the number of active constituents participating in the hard scattering subprocess. Two are most common. The handbag mechanism involves only one active constituent, while the pQCD mechanism involves three. In any given kinematic regime, both mechanisms may contribute. At “sufficiently high” energy, the pQCD mechanism is expected to dominate, but the anticipated point of onset of this regime is not known.

2.2 Results of the JLab 6-GeV RCS experiments

Two groups of RCS experiments have been performed at Jefferson Lab with 6 GeV. The E99–114 experiment (Hall A, 2002) yielded spin-averaged cross-sections over a broad kinematic range $6.8 < s < 11 \text{ GeV}^2$, $2 < -t < 7 \text{ GeV}^2$ [12], as well as polarization transfer asymmetries K_{LL} and K_{LT} at $s = 6.9 \text{ GeV}^2$, $-t = 4 \text{ GeV}^2$ [13].

The E07-002 experiment (Hall C, 2008) measured polarization observables K_{LL} , K_{TT} and P_N at $s = 8.0 \text{ GeV}^2$, $-t = 2.1 \text{ GeV}^2$ (analysis in progress). In spite of the immense increase in precision over older experiments from Cornell, and first measurements of RCS polarization observables ever, the factorization scheme issue could not be resolved unambiguously. There is evidence for factorization of the reaction mechanism and dominance of the handbag mechanism, but it is still inconclusive. As in elastic electron-proton scattering, the polarization observables in RCS have added insight: the process appears to strongly favor the leading-quark mechanism ($\alpha \approx 1$), but some kinematic points have not satisfied the wide-angle condition ($s, -t, -u \gg M^2$) due to small value of $-u$.

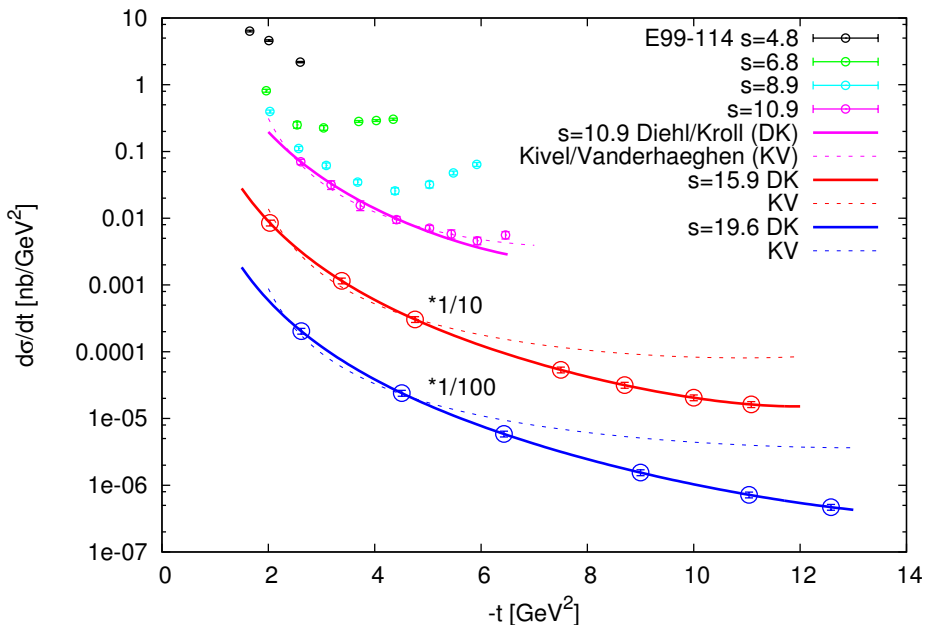


Fig. 3. The anticipated results in the proposed WACS experiment (the points at $s = 15.9$ and 19.6 GeV^2 plotted on the Diehl-Kroll parameterizations of cross-sections). Only the statistical uncertainties are shown.

2.3 Proposal for a JLab 12-GeV WACS experiment

To address the issues and avoid the deficiencies enumerated above, a new proposal has been forwarded for a measurement of WACS in Hall C that will exploit the forthcoming 12 GeV beam of CEBAF [14]. We intend to measure 13 kinematic points, with the main goal of determine the scaling power n of the cross-section in terms of s at fixed θ_{cm} , and from this information infer the dominant reaction mechanism. The most important feature of the experiment is the fulfillment of the wide-angle condition, i.e. $s, -t, -u \gg M^2$ will be satisfied in *all* settings. A broad

range in $-t$ will be covered, allowing us to extract the RCS form-factor $\mathcal{R}(t)$ and find solid evidence for factorization. The results will also provide constraints on GPDs at high Bjorken x and constraints on 2γ effects, which are also relevant for the interpretation of electron-proton elastic scattering at high Q^2 . The kinematics range covered will be

$$15.0 < s < 21.0 \text{ GeV}^2 \quad 2.0 < -t < 12.0 \text{ GeV}^2 \quad 3.0 < -u < 15.3 \text{ GeV}^2 .$$

The expected uncertainties, as given in the PR-12-13-009 proposal, are shown in Fig. 3. This proposal has been deferred by JLab PAC 40. We are presently working on its revision and will submit the new version to PAC 41 in early 2014.

References

1. P. Guichon et al., Nucl. Phys. A **591** (1995) 606.
2. M. Vanderhaeghen et al., Phys. Lett. B **402** (1997) 243.
3. B. Pasquini et al., Eur. Phys. J. A **11** (2001) 185.
4. D. Drechsel et al., Phys. Rep. **378** (2003) 99.
5. H. Fonvieille (spokesperson) et al. (A1 Collaboration), MAMI Proposal A1/1-09.
6. P. Bourgeois et al., Phys. Rev. Lett. **97** (2006) 212001.
7. J. Roche et al. Phys. Rev. Lett. **85** (2000) 708.
8. P. Janssens et al., Eur. Phys. J. A **37** (2008) 1.
9. G. Laveissière et al., Phys. Rev. Lett. **93** (2004) 122001.
10. M. Diehl, P. Kroll, [arXiv:1302.4604](https://arxiv.org/abs/1302.4604) [hep-ph].
11. N. Kivel, M. Vanderhaeghen, [arXiv:1212.0683](https://arxiv.org/abs/1212.0683) [hep-ph].
12. A. Danagoulian et al., Phys. Rev. Lett. **98** (2007) 152001.
13. D. J. Hamilton et al., Phys. Rev. Lett. **94** (2005) 242001.
14. B. Wojtsekhowski, D. Hamilton, S. Širca (spokespersons), Jefferson Lab Proposal PR-12-13-009 (submitted to PAC 40).

Povzetki v slovenščini

Vloga valenčnih in morskih kvarkov v lahkih barionih

Roelof Bijker^a in Elena Santopinto^b

^a Instituto de Ciencias Nucleares, Universidad Nacional Autónoma de México, A.P.70-543, 04510 México D.F., México

^b I.N.F.N., Sezione di Genova, via Dodecaneso 33, Genova, I-16146 Italy

V tem prispevku obravnavamo, kakšna je porazdelitev spina in okusa v protonu pri dveh posplošitvah kvarkovega modela, in sicer pri modelu z nedušeni kvarki in pri modelu s kiralnimi kvarki. Pri tem predstavimo vlogo valenčnih in morskih kvarkov v lahkih barionih.

Spektri barionov in oblikovni faktorji nukleona iz relativističnih kvarkovih modelov ter iz anti-de Sitterjev kvantne kromodinamike (AdS/QCD)

J. P. Day in W. Plessas

Theoretical Physics, Institute of Physics, University of Graz, A-8010 Graz, Austria

Nizkoenergijske hadrone obravnavamo z neperturbativnimi pristopi oziroma z efektivnimi modeli. Prelagamo relativistični konstituentni kvarkov model, ki hkrati opiše vse znane barione z okusom u , d , s , c in b kvarkov. Uspešnost pokažemo tako pri barionski spektroskopiji kot pri elektromagnetnih, aksialnih in gravitacijskih oblikovnih faktorjih. Potem pa prikažemo možnosti, ki jih nudi anti-de Sitterjeva kvantna kromodinamika na svetlobnem stožcu pri opisu istih količin: mezonskih in barionskih spektrov ter njihove strukture.

Spektroskopija hibridnih mezonov

Giuseppe Galatà

Instituto de Ciencias Nucleares, Universidad Nacional Autónoma de México, Apdo. Postal 70-543 04510 México, DF, México

Najpogosteje obravnavajo hibridne mezone, ki so sestavljeni iz kvarka, antikvarka in gluona. Mi smo jih proučevali z variacijskim pristopom h kromodinamiki v coulombski umeritvi. Pokazali smo, da jih omejuje v okviru variacijskega pristopa linearni potencial, ki sledi iz Dyson-Schwingerjevih enačb vsaj na hadronski skali. S tem potencialom smo najprej izračunali spekter gluonske kepe. To je idealiziran sistem gluonskih ekscitacij, vezanih na statični lokaliziran izvor s simetrijo barvnega okteta (npr. na zelo težek kvark in antikvark). V naslednjem koraku smo vpeljali dinamiko kvarkov in antikvarkov in izračunali spekter težkih hibridnih mezonov. Rezultati se lepo ujemajo z računi na mreži.

Vroča in gosta snov v kromodinamiki ter povrnitev simetrije $U_A(1)$

Dubravko Klabučar, Sanjin Benić^a, Davor Horvatić^a in Dalibor Kekez^b

^a Physics Department, Faculty of Science, Zagreb University, Bijenička c. 32, Zagreb 10000, Croatia

^b Rudjer Bošković Institute, Bijenička c. 54, 10000 Zagreb, Croatia

Pomembni nedavni rezultati v laboratoriju RHIC glede mnogoterosti mezonov η' pri trkih težkih ionov so jasno nakazali delno povrnitev simetrije $U_A(1)$ pri visoki temperaturi. S tem so nedvoumno zaznamovali tvorbo novega stanja snovi. Za razlago meritev kolaboracij STAR in PHENIX so predlagali minimalno posplošitev Wittenove in Venezianove relacije na končne temperature. V tem prispevku podajamo podrobno pedagoško razpravo in razlago. Najprej razložimo, zakaj se na podlagi teh rezultatov Wittenova in Venezianova relacija ne da posplošiti od temperature nič na temperature preblizu kiralnega prehoda in čez. Potem predlagamo količino, ki pri višjih temperaturah nadomesti Yang-Millovo topološko susceptibilnost v omenjeni relaciji, tako da ni več nesoglasja z eksperimenti pri končnih temperaturah. To prikažemo z odvisnostjo mas psevdoskalar-nih mezonov od temperature v kiralno korektnem Dyson-Schwingerjevem pristopu, vendar so naši rezultati in zaključki splošnejši in neodvisni od modela.

Fazni premiki pri resonancah, kot jih da kromodinamika na mreži: kanal pion-nukleon

C. B. Lang¹ in V. Verduci²

¹Institut für Physik, Universität Graz, A-8010 Graz, Austria

²School of Physics and Astronomy, University of Edinburgh, Edinburgh EH9 3JZ, Scotland

Uporabili smo regularizacijo mreže v evklidskem prostoru-času in izkoristili ogromen napredek pri računanju hadronskih lastnosti s simulacijami Monte Carlo. Za študij razpada hadronov je pomembna izbira interpolatorjev v vmesnem stanju. Pri barionih so doslej uporabili le trokvarkovske interpolatorje in so dobili le višja kvazi-vezana stanja. Zato smo vpeljali še interpolatorje tipa pion-nukleon (4 kvarke + 1 antikvark). Da smo dobili statistično zanesljiv rezultat, smo s tako imenovano destilacijsko metodo izbrali glavne prispevke v grafih. Z Lüscherjevo metodo smo potem izpeljali fazne premike.

Razcep barionskih elektromagnetnih oblikovnih faktorjev po okusih

M. Rohrmoser[†], Ki-Seok Choi* in W. Plessas[†]

[†] Theoretical Physics, Institute of Physics, University of Graz, A-8010 Graz, Austria

* Department of Physics, Soongsil University, Seoul 156-743, Republic of Korea

Preizkusili smo relativistični model s konstituentnimi kvarki in z izmenjavo Goldstonovih mezonov glede na nove fenomenološke podatke o porazdelitvi okusa pri elektromagnetnih oblikovnih faktorjih nukleona. Te raziskave smo potem razširili na vsa druga barionska osnovna stanja z okusi u, d in s. Za mnoga stanja težja od nukleona smo lahko naše rezultate primerjali z razpoložljivimi računi s kromodinamiko na mreži. Izkazalo se je, da relativistični model s konstituentnimi kvarki že v okviru trokvarkovske konfiguracije primerno dobro opiše elektromagnetno zgradbo do prenosov gibalnih količin $Q^2 \sim 4 - 5\text{GeV}^2$.

Prispevki kvarkovskih parov k šibkim oblikovnim faktorjem za prehode v težko-lahkih mezonih

Oliver Senekowitsch in Wolfgang Schweiger

Institut für Physik, Universität Graz, A-8010 Graz, Austria

Za ta namen smo uporabili relativistični model s konstituentnimi kvarki, prirejen v točkovni obliki. V krajevnem in časovnem območju prenosa gibalne količine smo preučevali oblikovne faktorje za prehode težko-lahkih mezonov v težko-lahke in lahko-lahke mezone. Raziskali smo vpliv ne-valenčnih prostostnih stopenj, ki prispevajo "dvokvarkovske tokove" pri šibkih prehodih. V ta namen smo najprej izračunali oblikovne faktorje v krajevnem območju prenosa gibalne količine, kjer menimo, da so dvokvarkovski prispevki zatrti. Nato smo jih analitično nadaljevali v časovno območje prenosa gibalne količine. Primerjava z neposrednimi računi razpada kaže na vlogo dvokvarkovskih prispevkov pri kinematiki razpada. Predlagamo preprost dinamični mehanizem, osnovan na modelu tvorbe parov s kvantnim številom 3P_0 .

Razvoj barionov po recipročnem številu barv v povezavi z Reggejevimi trajektorijami

N. Matagne^a in Fl. Stancu^b

^a Service de Physique Nucléaire et Subnucléaire, University of Mons, Place du Parc, B-7000 Mons, Belgium,

^b Institute of Physics, B5, University of Liège, Sart Tilman, B-4000 Liège 1, Belgium

Barione z mešano simetrijo, ki imakjo pozitivno in negativno parnost, smo opisali na podoben način. Uporabili smo metodo razvoja po recipročnem številu barv v kromodinamiki, pri kateri smo točno vgradili permutacijsko simetrijo. Na ta način smo lahko izrazili masno formulo z majhnim številom linearno neodvisnih operatorjev. Pokazali smo, da sledi vodilni prispevek drugačni Reggejevi trajektoriji kot pri simetričnih stanjih, če ga rišemo kot funkcijo pasovnega kvantnega števila N .

Elektroekscitacija resonanc v parcialnih valovih z $l = 2$

Bojan Golli^{a,c} in Simon Širca^{b,c}

^aPedagoška fakulteta, Univerza v Ljubljani, 1000 Ljubljana, Slovenija

^bFakulteta za matematiko in fiziko, Univerza v Ljubljani, 1000 Ljubljana, Slovenija

^cInstitut J. Stefan, 1000 Ljubljana, Slovenija

Predstavimo račun sipanja in elektroprodukcije mezonov v parcialnih valovih D_{13} , D_{33} in D_{15} z metodo sklopljenih kanalov, ki vsebujejo kvazivezana nukleonska vzbujena stanja, kot jih daje kvarkovski model. V nasprotju z rezultati v parcialnih valovih P_{11} , P_{33} in S_{11} kvarkovski model napoveduje nekoliko premajhne vrednosti za sklopitve resonančnih stanj z mezoni in fotonom, a kljub temu vodi do konsistentnih rezultatov v vseh obravnavanih kanalih.

Novi rezultati v spektroskopiji kvarkonijev in eksotičnih kvarkonijskih resonanc v "tovarnah" mezonov B

Marko Petrič

Institut J. Stefan, 1000 Ljubljana, Slovenija

V tem prispevku predstavimo nedavne zbrane rezultate meritev na detektorju Belle, ki so potekale na asimetričnem trkalniku KEKB za elektrone in pozitrone na inštitutu KEK v Tsukubi (Japonska). Vzorec podatkov se da uporabiti za razne nove preiskave v spektroskopiji. Obravnavamo odkritje eksotičnih stanj Z_b , meritev sevalnih prehodov $h_b(1, 2P) \rightarrow \eta_b(1, 2S)$, ki dajo prvo evidenco za stanje $h_b(2S)$, ter odkritje čarobnega stanja $Z^+(3900)$.

Čarmonijem podobna stanja in resonance K^* pri kromodinamiki na mreži

Saša Prelovšek

Institut J. Stefan, Jamova 39, 1000 Ljubljana in
Oddelek za fiziko, Univerza v Ljubljani, Jadranska 19, 1000 Ljubljana, Slovenija

Predstavila sem prvo evidenco za mezon $X(3872)$ z uporabo kromodinamike na mreži, prvo iskanje resonance Z_c^+ (3900) in prvo izpeljavo razpadne širine mezona $K^*(892)$ za razpad z močno silo.

Ali je pion sklopljen s posameznim kvarkom ali s celim nukleonom?

Mitja Rosina^{a,b} in Bogdan Povh^c

^aFakulteta za matematiko in fiziko, Univerza v Ljubljani, Jadranska 19, p.p. 2964, 1001 Ljubljana, Slovenija

^bInstitut J. Stefan, 1000 Ljubljana, Slovenija

^cMax-Planck-Institut für Kernphysik, Postfach 103980, D-69029 Heidelberg, Germany

Primerjamo dva modela; v prvem so mezoni π sklopljeni s posameznimi kvarki, v drugem pa so sklopljeni z nukleonom kot celoto. Pokazali smo, da imajo mnoge lastnosti nukleona, kot na primer asimetrija v številu antikvarkov \bar{u} in \bar{d} v nukleonskem oblaku, spinska polarizacija ter amplitude za vzbujanje nukleona z elektroni, enake vrednosti v obeh modelih. Napovedujemo pa, da bodo natančnejše meritve takih trkov elektrona s protonom, pri katerih odleti proton skoraj natanko v smeri naprej, lahko razlikovalale med obema modeloma.

Eksperimenti z realnim in virtualnim comptonским sipanjem pri MAMI in v Jeffersonovem laboratoriju

Simon Širca

Fakulteta za matematiko in fiziko, Univerza v Ljubljani, Jadranska 19, in
Institut J. Stefan, 1000 Ljubljana, Slovenija

Realno in virtualno comptonško sipanje sodita med najelementarnejše elektromagnetne procese na protonu. V prispevku opišemo dve dejavni smeri eksperimentalnih raziskav: virtualne comptonške poskuse v Mainzu, ki so namenjeni določitvi posplošenih protonskih polarizirnosti, in pred nedavnim podano pobudo v Jeffersonovem laboratoriju, da bi obstoječe podatke za realno comptonško sipanje obogatili tako, da bi meritve razširili k visokim vrednostim s in t .

BLEJSKE DELAVNICE IZ FIZIKE, LETNIK 14, ŠT. 1, ISSN 1580-4992

BLED WORKSHOPS IN PHYSICS, VOL. 14, NO. 1

Zbornik delavnice 'Pogled v hadrone',
Bled, 7. – 14. julij 2013

Proceedings of the Mini-Workshop 'Looking into Hadrons',
Bled, July 7 – 14, 2013

Uredili in oblikovali Bojan Golli, Mitja Rosina, Simon Širca

Članki so recenzirani. Recenzijo je opravil uredniški odbor.

Izid publikacije je finančno podprla Javna agencija za raziskovalno dejavnost RS iz sredstev državnega proračuna iz naslova razpisa za sofinanciranje domačih znanstvenih periodičnih publikacij.

Tehnični urednik Matjaž Zaveršnik

Založilo: DMFA – založništvo, Jadranska 19, 1000 Ljubljana, Slovenija

Natisnila tiskarna Birografika Bori v nakladi 90 izvodov

Publikacija DMFA številka 1915

Brezplačni izvod za udeležence delavnice
